PC

An objective method for forecasting hail and thunderstorms

by A. Woodroffe and J.H. Seymour

1. Introduction

The severe local storm, defined by Winston /1/ as a thunderstorm accompanied by very strong surface winds and large hail, is a rare occurrence in the British Isles. Consequently, the damage and inconvenience inflicted by these storms is small in comparison with that experienced in certain areas of the world, notably in parts of the USA and northern Italy. However, warnings of the less severe hail and thunderstorms are important for general purpose and aviation forecasting, as well as for the more specialised requirements such as the issue of lightning risk forecasts to the electricity boards. Aircraft, in particular, require warning of even modest thunderstorms because of the extreme turbulence and icing experienced in the cumulonimbus clouds. Damage by impact with hail is also a serious problem which becomes more serious as aircraft speeds increase, and it is certain that a SST would sustain considerable damage from the smallest hail if it was encountered during the supersonic phase of flight. Jones /2/ has emphasised that although airborne radar would assist in the avoidance of cumulonimbus clouds, detection would be required up to ranges of 200 n.mi in the most unfavourable circumstances, to enable appropriate avoiding action to be taken. At these ranges, there would be considerable imprecision in the measurement of the cloud heights, and accurate forecasts of the maximum heights to be expected would be very helpful in deciding whether a detour was necessary.

One of the major problems that the forecaster must face is attempting to predict the development of a meso-scale weather system using only the synoptic observations that are routinely available. In developing a technique with the present density of observations, it is necessary to relate the development of these storms with the synoptic-scale properties of the atmosphere, of which there are adequate observations.

/Numerous

Numerous techniques for forecasting hail and thunderstorms have been devised during the last 15 years or so, and almost invariably these methods take account in one way or another of the well-established relationship between the occurrence of these phenomena and the prior existence of static instability in the atmosphere. The recent emphasis, particularly in this country, has been on the use of indices which are so defined that they provide an approximate measure of the latent instability. Some indices, such as the one proposed by Jefferson /3/, also take account empirically of other parameters like humidity, but their essential properties are that they are simple to evaluate, while giving a fairly reliable indication of the likelihood of storms. Considering their simplicity, these indices have proved remarkably successful as predictors.

In the field of numerical weather prediction, Bushby and Timpson /4/ have recently reported on experiments with a ten-level primitive equation model incorporating humidity. The results of this work suggest that reliable forecasts of the thermal, dynamical and humidity properties of the atmosphere, on the smaller-synoptic scale, for periods up to about 24 hours ahead should be available on an operational basis within the next few years. These forecasts would provide a sound basis for an objective storm-forecasting scheme which could be handled entirely on the computer, and it would no longer be necessary to regard the time factor as imposing an upper limit to the permissible complexity of the scheme. The original purpose of this investigation was to develop such an objective technique for predicting the occurrence and also, if possible, the size of hail.

Many cases of hail would pass unrecorded if the forecasts were checked against the reports from the existing synoptic and climatological networks of observing stations. Individual hailstorms, with a few notable exceptions, affect areas with typical dimensions much less than the average distance between stations, so that it would be impossible to obtain a satisfactory verification of the forecasts, unless a special high-density observing network were set up. Hail and thunder are both by-products of the cumulonimbus cloud and since most theories of the separation of electric charge demand the presence of the ice phase in the cloud

(see

(see e.g. Mason /5/), hail of some size probably exists in all thunderstorms in middle and high latitudes, although it may not reach the ground. The basic problem is therefore one of forecasting the active cumulonimbus cloud, and for our purposes we shall regard the observation of hail, lightning or thunder as being evidence of its existence. To distinguish cases of hail reaching the ground from those where thunder alone is observed requires the consideration of the melting experienced by the ice particles during their fall below the freezing level. Considerable complications are introduced here as the melting depends on several factors besides the temperature profile. Mason /6/, in a theoretical treatment of the subject indicated that the melting depended on the initial size and density of the hail, the accretion of cloud droplets and the humidity of the air, as well as the temperature profile and the height of the freezing level above the ground.

Coles /7/ has stated that it is the practice in the Meteorological Office to include a mention of hail in forecasts when thunderstorms are expected; this implies that there are no recognised criteria for differentiating between those conditions which favour thunderstorms and those favouring hail, which is a reflection of the close relationship between these convective phenomena. The formulation of rules to make this distinction would require the analysis of observations similar to those provided by the network of voluntary hail observers which was set up by Ludlam in the late 1950's. Ludlam (private communication) has expressed the view that hail almost invariably reaches the ground at some stage during the lifetime of an active thunderstorm, although only a very small area may be affected. This is probably not true, however, when the air is unusually warm or when the storm is rather weak.

It was decided, on the basis of these considerations, that it would not be practicable with the observational material presently available to restrict this investigation to the forecasting of hail at the ground. Also, since hail and thunder are so closely related, there seems little point in attempting to discriminate between them until the present techniques for predicting the initial development and severity of either of these weather phenomena have been considerably improved. This report describes, therefore, a method for forecasting the

/occurrence

occurrence of hail and/or thunderstorms in S.E. England during the summer months. Hail and thunder will subsequently be regarded as alternative manifestations of a single weather phenomenon, the cumulonimbus thundercloud.

2. Theories of small-scale convection

The validity of a particular theory of small-scale convection is usually assessed by comparing the observed depths of convective clouds with the values predicted by the theory. The actual heights of clouds can easily be measured and forecasters have recognised for a long time that there is a fairly close relationship between the depth of the cloud and the severity of the associated weather phenomena. Douglas and Hitschfeld /8/ showed, for example, that the size of hail is strongly dependent on the height of the storm. The oldest theory of convection, the well-known parcel theory, fell out of favour for a long time, because it was shown that on any given day, the theory greatly overestimated the heights reached by a substantial majority of clouds.

Petterssen et alii /9/ showed theoretically that on the basis of the slice theory, introduced by Bjerknes /10/, the tops should extend only slightly above the level where the lapse rate first becomes less than the saturated adiabatic. Measurements of actual cloud heights confirmed that this conclusion was justified in many instances. The experimental work of Scorer /11/ with isolated thermals in water tanks, emphasised that the basic concept of the parcel theory, of a discrete volume of air ascending through the environment, without mixing, was extremely unrealistic. Substantial mixing occurs between the thermal and its surroundings, so that the buoyancy is quickly destroyed. An isolated cloudy thermal rising through a typical unsaturated environment can only penetrate vertically through a distance which is of the same order as the initial horizontal dimension of the thermal. Byers and Braham /12/, in their report on the Thunderstorm Project, had already shown that the rate of entrainment into a large cumulus is of the order of 100% per 500 mb. of ascent and that the updraught air does not become much warmer than the environmental air. This is contrary to expectations from the parcel theory where, under suitable lapse rate conditions, temperature excesses of 5°C or more may occur.

/Long

Long, Hanks and Beebe [13] in a report on tropopause penetrations by cumulonimbus clouds have noted that there has been "a rather steady return in recent years to the concept of the undiluted, saturated, steadily rising parcel or jet of air in the centre of a large thunderstorm. Such a concept became necessary when the tops of very tall thunderstorms exceeded the calculated maximum heights of rising jets or bubbles of entrained air by wide margins". Their observations showed that, in the case of 48 giant cumulonimbus clouds in the vicinity of Kansas City, most tops were within about 5,000 ft. of the values computed on parcel theory. Newton [14] has also commented on the necessity of returning to the idea of undiluted air to explain the great vertical development of some cumulonimbus clouds. He suggested that the efficiency of mixing will vary considerably, so that in the interior of a large-diameter cloud, the effects of entrainment may be quite small.

Ludlam, in several papers (e.g [15, 16]), has expressed the view that the assumptions of parcel theory (adiabatic ascent through an undisturbed environment) may not be unrealistic in the interior of a large, strongly-building cloud, particularly if the convection becomes organised, as it may do in the presence of vertical wind shear. The thermals cannot be regarded as isolated, and the mixing laws obtained by Scorer are consequently no longer applicable; instead they rise in rapid succession as the flux of buoyant air into the cloud increases, and in the limit may combine to form the type of strong, smooth, updraughts observed by sailplane pilots in cumulonimbus clouds over Germany (Wichmann [17]). Ludlam and Newton both regard the early thermals as expendable, being used to saturate and warm the immediate environment. Later thermals ascending from cloud base through the centre of the cloud encounter an environment which has been so modified that the effects of mixing are considerably reduced. Under these conditions, it is conceivable that the properties of the later thermals in the vicinity of the cloud core will approximate to the adiabatic values expected from parcel theory. The thermals are then able to ascend to great heights before losing their buoyancy.

/The

The development of a vigorous thundercloud depends, therefore, on a copious and persistent supply of buoyant air into the cloud. It is to be noted that the effects of friction drag, as well as entrainment, will become less important as the vigour of the convection increases. Ludlam /16/ has associated the development of a shower with the organisation of the convection. The flux of potentially warm air into the cloud is substantially increased and conditions are most likely to approximate to adiabatic. Ludlam gave examples of major storms which became organised with the help of wind shear and demonstrated that the tops reached the heights expected on parcel theory.

The slice method, although treating convective processes as adiabatic, considers also the compensating downward currents in the environment. The work of Petterssen /9/ indicated that this theory was useful for predicting the general level likely to be reached by convective clouds. In particular, it can explain why many clouds never attain the heights expected from the parcel method. However, the problem of forecasting hail and thunder demands that we should be concerned with the maximum development that is likely to occur in any given area, not the average value. A difficulty in the practical application of the slice method is that the stability depends on the fraction of the horizontal area occupied by the ascending currents. At the level reached by the highest tops, this fraction will be very small and the stability criteria approximate to those of the parcel method.

Saunders /18/ has reported on tests of thunderstorm forecasting methods carried out in the Manby Group in 1965. Siskin's technique /19/ was used to forecast hail, using cloud thickness predictions by both the parcel and slice methods. Although the forecasts were only tested over a six-month period and no special observations were available for checking the occurrence of hail, the results showed fairly conclusively that the forecasts using the parcel theory cloud thicknesses were superior. It was concluded that the Siskin "slice" method consistently under-estimated the cloud thickness and failed to provide a basis for forecasting hail.

Roach /20/ concluded from an analysis of severe storms in Oklahama that parcel theory seemed to indicate the maximum development attainable, or in other words, the worst possible conditions to be expected. Other factors must be considered in deciding whether this maximum will be attained on any given day.

This discussion of the various theories of convection indicates that the thermo-dynamic processes are strongly influenced by the scale and intensity of the convective processes. It appears that the use of the parcel method is most justified in dealing with the vigorous convection which is usually associated with the development of hail and thunderstorms. Consequently, parcel theory was used in this investigation to predict the variation with height of the temperature and vertical velocity in the updraught.

3. The parcel method and the maximum size of hail

The concept of the adiabatic motion of a discrete air parcel through an undisturbed environment forms the basis of the parcel theory of convection. These assumptions permit an evaluation of the energy available to the parcel due to the buoyancy forces, if it is displaced from an initial equilibrium position. The stability criteria, so obtained, can then be expressed as a function of the lapse rate alone. Consider a parcel of air surrounded by an environment which is in hydrostatic equilibrium. The equations of motion in the vertical, for the parcel of air and the environment respectively are:-

$$\frac{dw}{dt} = -\alpha \frac{\partial p^1}{\partial z} - g \qquad - (1)$$

$$0 = -\alpha^1 \frac{\partial p^1}{\partial z} - g \qquad - (2)$$

where w = vertical velocity of the parcel

α = specific volume of the parcel

α^1 = specific volume of the environment

p^1 = pressure of the environment

z = a vertical co-ordinate

g = gravitational acceleration.

Note that in deriving Eq. (1), it is assumed that the pressure gradient in the vertical is the same for the parcel as exists in the environment. From Eqs. (1) and (2):-

$$\frac{dw}{dt} = g \frac{\alpha - \alpha^1}{\alpha^1}$$ and using the equation of state:

$$\frac{dw}{dt} = g \frac{T - T^1}{T^1} \qquad - (3)$$

/where

where T and T^1 are the absolute temperatures of the parcel and environment respectively. Thus the buoyancy force is proportional to the excess temperature. The temperature of the parcel will follow either a saturated or dry adiabatic, depending on whether condensation is occurring. Consequently, if the vertical temperature profile of the environment is specified, parcel theory determines the kinetic energy that will be acquired by the parcel in moving through a given distance in the vertical ($T > T^1$) or alternatively the work that must be done in moving the parcel through a given distance in the vertical ($T < T^1$). By applying this theory to the ascent of thermals in the interior of a cumulonimbus cloud, we can deduce the variation with height of the vertical velocity and temperature in the updraught.

The conditions of temperature and humidity in the environment, as measured by a radio-sonde ascent, are generally plotted on a tephigram, which is an equal-area transformation of a p-v diagram. A full discussion of the use of the tephigram in the application of the parcel theory is given in the paper by Petterssen /9/ Fig.1 is a schematic diagram of a tephigram for a conditionally unstable environment. The positive area between the environment temperature curve AA^1 and the saturated adiabatic BB^1 is a direct measure of the available energy. BB^1 is the saturated adiabatic corresponding to the wet-bulb potential temperature of the ascending parcel (θ_{wp}). θ_{wp} is determined from the values of temperature and humidity near the ground. The maximum upward velocity is attained at the level Z_E, where there is zero excess temperature. The parcel oscillates about this level, the upper limit of the oscillation being Z_u (the positive and negative areas being equal). Thus, the cloud top will reach the level Z_u on parcel theory.

Measurement of the positive area is difficult and is very rarely done in current forecasting practice. The height, Z_E, is the parameter which is usually determined from the tephigram, since forecasters' experience has shown that this quantity is useful for assessing the heights of the tallest clouds. The relationship between the depths of convective clouds and the severity of the associated weather phenomena has already been noted; in general, there is also a broad connection between the height Z_E and the latent instability as measured by the positive area on the tephigram. In 1961, Coles /1/ observed that the forecasters in the Meteorological Office use their experience in applying the relationship that exists between the energy gained by an ascending parcel and the intensity

/of

of the convective phenomena. Since then, several simple numerical measures of the latent instability have become available to the forecaster, in the form of the instability indices mentioned previously.

A particular aspect of this problem concerns the forecasting of the maximum size of hailstone. Although large hail is rare in this country, it is important that we should recognise those occasions when it is liable to occur. Ludlam [15] showed theoretically that if the stone is grown in a steady updraught and all the accreted water is frozen (dry growth), the fall speed of the stone as it leaves the supercooled region will be about twice the speed of the updraught. If wet growth occurs and the excess water is lost, the ratio of fallspeed to updraught decreases to about 1.4. Any reasonable theory of the growth of large hail requires that more than a simple ascent and descent should be made through the supercooled part of the cloud. A consideration of more realistic models of the hail-growth mechanism suggests that, in practice, the fallspeed-updraught ratio will be much nearer to unity than in the simple model described above. Ludlam concluded that the fallspeed of the largest stones cannot substantially exceed the maximum updraught occurring in the cloud.

If this conclusion is assumed to be correct, the size of the largest hail can readily be calculated from the maximum speed in the updraught. When the stone reaches its terminal velocity, the air resistance or drag force equals the gravitational force. Equating these two quantities gives:

$$\pi r^2 \frac{1}{2} \rho V^2 C_D = \frac{4}{3} \pi r^3 (\sigma - \rho) g \qquad - (4)$$

where r is the radius of the hailstone

V is the terminal velocity of the stone

σ is the density of the stone

ρ is the density of the air

g is the gravitational accelecation, and

C_D is the drag coefficient of the stone.

The drag coefficient is a non-dimensional parameter defined by the following equation:-

/C_D

$$C_D = \frac{D}{\frac{1}{2}\rho V^2 A}$$

where D is the drag force acting on a particle

V is the velocity of the particle

A is the cross-sectional area of the particle, and

ρ is the density of the environment.

The Reynolds number appropriate to hailstones in the high troposphere is of the order of 10^3 for stones of 1 mm. radius and of the order 10^5 for stones of 3 cm. radius. The drag coefficient for rigid spheres has been determined experimentally and tabulated by McDonald [21] for a wide range of Reynolds number. In the interval appropriate to hailstones, the drag coefficient varies only between 0.40 and 0.46 with an average value of 0.43. The following values will be used in Eq. (4):- $C_D = 0.43$, $\rho = 5 \times 10^{-4}$ gm/cc, $\sigma = 0.9$ gm/cc, $g = 980$ cm/sec^2. The air density and drag coefficient have been taken to represent conditions in the upper troposphere, where the maximum updraught is usually situated. It is to be noted that this value of the drag coefficient is applicable to spherical hailstones. Large stones often have protuberances and tend to be of a more oblate spheroidal shape, which results in increased air resistance. However, in the British Isles, hail with a radius greater than about 1 cm. is rare. Even in the case of larger stones, this assumption of a sphere is probably not inconsistent with the accuracy of the other approximations and assumptions which have been made.

Substituting these values into Eq. (4), we obtain:-

$$r \simeq 9 \times 10^{-8} V^2 \qquad - (5a)$$

where V is measured in cm/sec and r in cm.

On the basis of Ludlam's investigations, we now equate the terminal velocity of the largest hailstones (radius r_{max}) to the maximum speed in the updraught (U_{max}). Thus:-

$$r_{max} \simeq 9 \times 10^{-4} U^2_{max} \qquad - (5b)$$

where U_{max} is measured in m/sec and r_{max} in cm, or alternatively:-

$$r \simeq 9 \times 10^{-4} E_{max} \qquad - (5c)$$

where E_{max} is the maximum kinetic energy acquired by unit mass of air in the updraught. r_{max} is measured in cm. and E_{max} in joules/kg (j/kg). If E_{max} is

/calculated

calculated using parcel theory, the maximum size of hail may then be obtained from Eq. (5c). Thus, the radius will be proportional to the maximum kinetic energy per unit mass in the updraught. In this report, the energies will be expressed in units of j/kg, which is the same numerically as the square of the vertical velocity, if the velocity is measured in m/sec. If, for example, E_{max} = 400 j/kg, U_{max} = 20 m/sec. Table I shows E_{max} and r_{max} for selected values of U_{max}.

Two methods for forecasting the maximum size of hail have been developed in the United States by Fawbush and Miller [22] and Foster and Bates [23]. Remarkable claims have been made for the success of their predictions, which use parcel theory as a basis for calculating the updraught speed in the region of hail growth (taken as the -5°C or -10°C level). The methods are essentially

TABLE I:- Relationship between the maximum velocity and energy in the updraught and the maximum size of hail.

U_{max} m/sec	E_{max} Joules/kg	r_{max} cm
10	100	0.09
20	400	0.36
30	900	0.82
40	1600	1.46
50	2500	2.27

similar to the procedure described above, except that Fawbush and Miller applied empirical adjustments to obtain the best overall forecasts of hail size. Also, the maximum vertical velocity is not used; instead the value at a fixed level fairly low in the cloud is calculated. There is likely to be a close correlation, however, between the vertical velocities at different levels, so that the results may be comparable with those of the scheme described above.

Severe storms occur relatively frequently in the parts of the USA where these techniques have been successfully applied, and the instabilities associated with these storms are correspondingly much greater than the typical values experienced in this country. Ludlam [16] emphasised that it is the occurrence

/of

of small hail which is most difficult to forecast, because the required vertical velocities can be generated with an updraught temperature excess of about 1°C. This temperature difference is of the same order as the accuracy of the radiosonde temperature soundings. It may be difficult, therefore, to distinguish between those occasions when small hail occurs and when no storms develop. Alternatively, the updraughts associated with large hail are generated by temperature excesses of several centigrade degrees and the same uncertainty in the temperature sounding has a proportionally smaller effect on the forecast hail size.

4. The calculation of the maximum kinetic energy, E_{max}

It was shown in the preceding section that a forecast of the likely severity of storms (expressed in this instance in terms of maximum hail size) may be made on the basis of the energy acquired by a parcel during adiabatic ascent.

The evaluation of the energy on a tephigram is tedious and rather imprecise. Also, subjective estimates of the changes in the conditions during the forecast period are often not sufficiently accurate for this type of analysis. The solution to this problem appeared to depend on the development of a satisfactory objective method for calculating the energy. The technique should clearly be capable of making use of the numerically forecast fields of temperature and humidity, which will eventually be available from the type of model developed by Bushby and Timpson.

The vertical temperature profile in the environment may be specified either in terms of temperatures at a number of discrete levels, or as values of partial thickness between various pressure levels. There are certain advantages in using the latter. Thickness measures the mean temperature through a certain layer of the atmosphere, and so takes account of the detailed fluctuations of temperature in the vertical. The temperature at a particular height may be unrepresentative of conditions both above and below that level. Also, temperature is not forecast explicitly by numerical models of the type developed by Bushby and Timpson, whereas thickness is.

Although the size of the largest hail has been related to the maximum speed in the updraught, it must be remembered that at heights where the temperature is below about -40°C (Schaefer point), the cloud consists entirely of ice particles. The growth of hail by accretion ceases when the stone enters this zone. The

/size

size depends, therefore, on the maximum updraught in the supercooled region, which extends from cloud base up to the -40°C level. Over the British Isles, in summer, the temperature at 300 mb is usually close to -40°C, so that the available energy above about 300 mb should not be included in E_{max}. It seemed appropriate to calculate the energy released during the adiabatic ascent of a parcel from the 850 mb level to 300 mb. This energy is identified with E_{max} in Eq. (5c). A convenient method of specifying conditions in the environment is in terms of the partial thicknesses between the following standard pressure levels:- 850, 700, 500 and 300 mb.

Let E_1, E_2 and E_3 be the available energies within the layers 850-700 mb, 700-500 mb. and 500-300 mb. respectively. This is shown diagramatically in Fig. 2. The following rules were formulated for calculating E_{max}:-

1. If the partial energies E_1, E_2 and E_3 are all positive, E_{max} is simply the sum of these quantities.

2. If there are both positive and negative energy contributions from E_1, E_2 and E_3, E_{max} is obtained by summing only the positive contributions. This situation usually occurs when either E_3 or both E_2 and E_3 are negative, and implies that the maximum updraught is below the 500 mb. level. It is realised that if the sign of the temperature excess reverses within a layer, the maximum energy, which occurs at the level of zero temperature excess, will be underestimated. This is not thought to be serious in the vast majority of cases, considering the accuracy of the other assumptions and approximations.

3. If E_1, E_2 and E_3 are all negative, E_{max} is identified with the least negative of these quantities (usually E_1). E_{max} now serves as a measure of the stability of the ascent.

There is often a forced component of vertical motion in a storm, due to the horizontal inflow of potentially warm air. The presence of wind shear in the vertical provides suitable conditions for this relative inflow to occur at low levels, and in extreme situations may contribute substantially to the updraught. In the majority of cases, the kinetic energy resulting from the relative horizontal motion is small in comparison with that generated by the buoyancy forces and the effect was neglected in this investigation.

/Consider

Consider, now, the kinetic energy acquired by a parcel during adiabatic ascent through the layer between the pressure levels p_o and p_1 mb. ($p_o > p_1$). Let ΔT be the temperature excess of the parcel relative to the environment, S the thickness of the layer and E the kinetic energy acquired by the parcel during ascent through the layer.

The instantaneous vertical acceleration of the parcel is, from Eq. (3):-

$$\frac{dw}{dt} = g \frac{T-T^1}{T^1} = g \frac{\Delta T}{T^1}$$

Hence, the mean acceleration of the parcel ($\bar{w}$) is given approximately by:-

$$\bar{w} = g \frac{\overline{\Delta T}}{\overline{T^1}}$$

where the bar denotes the mean value through the layer. Therefore:-

$$E = \frac{2 g \overline{\Delta T} S}{\overline{T^1}}$$

Now by applying the Gas equation to an atmosphere in hydrostatic equilibrium, we obtain an expression for the thickness of the layer in terms of its mean temperature:-

$$S = \frac{\overline{RT^1}}{g} \log_e \left(\frac{p_o}{p_1}\right) \qquad - (6)$$

where R is the gas constant for dry air.

$\therefore$ $E = 2R \log_e \left(\frac{p_o}{p_1}\right) \overline{\Delta T}$

or $\underline{E = k \overline{\Delta T}}$ - (7)

where $k = 2R \log_e \left(\frac{p_o}{p_1}\right)$

If R is measured in units of j/kg/°C, E is given in j/kg by Eq. (7). Now R = 287.0 j/kg/°C. Hence the values of k for the three layers used in this work are:-

$p_o - p_1$ (MB)	k (J/KG/°C)
850-700	111.3
700-500	193.2
500-300	293.0

The gain in the kinetic energy of the parcel within each of the layers may be calculated by substituting the above values of k into Eq. (7). The mean temperature excess in the updraught ($\overline{\Delta T}$) is determined by the thickness of the layer and the wet-bulb potential temperature of the ascending parcel (θ_{wp}). If the thickness is known, the mean temperature of the environment can be calculated

/from

from Eq. (6). There is no simple expression relating the mean dry-bulb temperature of the parcel to θ_{wp}; the easiest method of specifying the relationship is in terms of selected values read from a tephigram.

The effect of water vapour on air density has been ignored, so far. It is necessary to work in terms of virtual temperature to take account of the reduction in density when water vapour is present. Upper-air thicknesses are evaluated from virtual temperatures, so it is only necessary to correct the dry-bulb temperature of the ascending parcel. Virtual temperature is related to the dry-bulb temperature by the approximate expression:-

$$T_v - T \approx 0.61\, rT \qquad - (8)$$

where T_v is the virtual temperature of the air (^oA)

T is the dry-bulb temperature (^oA)

and r is the mixing ratio of water vapour in grams per gram of dry air.

Above the condensation level, the ascending parcel is always close to saturation, so that in Eq. (8) r may be replaced by r_s, the saturated mixing ratio. The mean value of r_s within a layer can be determined on a tephigram for any particular wet-bulb potential temperature, and the appropriate temperature correction calculated from Eq. (8). It seemed unnecessary, at least initially, to include corrections for the effect on the buoyancy of the weight of condensed water and the release of latent heat of fusion. The inclusion of these factors would require basic assumptions to be made concerning the proportion of the condensed water that is carried with the parcel and the proportion that is eventually frozen. Ludlam [16] did not consider that these refinements were necessary in a first approach, especially since the two effects tend to cancel out if the cloud reaches the glaciation level.

5. Practical details on the preparation and verification of the forecasts

The theoretical considerations of the preceding sections provide a basis for a practical method of forecasting hail and thunderstorms. Practical details, such as the forecast area and the method of checking the forecasts will be described in this section.

Forecast area. The area for which the forecasts were to be prepared is shown in Fig. 3. It seemed advisable to restrict the investigation to a relatively small region, since the value of the forecasts is reduced considerably if they

/are

are made in general terms for a very large area. S.E. England was selected for three reasons:

(a) There is a good coverage of synoptic and climatological observing stations in S.E. England. In the period 1958-1962, reports from 72 stations were available and this was increased to 104 stations in 1963 and 1964.

(b) The Crawley and Hemsby radio-sonde stations are well situated for the determination of representative upper-air conditions over the area.

(c) The overall frequency and intensity of storms is higher in this area than in any other region of the British Isles.

To see how the apparent skill of the forecasts depended on the size of the area, S.E. England was sub-divided as shown in Fig. 3. Forecasts were prepared for area B and for the combined area, A and B. The predictions for area B, which corresponds roughly to the CFO definition of the S.E. region, were based on Crawley upper-air data, while those for the combined area were based on the mean of the Crawley and Hemsby ascents.

Period of the investigation. The investigation was confined to the forecasting of hail and thunder during the months May to September inclusive. Statistics given by Atkinson (24) for the occurrence of thunder over S.E. England show that approximately 75% of the outbreaks occur during these five months of the year. Forecasts were to be prepared on a daily basis over this period. The forecasting rules were formulated using data from 1960-1962. These criteria were then tested on independent data for the years 1958-1959 and 1963-1964.

Time of validity of the forecasts. The occurrence of hail and thunder undergoes a marked diurnal variation, especially at inland stations. Miller and Starrett [25] produced a diagram portraying the isochrones of maximum thunderstorm activity in Great Britain. In S.E. England, the maximum occurs between about 1200 GMT and 1900 GMT depending on the location. There is also a much smaller secondary maximum which occurs, again depending on location, between 2000 GMT and 0400 GMT. The diurnal minimum of thunderstorm activity is at about 0700 GMT.

The greatest difficulty is experienced in the preparation of the forecast for the daytime period, when the activity is greatest, based on data for 0000 GMT and 0600 GMT. This forecast usually has to be issued before any storms have developed. It was decided that two different verifying periods should be used:- 0600-1800 GMT and 0600-2400 GMT. The "start" time of 0600 GMT was chosen because it is

/near

near the time of the diurnal minimum of storms, so that the results are least likely to be affected by decaying storms which have lingered on from the previous day. It also seemed advisable to base the investigation on the mid-day ascents rather than attempt to predict the values of the parameters or use the midnight soundings. This implies that the various predictors can be forecast accurately, but it avoids obscuring the physical relationships because of errors in the predictors themselves.

Verification of the forecasts. The records of the synoptic and climatological stations in the forecast area were examined and reports of hail or thunderstorms were noted, together with the time of occurrence. In cases where hail was actually observed, the maximum size of the stones was recorded. The SFLOC reports were also analysed and were regarded as equivalent to a direct observation of a thunderstorm.

The weather for a particular area and verifying period was recorded by a simple two-character code which is defined as follows:-

X denotes that there were no reports of hail, thunderstorms or SFLOCS.

H denotes that there was at least one report of hail, either with or without reports of thunderstorms and SFLOCS.

T denotes that there was at least one report of a thunderstorm or SFLOC with no reports of hail.

Ice pellets were regarded as a form of hail. The code letters H and T are followed by a digit, n, representing the total number of thunderstorm and SFLOC reports. The 7-point scale for n is given in Table 2.

TABLE 2:- Code for total number of thunderstorms and SFLOCS

Code n	Total number of thunderstorms/SFLOCS
0	0*
1	1
2	2-4
3	5-19
4	20-39
5	40-99
6	≥ 100

*Only occurs in conjunction with the symbol H.

/The

The limits for each value of n were not defined from strict statistical considerations, but were founded on a subjective assessment of the most useful type of classification. In general, as n increases the number of cases within that category will tend to decrease, so that days with the highest value of n may number only one or two in a summer. It was not considered worthwhile to specify the number of individual hail reports in the code. Hail was observed at only one or two stations on most hail days, and days with more than six reports were rare.

This type of classification is much more informative than a simple statement of whether the phenomenon did or did not occur. The code indicates how widespread the outbreaks were, which in turn is likely to give a measure of the general severity of the storms. The above classification is used on the diagrams in this report.

Comparison with other forecasting techniques. The usefulness of any new technique must be judged in relation to the success already achieved by the established forecasting methods. A fair comparison requires an objective assessment of the skill shown by the different techniques under identical conditions. Saunders [18, 26] has reported on tests of various methods for forecasting hail and thunderstorms, which were carried out in the Manby Group of stations during the summers of 1965 and 1966. None of the techniques quite reached the standard achieved by forecasters using "general practice" methods. The tests indicated that the stability indices devised by Rackliff [27] and Boyden [28] are the most useful aids currently available. These two indices serve as a standard for assessing any new technique. The results were also compared with two indices which were claimed by Jefferson [29, 3] to be an improvement on the Rackliff index. These four indices are defined as follows:-

Rackliff index (ΔT) : $\Delta T = \theta_{w900} - T_{500}$.

Boyden index (I) : $I = Z - T - 200$.

Jefferson index (T_J) : $T_J = 1.6\,\theta_{w900} - T_{500} - 11$.

Modified Jefferson index (T_{MJ}) : $T_{MJ} = 1.6\,\theta_{w900} - T_{500} - \frac{1}{2} T_{D700} - 8$.

/where

where Θ_{W900} is the 900 mb. wet-bulb potential temperature,

T_{500} is the 500 mb. dry-bulb temperature,

Z is the 1000-700 mb. thickness in dekametres,

T is the 700 mb. temperature (^{o}C), and

T_{D700} is the dew-point depression in ^{o}C at 700 mb.

6. Calculation of the partial energies on the computer.

The available energy between 850 and 300 mb. may readily be calculated on the computer, using the method outlined in section 4. Hand calculations on seven years' data for both individual and meaned ascents would have resulted in a very slow and tedious analysis process. The upper-air observations from Crawley and Hemsby were available on magnetic tape for the whole of the seven-year period covered by this investigation.

A programme was written to calculate the partial energies, using temperatures and humidities either from a single ascent or from the mean of two separate soundings. Eq. (7) gives the kinetic energy, E, acquired by a parcel during ascent through a particular layer of the atmosphere:-

i.e. $E = k\,\overline{\Delta T}$

or $E = k\,(\overline{T} - \overline{T^{1}})$ - (9)

where $\overline{T}$ and $\overline{T^{1}}$ are the mean temperatures of the parcel and environment respectively. The value of k for each of the layers has already been derived in section 4. The programme utilised Eq. (6) to evaluate $\overline{T^{1}}$ from the thickness of the layer, S. The mean temperature of the parcel, $\overline{T}$, and the corresponding virtual temperature correction were interpolated from tables expressing these quantities as a function of the parcel wet-bulb potential temperature (Θ_{wp}). These tables were originally derived from careful measurements made on a tephigram. It now only remains to discuss the method for determining Θ_{wp}.

The air entering the updraught mainly originates in the lowest kilometre or so of the atmosphere. Consequently, Θ_{wp} depends on the average conditions which exist from the surface up to about the 900 mb. level. However, the wet-bulb potential temperature of the air near the ground is influenced by local surface features and by non-adiabatic radiation effects. The incoming solar radiation during the daytime, and the outgoing terrestrial radiation at night cause a marked diurnal fluctuation in the observed values of temperature and humidity, below about the 900 mb. level. Current numerical forecasting models can only take account of

/these

these boundary effects through a simple empirical approach, so that the predictions of the wet-bulb potential temperature, in the lowest layers, are likely to be much less accurate than in the free atmosphere.

It was decided, therefore, that θ_{wp} should be determined from the temperature and humidity at 900 mb., because this level is fairly representative of conditions in the lowest layer but is not affected markedly by the factors discussed above. The 900 mb. wet-bulb potential temperature (θ_{w900}) was interpolated from a table expressing this quantity as a function of the temperature and humidity mixing ratio. Observations show that θ_{w900} is usually lower than the average wet-bulb potential temperature between 900 mb. and the surface. A correction was applied to θ_{w900} to compensate for this systematic difference. Thus:-

$$\theta_{wp} = \theta_{w900} + C \qquad - (10)$$

where C is an empirical constant.

C was determined from a statistical analysis of 1200 GMT Crawley and Hemsby upper-air data for the years 1960 and 1961 (May-September). The results are summarised in Table 3 for various groups of weather categories:

TABLE 3: Relationship between the wet-bulb potential temps. at the surface, 950 mb. and 900 mb. (May-Sept. 1960-1961)

Weather classification area A+B 0600-1800 GMT	Average wet-bulb potential temperature Mean of Crawley and Hemsby (1200 GMT)				Mean-θ_{w900}
	Surf θ_{wsur} (°C)	950 mb θ_{w950} (°C)	900 mb θ_{w900} (°C)	$\theta_{wsur}+\theta_{w950}+\theta_{w900}/3$ (°C)	(°C)
H0-H6	10.3	8.5	7.9	8.9	1.0
T2-T6	14.1	12.5	12.0	12.9	0.9
T1	15.2	13.1	12.7	13.7	1.0
X	12.7	10.8	10.5	11.3	0.8

θ_{w900} was compared with the mean of the wet-bulb potential temperatures at the surface, 950 mb. and 900 mb. Table 3 shows that the difference between the mean wet-bulb potential temperature and the value at 900 mb. did not depend particularly on whether the day was a "convection day". Therefore θ_{wp} was determined from

/Eq.

Eq. (10) with C = 1.0°C. After calculating the available energy for each of the three layers the programme computed E_{max}, following the rules laid down in section 4, and finally printed out the values of θ_{wp}, E_1, E_2, E_3 and E_{max}.

7. The development of the forecasting scheme.

The aim of this investigation was to relate the occurrence and severity of hail and thunderstorms with the maximum kinetic energy, as defined above, acquired by a parcel during adiabatic ascent. Since the vast majority of hail that falls in this country is less than 1 cm. in diameter, the size of the hail is not, in general, a particularly useful indicator of the severity of the storms. It was mentioned, in section 5, that the total number of reports of thunderstorms and SFLOCS may be taken as a rough measure of the severity of the outbreaks. The forecasting of hail size will be considered again, later in the report.

The criteria for forecasting storms were based on an analysis of actual (1200 GMT) upper-air data, for each day during the period May-September 1960-1962. The procedure for preparing and verifying the "forecasts" has already been described. Rules were initially developed for forecasting storms over area B (see Fig. 3) and similar techniques were then applied to the combined area (A+B). The methods adopted for the small and large areas were identical, apart from minor differences in the critical values of the predictors and the use of meaned ascents in the case of the combined area. The criteria were determined on the basis of the weather during the period 0600-1800 GMT, which includes the time of the diurnal maximum of storms for most of S.E. England. The relationship between the occurrence and intensity of storms and the available energy is likely to be most clearly defined for this interval, centred on the time of the midday upper-air ascent. Results for the period 0600-2400 GMT are complicated by the changes occurring in the conditions between midday and midnight, and by the migration of storms from the Continent.

a) Analysis for area B

The upper-air observations from the 1200 GMT Crawley ascent were taken to be representative of conditions over area B, during the period 0600-1800 GMT. The partial energies and the maximum kinetic energy were calculated on the computer, following the procedure described in the previous section.

/The

The first step in the analysis was the determination of the minimum value of E_{max} for which there was a significant probability of storms. The distribution of occasions of hail and thunder as a function of E_{max} is recorded in Table 4. The results show clearly the broad relationship which exists between the occurrence of storms and the available energy. It was decided, from these statistics, to exclude the possibility of a positive forecast of hail or thunder whenever E_{max} was less than -200 j/kg. The table shows that, on such days, the probability of hail, or more than a single report of thunder, was only 4%. Also, there was not a single occasion of widespread storms (defined as days with $n > 3$) in the 177 days with values of E_{max} below this limit. The probability of storms did not show any significant change over the range of E_{max} from -200 to -400 j/kg. Days with E_{max} less than -200 j/kg. were classified as cases of "large negative energy" (LN). This category was identified with a definite forecast of no hail or thunder.

The production of hail and according to most theories, the development of thunderstorm electricity demand the presence of the ice phase in the cloud. Therefore, it is also necessary to consider whether the convection will extend sufficiently far above the freezing level for ice particles to form. The vast majority of natural freezing nuclei do not become active until the water droplets are cooled below about -10°C. Dorsch and Hacker [30] found that supercooled water droplets did not freeze spontaneously at a unique temperature. On average, the larger drops were observed to freeze at higher temperatures, but there was a wide range of temperature at which spontaneous freezing occurred for a given droplet size. Findeisen and Schulz [31] investigated the formation of ice crystals in expansion chambers. They demonstrated that the rate of cooling at the time of cloud formation was important in determining the temperature at which significant numbers of ice particles first formed. Both these experiments indicated that significant concentrations of ice crystals are unlikely to form in a growing cumulus unless the top reaches a level where the temperature is between about -10°C and -18°C. In the period from May to September, the average Crawley upper-air temperatures at 700 and 500 mb. are -2°C and -17°C, respectively (mean of 0300 and 1500 GMT ascents for the years 1951-1955 inclusive). The growth of a cumulus cloud to the glaciation level is likely to depend strongly on the

/available

TABLE 4:- RELATIONSHIP BETWEEN E_{MAX} (CRAWLEY 1200 G.M.T. ASCENT) AND THE WEATHER IN AREA B (0600-1800 G.M.T.) PERIOD MAY-SEPT 1960-62

(a) NUMBER OF DAYS WITH E_{MAX} (CRAWLEY 1200 G.M.T ASCENT) BETWEEN SPECIFIED LIMITS FOR VARIOUS WEATHER CATEGORIES (AREA B 0600-1800 G.M.T.)

WEATHER CLASSIFICATION AREA B 0600-1800 G.M.T.	E_{MAX} (JOULES/KG)																			
	≤-500	-499 TO -450	-449 TO -400	-399 TO -350	-349 TO -300	-299 TO -250	-249 TO -200	-199 TO -150	-149 TO -100	-99 TO -50	-49 TO 0	+1 TO 50	51 TO 100	101 TO 150	151 TO 200	201 TO 250	251 TO 300	301 TO 350	351 TO 400	401 TO 450	451 TO 500	>500
X	62	10	13	17	20	12	31	26	20	25	19	29	18	12	6	2	2	1	0	0	0	4
T1	1	1	0	1	0	1	1	2	1	6	1	5	2	4	1	0	0	0	1	1	0	0
T2-T6/H2-H6	1	0	0	2	2	0	3	4	4	6	8	9	9	13	9	3	4	4	4	2	2	7
TOTAL	64	11	13	20	22	13	35	32	25	37	28	43	29	29	16	5	6	5	4	3	2	11
T4-T6/H4-H6	0	0	0	0	0	0	0	1	1	3	4	3	4	8	3	0	1	3	2	1	2	5

(b) NUMBER OF DAYS WITH E_{MAX} (CRAWLEY 1200 G.M.T. ASCENT) BELOW SPECIFIED LIMITS FOR VARIOUS WEATHER CATEGORIES (AREA B 0600-1800 G.M.T.)

WEATHER CLASSIFICATION AREA B 0600-1800 G.M.T.	E_{MAX} (JOULES/KG)																				WHOLE RANGE
	≤-500	≤-450	≤-400	≤-350	≤-300	≤-250	≤-200	≤-150	≤-100	≤-50	≤0	≤50	≤100	≤150	≤200	≤250	≤300	≤350	≤400	≤450	≤500	
X	62	72	85	102	122	134	165	191	211	236	255	284	302	314	320	322	324	325	325	325	325	329
%	(97)	(96)	(97)	(94)	(94)	(94)	(93)	(91)	(90)	(87)	(88)	(83)	(81)	(79)	(77)	(76)	(76)	(75)	(74)	(74)	(74)	(73)
T1	1	2	2	3	3	4	5	7	8	14	15	20	22	27	27	27	27	27	27	28	28	28
%	(2)	(3)	(2)	(3)	(2)	(3)	(3)	(3)	(3)	(5)	(5)	(6)	(6)	(7)	(6)	(6)	(6)	(6)	(6)	(6)	(6)	(6)
T2-T6/H2-H6	1	1	1	3	5	5	8	12	16	22	30	39	48	61	70	75	77	81	85	87	89	96
%	(2)	(1)	(1)	(3)	(4)	(3)	(4)	(6)	(7)	(8)	(10)	(11)	(13)	(15)	(17)	(17)	(18)	(19)	(19)	(20)	(20)	(21)
TOTAL	64	75	88	108	130	143	178	210	235	272	300	343	372	401	417	424	428	433	437	440	442	453
T4-T6/H4-H6	0	0	0	0	0	0	0	1	2	5	9	12	16	24	27	27	28	31	33	34	36	41
%	(0)	(0)	(0)	(0)	(0)	(0)	(0)	(0)	(1)	(2)	(3)	(3)	(4)	(6)	(6)	(6)	(7)	(7)	(8)	(8)	(8)	(9)

BRACKETED FIGURES ARE THE PERCENTAGES OF THE TOTAL

available energy between the 700 and 500 mb. levels (i.e. E_2).

A diagram was plotted (Fig. 4) showing the weather category for area B, as a function of E_2 and Θ_{wp}. Cases of large negative energy (LN) were omitted from this diagram, but the weather for the remaining days was plotted, using the code defined in section 5. When E_3 is positive, ascent well above the freezing level is likely to occur, irrespective of the value of E_2. These cases are included within square brackets in Fig.4. The intention was to determine for any given Θ_{wp}, the critical value of E_2 which was necessary for the occurrence of hail and thunder. However, the total available energy, E_{max}, is an equally important factor controlling the development of storms; in particular, it seemed probable that E_{max} must also exceed a certain threshold for vigorous convection to be initiated. To enable these two factors to be considered in conjunction, E_{max} was plotted adjacent to the weather symbols on the original working diagram.

Careful examination of the data indicated that the critical relationship between E_2 and Θ_{wp} was of the form given by the curve in Fig.4, with a threshold value for E_{max} of 30 j/kg. The areas to the left and right of the curve will be referred to, respectively, as the "cold" and "warm" zones. The term "cold" is used in the sense that the values of E_2 and Θ_{wp} are consistent with the convection extending to levels where the temperature is low enough for substantial concentrations of ice particles to form. When E_3 is positive, this requirement is likely to be satisfied, irrespective of Fig.4. These occasions were automatically classified as cold zone cases, and were disregarded in the analysis of the critical curve. Table 5 summarises the weather for the cold zone cases, as a function of E_{max}.

It was impracticable to reproduce the values of E_{max} with the weather symbols in Fig.4. Consequently, the diagram does not show clearly the critical relationship between E_2 and Θ_{wp}, because days with E_{max} both above and below the threshold of 30 j/kg. are included. Fig.5 is similar to Fig.4, except that the diagram is restricted to those occasions when E_{max} exceeded the threshold value. The distinction between the cold and warm zones is shown more clearly on this diagram; the corresponding statistical summary is given in Table 6.

/TABLE

TABLE 5:- Summary of the weather categories for the cold zone cases as a function of E_{max}.
Crawley 1200 GMT ascent. Area B (0600-1800 GMT).
Period May-Sept. 1960-1962.

E_{max} Joules/kg	Number of days in weather category	
	x	Ho-H6 T1-T6
<0	38	5
0-9	0	1
10-19	4	0
20-29	1	1
30-39	1	2
40-49	1	1
50-59	1	1
⩾60	13	54

TABLE 6:- Summary of the weather categories for the cold and warm zones for days with $E_{max} \geqslant 30$ j/kg.
Crawley 1200 GMT ascent. Area B (0600-1800 GMT)
Period May-Sept. 1960-1962.

Zone	Number of days in weather category		
	x	T1	Ho-H6 T2-T6
Cold zone	16	4	54
Warm zone	43	5	7

Cold zone cases with E_{max} greater than or equal to 30 j/kg. were classified as days of "large positive energy" (LP). On these occasions there is sufficient instability to initiate convection and the cloud should reach the glaciation level unhindered, providing there are no other factors to inhibit their development. Hail or thunder were observed on about 80% of these days.

In general, the temperature at the equilibrium level is not determined uniquely by θ_{wp} and the partial energies. However, on the assumption that the environment temperature varies linearly with pressure between 700 and 500 mb., the equilibrium temperature (T_E) may be evaluated for the particular case when the critical value of E_2 is zero. In Fig.4, the curve intercepts the θ_{wp} axis at

/o

θ_{wp} = 14.1°C. It is readily shown on a tephigram that the corresponding value of T_E is approximately -10°C. T_E will be lower, of course, if E_2 exceeds the critical value, and vice versa.

It was indicated previously that significant concentrations of ice particles are unlikely to form in a growing cumulus cloud unless the top extends, at least, to the -10°C level. The inference is that glaciation and the subsequent development of hail and thunder are improbable unless E_2 exceeds the critical values defined by the curve in Figs. 4 and 5. When the air is cold, storms may occur with large negative values of available energy between 700 and 500 mb. Conversely, in very warm air masses, storms may not develop even when the energy contribution from this layer is positive.

A consequence of glaciation that has not been stressed is the additional buoyancy which results from the release of latent heat of fusion. This source of energy was excluded from the calculations for the reasons given in section 4. However, rapid growth of the cloud is often observed immediately after the onset of glaciation, this usually being the critical stage in the development of an active cumulonimbus. The result is the accentuation of the importance of the critical energy level in the middle layer.

Although the majority of storms are associated with the large positive energy (LP) category, it is clear that a significant proportion is included within the warm zone in Fig.4. Other processes must be considered to account for these outbreaks, especially as E_{max} is negative in many instances. A study of the data revealed a tendency for warm zone storms to occur with positive or small negative values of (E_2-E_1). This is not surprising since large negative values of (E_2-E_1) imply the presence of a much-reduced lapse rate, in the vicinity of the 700 mb. level. Fig.6 shows the weather category for the warm zone cases as a function of (E_2-E_1) and θ_{wp}. The diagram was sub-divided into two areas. In the area below the line, the probability of hail or more than a single thunderstorm report was under 6% on any given day. Days included in this area were classified as "warm stable type" (WST), this category being identified with a definite forecast of no hail or thunder. Above the line, storms occurred on about 50% of the days, so that other factors must be considered before a definite forecast can be made. These cases were classified as "unstable type" (UT). Table 7 summarise the weather for both

/these

these categories.

TABLE 7:- Summary of the weather categories for the WST and UT cases in Fig.6. Crawley 1200 GMT ascent. Area B (0600-1800 GMT). Period May-Sept 1960-1962.

Classification	Number of days in weather category		
	x	T1	Ho-H6 T2-T6
WST	89	8	6
UT	34	10	24

The parameter (E_2-E_1) is basically similar to the predictor $\Delta_{\Delta h}$ used by Hanssen [32] in his objective method for forecasting thunderstorms. $\Delta_{\Delta h}$ was defined as the 1000-700 mb. thickness minus the 700-500 mb. thickness.

The cold zone cases with E_{max} less than the threshold of 30 j/kg. were analysed in a similar manner. As with the warm zone thunderstorms, other processes apart from the direct release of latent instability are likely to be involved in the development of these storms. The weather for those cold zone cases with E_{max} less than 30 j/kg. is plotted in Fig.7, as a function of (E_2-E_1) and θ_{wp}. Although it was difficult to draw definite conclusions from such a small number of cases, the diagram was tentatively divided into two areas. Cases below the line were classified as "cold stable type" (CST), a category analogous to the warm stable type of Fig.6. The few cases above the line were incorporated in the unstable type (UT) category, along with those from Fig.6. Approximately half of the occasions included in the latter category were associated with hail or thunder.

Storms associated with UT category are not explicable simply in terms of the available energy at 1200 GMT. Forecasters have recognised for a long time that convection is enhanced when the sea-level isobars are curved cyclonically. Petterssen [9] noted that there is a close association between the occurrence of subsidence, which is a stabilising process, and the existence of anticyclonic vorticity in the free atmosphere. Their investigation established that deep convection (defined as cases when the cloud tops extend to or above the 600 mb. level) is very strongly linked with cyclonic vorticity at the 750 mb. level.

/Atkinson

Atkinson [24], in his analysis of thunder outbreaks over S.E. England, produced statistics showing that under 10% of the non-frontal storms occur with anticyclonic curvature of the surface isobars. The outbreaks in these anticyclonic airstreams are usually small and located on the edge of the high-pressure system. Therefore, cyclonic vorticities are probably associated with areas where there is ascent by convergence, and on unstable type days this process is likely to result in the development of lapse rates favourable for deep convection on the basis of the energy criteria.

The geostrophic vorticity (ζ) is given by:-

$$\zeta = \frac{g}{f} \nabla^2 h \qquad - (11)$$

where f is the Coriolis parameter and h is the contour height. The Laplacian in Eq. (11) may be evaluated from the working analyses, using the finite difference grid shown in Fig.8. The distance from the central grid point to each of the four surrounding points was 300 n.mi. This grid length was chosen as the value most appropriate to the scale of troughs and other synoptic features which are known to favour the development of storms. The finite-difference form of the Laplacian is:-

$$\nabla^2 h = \frac{h_A + h_B + h_C + h_D - 4\,h_o}{a^2} \qquad - (12)$$

where a is the grid-length. For comparative purposes, it is only necessary to calculate the value of the numerator on the right-hand side of Eq. (12); this quantity will be referred to as the vorticity index (I). Thus:-

$$I = h_A + h_B + h_C + h_D - 4\,h_o$$

where the heights are measured in dekametres. To avoid unnecessary conversions, the vorticity index at the surface (I_s) was defined in terms of the surface pressure (p). Thus:-

$$I_s = p_A + p_B + p_C + p_D - 4\,p_o$$

where the pressures are measured in millibars. Positive indices denote cyclonic geostrophic vorticity.

The vorticity indices at the surface, 700 and 500 mb. were evaluated from the 1200 GMT analyses for all the days included in the unstable type (UT) category. Examination of the results indicated that the vorticities at the surface and 700 mb. were most effective in separating out the days of hail and thunder. Fig.9 is a

/diagram

diagram of the weather categories for the UT days as a function of the vorticity indices at these two levels. There was a marked preference for hail and thunder when the indices were both positive. The diagram was sub-divided, the areas above and below the line being classified as the positive (UT+) and negative (UT-) zones, respectively. The weather categories for the two areas are summarised in Table 8.

TABLE 8:- Summary of the weather categories for the UT+ and UT- cases. Crawley 1200 GMT ascent.
Area B (0600-1800 GMT). Period May-Sept 1960-1962.

Classification	Number of days in weather category		
	x	T1	H0-H6 T2-T6
UT-	26	5	3
UT+	11	5	24

Days in the UT- category were identified with a definite forecast of no hail or thunder.

Fig.9 shows that the widespread occurrence of hail and thunder is unlikely on days in the unstable type category, unless there is cyclonic vorticity at the surface or at 700 mb. In the majority of the large positive energy (LP) cases, storms may be expected to develop freely, even in situations of weak anticyclonic vorticity. However, their development may still be inhibited by dynamical effects, if there is pronounced anticyclonic vorticity in the lower troposphere. The weather for the days in the large positive energy (LP) category is plotted in Fig.10, as a function of the 1200 GMT vorticity indices at the surface and 700 mb. This diagram is consistent with the ideas just put forward; in particular, the most striking difference from Fig. 9 is in the considerable number of hail and thunder cases which are associated with small negative values of I_s. Nevertheless, there is some evidence in the diagram that storm development is hindered by large negative vorticity indices, and a tentative division was made. The areas above and below the line were classified as the positive (LP+) and negative (LP-) zones, respectively. Days in the LP- category were identified with a definite forecast of no hail or thunder.

Table 4 shows that there were 13 days in the large negative energy (LN)

/category

category on which hail or thunder were recorded. It seems certain that dynamical processes must be responsible for initiating the convection under these circumstances, as with the unstable type cases. Examination of the data suggested that it would be useful to define a new category to include those LN cases where (E_2-E_1) was positive and the vorticity indices were in the positive zone in Fig.9. Under these conditions, although the stratification is very stable for a parcel ascending from near the surface, convection may be triggered off in the lower troposphere by dynamical causes. This additional category will be referred to as the "unstable large negative energy" (ULN) category.

This almost completes the description of the forecasting scheme and the procedure is summarised in the form of a flow diagram in Fig.11. A positive forecast of hail and thunder is only possible for three of the categories (LP+, UT+, ULN). The scheme has been designed to take account, in a realistic way, of the main physical processes that are involved in the development of hail and thunderstorms.

Another important consideration concerns the extent to which the growth of a cumulonimbus cloud is inhibited by the presence of dry air aloft. If the environment is dry, the buoyancy of the cloudy air will be destroyed rapidly by turbulent mixing and the consequent evaporative cooling. This may be the reason why clouds sometimes remain quite shallow, although the air is unstable through a deep layer. The effect will be most pronounced in the early stages of development, because, as the cloud grows, the updraught becomes shielded from the environment by the decaying outer portions of the cloud. Faust [33] proposed a measure of instability known as "potential evaporation instability" which takes account of the humidity aloft. More recently, Jefferson [3] has shown how the variations in the mid-level moisture may be represented in a simple instability index. However, neither of these techniques has demonstrated any superiority over other methods which disregard the humidity profile. Hanssen [32] used the sum of the saturation deficits at 850 and 700 mb. as one of the parameters in his objective method for forecasting thunderstorms in the Netherlands. He pointed out that this quantity has a rather low predictive value and suggested that only extreme dryness is important (i.e. sum of the dew-point depressions at 850 and 700 mb. in excess of $30^{\circ}C$).

To investigate the relationship between the humidity profile and the

/occurrence

occurrence of storms, the Crawley and Hemsby 0000 GMT dew-point depressions at the surface, 850, 700 and 500 mb. were extracted for the period May to September 1958-1964. The reason for using the midnight rather than the mid-day sounding will be discussed later. The average of the Crawley and Hemsby dew-point depression was taken as representative of conditions, at each of the four levels. Totals for all possible combinations of the levels were also evaluated. The mean of two ascents was used, because humidity is a particularly variable quantity, and a single reading may be unrepresentative of the general conditions. Days included in the LP+, UT+ and ULN categories were analysed separately from the remainder.

It was not found possible to demonstrate any clear connection between the humidity at one or more of the levels and the occurrence of storms. The results suggested that the growth of cumulonimbus clouds is not influenced to any great extent by the humidity profile, except on occasions when the environment is exceptionally dry. The most useful parameter appeared to be the total of the dew-point depressions at 850 and 700 mb., and these results are summarised in Table 9. The probability of storms does not vary much with different humidities at 850 and 700 mb., unless the total dew-point depression at the two levels exceeds 30°C. This value is identical with the threshold suggested by Hanssen. When a positive forecast of hail and thunder was possible from the scheme summarised in Fig.11 consideration was then given to the humidity profile. If the total dew-point depression at 850 and 700 mb. exceeded 30°C, the day was re-classified as a "dry" case and a definite forecast of no hail or thunder was made. Otherwise, the original classification held, when a positive forecast of hail and thunderstorms was appropriate. In practice, the humidity would be considered before entering the flow diagram in Fig.11.

/TABLE

TABLE 9:-

Summary of the weather categories for the LP+/UT+/ULN cases (Crawley 1200 GMT ascent) as a function of the sum of the 850 and 700 mb. dew-point depressions (mean of Crawley and Hemsby 0000 GMT ascents). Area B (0600-1800 GMT). Period May-Sept. 1958-1964.

Sum of 850 and 700 mb dew-point depns. (mean of Crawley and Hemsby) °C	Number of days in weather category			% prob of hail or thunder
	x	H0-H6 T1-T6	Total	
0-5	7	15	22	68
5-10	27	70	97	72
10-15	18	53	71	75
15-20	12	26	38	69
20-25	9	17	26	65
25-30	1	3	4	75
>30	5	1	6	17

The scheme that has just been described will be referred to as the adiabatic energy method. It is based on various parameters that the investigation has proved to be useful as predictors. Numerous other physical and dynamical properties of the air mass were investigated, as the following list shows:-

a) Surface pressure and pressure tendency.

b) Maximum surface temperature and surface dew-point.

c) Type, location and speed of movement of fronts.

d) Vertical wind shear in the layers 900-500 mb. and 900-300 mb.

e) Potential instability in the layers 900-700 and 700-500 mb.

f) The relationship between the thickness tendencies in the layers 1000-850 mb., 850-700 mb. and 700-500 mb.

g) The temperature lapse through 100 mb. layers (1000-300 mb).

h) Wind velocity at 850, 700 and 500 mb. with particular reference to differential thermal advection.

i) Location of SFLOCS prior to 0600 GMT.

All these parameters were discarded, because, when used in conjunction with the above scheme, none of them produced any noticeable improvement in the standard of discrimination.

The results of the analysis for area B, during the months May to September

/1960

1960-1962, are given in Appendix 1. The contingency tables show, for the two verifying periods, the distribution of weather categories associated with each type of classification. The three classes below the horizontal line have been identified with a positive forecast of hail and thunderstorms. The Rackliff, Boyden, Jefferson and modified Jefferson indices were also calculated from the 1200 GMT Crawley soundings for the same period, and the results are tabulated in Appendix 2. The relative merits of the different techniques may be assessed more readily by treating the phenomenon on an occurrence/non-occurrence basis. A statistical summary of the analyses by the adiabatic energy method and the conventional instability indices is given in Table 10. The percentage accuracy of the dichotomous classification and the percentage of thunderstorm days accommodated by the technique are recorded. However, Johnson [34] has pointed out that, on their own, such statistics can be misleading. One of the most useful of the simple verification statistics for this type of classification is the Heidke "skill score" (S) which is defined by:-

$$S = \frac{\text{number of correct forecasts - number correct by chance}}{\text{total number of forecasts - number correct by chance}}$$

S is 1 for complete accuracy and 0 for forecasts that are no better than chance. The skill score for each of the techniques is included in Table 10. The critical values of the instability indices were selected to give the highest skill scores, and were not necessarily the same as the values suggested originally by the authors. With the exception of the Boyden index, there was little difference between two adjacent critical indices and in these cases the results are presented for both values.

It is clear from the contingency tables in Appendices 1 and 2 that, when thunder is observed in apparently stable air masses, the outbreaks are often quite local features. On a substantial proportion of these occasions, thunder is reported by only a single station (or a single SFLOC) i.e. the weather category is T1. Such outbreaks are of relatively little importance, and it seemed worthwhile to re-calculate the verification statistics with the T1 cases excluded. These results are recorded in brackets in Table 10, and it will be noted that the percentage accuracy and skill scores generally show a definite increase with the exclusion of these borderline situations. The statistics in Table 10 demonstrate that the adiabatic energy method is capable of discriminating more closely than

/the

TABLE 10:- VERIFICATION STATISTICS FOR "FORECASTS" BASED ON ACTUAL 1200 G.M.T DATA

AREA B MAY-SEPT 1960-62 (DEPENDENT DATA)

BRACKETS INDICATE STATISTICS EXCLUDING TI CASES

1) VERIFYING TIME 0600-1800 G.M.T.

TECHNIQUE AND CRITICAL INDEX	OVERALL ACCURACY OF FORECASTS			ACCURACY OF 'THUNDERSTORM' FORECASTS			ACCURACY OF 'NO THUNDERSTORM' FORECASTS			INCLUSION IN FORECASTS OF THUNDERSTORMS WHICH OCCURRED			SKILL SCORE	
	NUMBER OF FORECASTS	NUMBER CORRECT	% CORRECT	NUMBER OF FORECASTS	NUMBER CORRECT	% CORRECT	NUMBER OF FORECASTS	NUMBER CORRECT	% CORRECT	NO. OF THUNDERSTORM DAYS	NO. CORRECTLY FORECAST	% CORRECT		
ADIABATIC ENERGY	453 (423)	394 (355)	87 (91)	109 (100)	87 (78)	80 (78)	344 (325)	307 (307)	89 (94)	124 (96)	87 (78)	70 (81)	0.66	(0.73)
MOD. JEFFERSON 25/26	459 (431)	372 (366)	81 (85)	103 (87)	70 (64)	68 (64)	356 (334)	302 (302)	85 (90)	124 (96)	70 (64)	56 (67)	0.50	(0.57)
MOD. JEFFERSON 24/25	459 (431)	369 (355)	80 (83)	128 (117)	81 (70)	63 (60)	331 (314)	288 (285)	87 (91)	124 (96)	81 (70)	65 (73)	0.51	(0.55)
RAUCLIFF 30/31	459 (431)	372 (366)	81 (85)	85 (79)	61 (55)	72 (70)	374 (352)	311 (311)	83 (88)	124 (96)	61 (53)	49 (57)	0.47	(0.54)
CAULIFF 29/30	459 (431)	361 (352)	79 (82)	128 (119)	77 (68)	60 (57)	331 (312)	284 (284)	86 (91)	124 (96)	77 (68)	62 (71)	0.46	(0.51)
OXYGEN 94/35	459 (431)	356 (346)	78 (80)	131 (121)	76 (66)	58 (55)	328 (310)	280 (280)	85 (90)	124 (96)	76 (64)	61 (67)	0.45	(0.48)
JEFFERSON 25/26	459 (431)	355 (346)	78 (81)	123 (113)	73 (63)	59 (56)	336 (318)	282 (283)	84 (89)	124 (96)	73 (63)	59 (66)	0.44	(0.48)
JEFFERSON 24/25	459 (431)	341 (335)	76 (79)	162 (145)	88 (74)	54 (50)	297 (286)	253 (261)	88 (91)	124 (96)	88 (74)	71 (77)	0.45	(0.46)

2) VERIFYING TIME 0600-2400 G.M.T.

TECHNIQUE AND CRITICAL INDEX	OVERALL ACCURACY OF FORECASTS			ACCURACY OF 'THUNDERSTORM' FORECASTS			ACCURACY OF 'NO THUNDERSTORM' FORECASTS			INCLUSION IN FORECASTS OF THUNDERSTORMS WHICH OCCURRED			SKILL SCORE	
	NUMBER OF FORECASTS	NUMBER CORRECT	% CORRECT	NUMBER OF FORECASTS	NUMBER CORRECT	% CORRECT	NUMBER OF FORECASTS	NUMBER CORRECT	% CORRECT	NO. OF THUNDERSTORM DAYS	NO. CORRECTLY FORECAST	% CORRECT		
ADIABATIC ENERGY	453 (418)	377 (367)	83 (88)	109 (91)	81 (71)	82 (78)	344 (327)	298 (296)	87 (90)	145 (110)	89 (71)	61 (72)	0.59	(0.67)
MOD. JEFFERSON 24/25	459 (424)	356 (345)	78 (81)	128 (117)	85 (74)	66 (63)	331 (307)	271 (271)	82 (88)	145 (110)	85 (74)	59 (67)	0.46	(0.54)
MOD. JEFFERSON 25/26	459 (424)	353 (345)	77 (81)	103 (86)	72 (65)	70 (76)	356 (338)	283 (280)	79 (83)	145 (110)	72 (65)	50 (59)	0.43	(0.51)
RAUCLIFF 29/30	459 (424)	330 (340)	76 (80)	128 (110)	82 (72)	64 (65)	331 (314)	268 (268)	81 (85)	145 (110)	82 (72)	57 (65)	0.43	(0.50)
RAUCLIFF 30/31	459 (424)	353 (349)	77 (82)	85 (71)	62 (53)	73 (75)	374 (353)	291 (296)	78 (84)	145 (110)	62 (53)	43 (48)	0.40	(0.50)
OXYGEN 94/35	459 (424)	341 (339)	74 (80)	131 (120)	83 (72)	63 (60)	328 (304)	258 (267)	79 (88)	145 (110)	83 (72)	57 (65)	0.43	(0.49)
JEFFERSON 24/25	459 (424)	338 (324)	74 (76)	162 (145)	93 (79)	57 (55)	297 (279)	245 (245)	82 (88)	145 (110)	93 (71)	64 (72)	0.41	(0.49)
JEFFERSON 25/26	459 (424)	345 (334)	75 (79)	123 (114)	76 (67)	62 (59)	336 (310)	267 (267)	79 (86)	145 (110)	76 (67)	52 (61)	0.39	(0.45)

the simple instability indices, between those conditions which are favourable for the occurrence or non-occurrence of storms. The skill scores for all the techniques are lower for the verification period 0600-2400 GMT than for the period 0600-1800 GMT, a result which was expected. Examination of the contingency tables in Appendix 1 reveals that very few of the occasions of widespread storms (defined as days with $n > 3$) were not associated with either the UT+ or LP+ categories. For example, in the verifying period 0600-1800 GMT, there were 41 occasions with more than 20 reports of hail, thunder or SFLOCS over area B. 38 of these days were included in the UT+ or LP+ classes. Similar proportions were achieved by the Rackliff [29/30] and the Jefferson [24/25] indices, but only at the expense of a disproportionate increase in the total number of unstable classifications. 38 of the 44 occasions on which hail was actually observed were included in the UT+ or LP+ classes, 32 of these being in the latter category. This result suggests that the chance of hail occurring at a particular station may only be significant on days included in the LP+ classification. The increase in the skill score when the T1 cases are excluded is due to the fact that as many as one half of all the occasions of hail and thunder, that are associated with the stable classes come in this weather category.

The statistics in Table 10 indicate that the modified Jefferson index is the most successful of the conventional instability indices. This result is contrary to the findings of Saunders [18] [26], from his tests carried out during the summers of 1965 and 1966. The Boyden and Rackliff indices were generally found to be the most useful aids for area forecasting. This apparent anomaly probably stems from the fact that the indices used in his tests were forecast from the midnight soundings and were not analysed midday values. The modified Jefferson index involves the dew-point depression at 700 mb and no really satisfactory methods for forecasting this parameter are currently available. In fact, the midday depression at 700 mb. probably depends to a certain extent on whether convection has reached that level, or in other words, the parameter is dependent on the phenomenon that is to be forecast. Lowndes (unpublished work) found that the RMS change in the Crawley 700 mb. dew-point depression between 0000 and 1200 GMT was 12.0°C (May-Sept. 1962). When an attempt was made to forecast the midday value from the midnight data, the RMS error in the predicted depression was still 9.1°C,

/corresponding

corresponding to an error of more than 4 units in the index. It is clear from Appendix 2 that the difference between the actual value and the critical value is equal to or less than 4 units on a substantial proportion of occasions. Therefore, although the modified Jefferson index may appear to be superior to the other indices when used diagnostically, it will not be particularly useful as a forecasting tool. This considerable uncertainty in the forecasts of the dew-point depression also explains why the midnight humidity data were used in the adiabatic energy method, to define occasions of extreme dryness.

b) Analysis for area A+B

The mean of the Crawley and Hemsby 1200 GMT upper-air soundings was taken to be representative of conditions over the combined area (A and B) during the period 0600-1800 GMT. The analysis procedure was identical to that adopted for area B, except for minor changes in the critical values of the various parameters. The diagrams appropriate to the combined area are shown in Figs. 12-17 and correspond to Figs. 4-7 and 9-10 respectively, for area B. Similarly, Tables 11-16 are the double-area equivalents of Tables 4-8 and 10.

The distribution of occasions of hail and thunder as a function of E_{max} is recorded in Table 11. It was decided on the basis of these statistics, that the upper limit to E_{max} for the large negative energy (LN) category should be changed to -250 j/kg. for the combined area. The probability of hail or thunder occurring somewhere in the area was as high as 10% for those days with values of E_{max} less than -200 j/kg. (the limiting value for area B). By using the slightly stricter criterion, this probability was reduced to 4%.

Fig.12 shows the weather category for the combined area, as a function of E_2 and θ_{wp}. Examination of the data indicated that the critical relationship between E_2 and θ_{wp} was of the form indicated by the curve in Fig.12, with a threshold value for E_{max} of 0 j/kg. The analysis was made quite independently of that performed earlier for area B, so that the criteria are based wholly on the data for the combined area. Table 12 summarises the weather for the cold zone cases in Fig.12, as a function of E_{max}.

/TABLE

TABLE II :- RELATIONSHIP BETWEEN EMAX (MEAN OF CRAWLEY AND HEMSBY 1200 G.M.T. ASCENTS) AND THE WEATHER IN AREAS A AND B 0600-1800 G.M.T.

PERIOD MAY-SEPT 1960-62

(a) NUMBER OF DAYS WITH EMAX (MEAN OF CRAWLEY AND HEMSBY 1200 G.M.T) BETWEEN SPECIFIED LIMITS FOR VARIOUS WEATHER CATEGORIES (AREA A+B 0600-1800 G.M.T).

WEATHER CLASSIFICATION AREA A+B 0600-1800 G.M.T.	EMAX (JOULES/KG.)																				
	≤-500	-499 TO -450	-449 TO -400	-399 TO -350	-349 TO -300	-299 TO -250	-249 TO -200	-199 TO -150	-149 TO -100	-99 TO -50	-49 TO 0	1 TO 50	51 TO 100	101 TO 150	151 TO 200	201 TO 250	251 TO 300	301 TO 350	351 TO 400	401 TO 450	451 TO 500	>500
X	49	12	11	26	14	20	24	22	19	34	14	19	11	12	3	0	0	1	0	0	0	0
T1	0	0	0	1	0	0	7	2	2	7	4	5	6	1	0	0	0	0	0	0	0	1
T2-T6/H0-H6	0	0	0	1	0	3	4	3	6	12	11	10	21	19	14	1	6	1	1	0	1	2
TOTAL	49	12	11	28	14	23	35	27	27	53	29	34	38	32	17	1	6	2	1	0	1	3
T4-T6/H4-H6	0	0	0	0	0	1	2	2	0	2	4	5	11	10	7	1	0	1	0	0	1	1

(b) NUMBER OF DAYS WITH EMAX (MEAN OF CRAWLEY AND HEMSBY 1200 G.M.T) BELOW SPECIFIED LIMITS FOR VARIOUS WEATHER CATEGORIES (AREA A+B 0600-1800 G.M.T.)

WEATHER CLASSIFICATION AREA A+B 0600-1800 G.M.T	EMAX (JOULES/KG.)																				WHOLE RANGE
	≤-500	≤-450	≤-400	≤-350	≤-300	≤-250	≤-200	≤-150	≤-100	≤-50	≤ 0	≤ 50	≤ 100	≤ 150	≤ 200	≤ 250	≤ 300	≤ 350	≤ 400	≤ 450	≤ 500	
X	49	61	72	98	112	132	156	178	197	231	245	264	275	287	290	290	290	291	291	291	291	291
%	(16)	(20)	(24)	(33)	(38)	(45)	(53)	(61)	(67)	(78)	(83)	(90)	(94)	(98)	(99)	(99)	(99)	(100)	(100)	(100)	(100)	(100)
T1	0	0	0	1	1	1	8	10	12	19	23	28	34	35	35	35	35	35	35	35	35	36
%	(0)	(0)	(0)	(3)	(3)	(3)	(23)	(28)	(34)	(53)	(64)	(78)	(94)	(97)	(97)	(97)	(97)	(97)	(97)	(97)	(97)	(100)
T2-T6/H0-H6	0	0	0	1	1	4	8	11	17	29	40	50	71	90	104	105	111	112	113	113	114	116
%	(0)	(0)	(0)	(1)	(1)	(3)	(7)	(9)	(15)	(25)	(34)	(43)	(61)	(78)	(90)	(91)	(96)	(97)	(97)	(97)	(98)	(100)
TOTAL	49	61	72	100	114	137	172	191	226	279	308	342	380	412	429	430	436	438	439	439	440	443
T4-T6/H4-H6	0	0	0	0	0	1	3	5	5	7	11	16	27	37	44	45	51	52	52	52	53	54
%	(0)	(0)	(0)	(0)	(0)	(1)	(2)	(3)	(2)	(3)	(4)	(5)	(7)	(9)	(10)	(10)	(12)	(12)	(12)	(12)	(12)	(12)

BRACKETED FIGURES ARE THE PERCENTAGES OF THE TOTAL

TABLE 12:-

Summary of the weather categories for the cold zone cases as a function of E_{max}. Mean of Crawley and Hemsby 1200 GMT ascents. Area A+B (0600 1800 GMT). Period May-Sept. 1960-1962.

E_{max} Joules/kg	Number of days in weather category	
	x	H0-H6 T1-T6
< -30	10	5
-30 to -21	0	2
-20 to -11	3	2
-10 to - 1	0	0
0 to 9	1	2
10 to 19	0	3
20 to 29	0	1
⩾ 30	11	66

Fig.13 is similar to Fig.12, except that the diagram is restricted to those occasions when E_{max} exceeded the threshold value. The corresponding statistical summary is given in Table 13.

TABLE 13:-

Summary of the weather categories for the cold and warm zones for days with E_{max} ⩾ 0 j/kg. Mean of Crawley and Hemsby 1200 GMT ascents. Area A+B (0600-1800 GMT). Period May-Sept. 1960-1962.

Zone	Number of days in weather category		
	x	T1	H0-H6 T2-T6
Cold zone	12	3	69
Warm zone	36	11	11

Cold zone cases with E_{max} greater than or equal to 0 j/kg. were classified as days of "large positive energy" (LP). Hail or thunder were observed on 86% of these occasions. In Fig.12, the curve intercepts the θ_{wp} axis at $\theta_{wp} = 15.2^{\circ}C$. The corresponding equilibrium temperature is $-8^{\circ}C$, which compares with $-10^{\circ}C$ from the area B analysis. This slight difference does not affect the inferences that were made at that stage.

A substantial number of occasions of hail and thunder are included within the warm zone in Fig.12, and as in the case of the single-area analysis, there is a tendency for warm zone storms to occur with positive or small negative values of (E_2-E_1). Fig.14 shows the weather category for the warm zone cases as a function of (E_2-E_1) and θ_{wp}. In the warm stable type (WST) area, below the line, the probability of hail or more than a single thunderstorm report was about 8% on any given day. It is interesting that numerous instances of single thunderstorm (T1) reports were associated with this category. Storms occurred on approximately 55% of the days in the unstable type (UT) area (above the line). Table 14 summarises the weather for the warm stable type (WST) and unstable type (UT) categories.

TABLE 14:-

Summary of the weather categories for the WST and UT cases in Fig.14. Mean of Crawley and Hemsby 1200 GMT ascents. Area A+B (0600-1800 GMT). Period May-Sept. 1960-1962.

Classification	Number of days in weather category		
	x	T1	H0-H6 T2-T6
WST	106	18	11
UT	28	12	24

The weather for the cold zone cases with E_{max} less than 0 j/kg is plotted in Fig.15, as a function of (E_2-E_1) and θ_{wp}. As before, the diagram was divided into two areas, days below the line being classified as "cold stable type" (CST) and days above the line as "unstable type" (UT).

/The

The surface and 700 mb. vorticity indices used in the analysis of area B were also taken to be representative of conditions over the combined areas. Fig.16 is a diagram of the weather categories for the unstable type (UT) days as a function of the 1200 GMT vorticity indices at these two levels. The effects of cyclonic vorticity were not quite so well marked as in Fig.9, but it was still possible to divide the diagram into the positive (UT+) and negative (UT-) zones. The weather categories for the two areas are summarised in Table 15.

TABLE 15:-

Summary of the weather categories for the UT+ and UT- cases.

Mean of Crawley and Hemsby 1200 GMT ascents. Area A+B (0600-1800 GMT). Period May-Sept. 1960-1962.

Classification	Number of days in weather category		
	x	T1	H0-H6 T2-T6
UT- UT+	15 14	7 7	8 22

The weather for the days in the large positive energy (LP) category is plotted in Fig.17, as a function of the 1200 GMT vorticity indices at the surface and 700 mb The diagram was tentatively sub-divided, the areas above and below the line being classified as the positive (LP+) and negative (LP-) zones, respectively.

The flow diagram of the analysis procedure for area B (Fig.11) is equally valid for the combined area, providing the threshold energies and figure numbers, which are appropriate to this area, are used. The same extreme dryness criteria were applied, as were used for area B. A summary of the analysis for the combined area (A+B) during the months May to September 1960-1962 is given in Appendix 3, the form of the contingency tables being identical with Appendix 1. Classes below the horizontal dividing line are identified with a positive forecast of hail and thunderstorms. The Rackliff index was calculated from the mean of the 1200 GMT Crawley and Hemsby soundings for the same period, and these results are tabulated in Appendix 4. To save unnecessary labour, only the Rackliff index was evaluated for comparison in this instance, because this index appeared to be at least as

/useful

useful as the Boyden and Jefferson indices on the previous work. By treating the phenomenon on an occurrence/non-occurrence basis, one obtains the statistics in Table 16. As before the critical value of the instability index was chosen to give the highest skill score. The percentage successes and skill scores have been evaluated both for every day and for those days when the weather is not in the borderline T1 weather category (bracketed).

The statistics in Table 16 are broadly similar to those presented in Table 10 for the small area. However, the superiority of the adiabatic energy method over the Rackliff index is slightly less for the combined area. In the verifying period 0600-1800 GMT, there were 54 days with more than 20 reports of hail, thunder or SFLOCS over the area and 51 of these occasions were included in the UT+ or LP+ classes. 42 of the 50 occasions on which hail was actually observed were included in these two classes, 39 being in the LP+ category. The fact that the occurrence of hail appears to be particularly associated with the LP+ category is in accordance with the ideas behind the structure of the scheme.

8. Tests on independent data.

The adiabatic energy method was tested on independent data for the years 1958, 1959, 1963 and 1964. 1200 GMT actual upper-air and surface data were analysed for each day in the period May to September, during these four years. The procedure defined by the flow diagram in Fig.11 was strictly followed to determine the classification on each day. It must be emphasised that these were not forecasts in the true sense of the word, since no attempt was made to predict the midday values of the parameters from the midnight data. Actual midday values of the predictors were used so that the skill scores and various other statistics are appropriate to the situation where the predictors can be forecast with 100% accuracy.

Results for area B are presented as contingency tables in Appendix 5. With the exception of the modified Jefferson index, which was excluded for the reasons given in section 7, the instability indices listed in Table 10 were again used as a standard. The contingency tables for these other indices are given in Appendix 6. By taking the critical index (or indices) which gave the best skill scores over the period 1960-1962, one was also testing these other techniques on independent data. A statistical summary of the results achieved by the adiabatic energy method and the conventional instability indices is given in Table 17.

/Comparison

TABLE 16 VERIFICATION STATISTICS FOR "FORECASTS" BASED ON ACTUAL 1200 GMT DATA

AREA A & B MAY-SEPT 1960-62 (DEPENDENT DATA)

BRACKETS INDICATE STATISTICS EXCLUDING TI CASES

1) VERIFYING TIME 0600-1800 G.M.T.

TECHNIQUE AND CRITICAL INDEX	OVERALL ACCURACY OF FORECASTS			ACCURACY OF 'THUNDERSTORM' FORECASTS			ACCURACY OF 'NO THUNDERSTORM' FORECASTS			INCLUSION IN FORECASTS OF THUNDERSTORMS WHICH OCCURRED			SKILL SCORE
	NUMBER OF FORECASTS	NUMBER CORRECT	% CORRECT	NUMBER OF FORECASTS	NUMBER CORRECT	% CORRECT	NUMBER OF FORECASTS	NUMBER CORRECT	% CORRECT	NO. OF THUNDERSTORM DAYS	NO. CORRECTLY FORECAST	% CORRECT	
ADIABATIC ENERGY	443 (407)	369 (351)	83 (86)	124 (114)	101 (91)	81 (80)	319 (293)	263 (260)	84 (91)	152 (114)	101 (91)	66 (78)	0.61 (0.71)
BLACKLIFF 29/29½	445 (407)	350 (337)	79 (83)	141 (130)	99 (88)	70 (67)	304 (277)	251 (251)	83 (90)	152 (116)	99 (88)	65 (76)	0.52 (0.59)

2) VERIFYING TIME 0600-2400 G.M.T.

TECHNIQUE AND CRITICAL INDEX	OVERALL ACCURACY OF FORECASTS			ACCURACY OF 'THUNDERSTORM' FORECASTS			ACCURACY OF 'NO THUNDERSTORM' FORECASTS			INCLUSION IN FORECASTS OF THUNDERSTORMS WHICH OCCURRED			SKILL SCORE
	NUMBER OF FORECASTS	NUMBER CORRECT	% CORRECT	NUMBER OF FORECASTS	NUMBER CORRECT	% CORRECT	NUMBER OF FORECASTS	NUMBER CORRECT	% CORRECT	NO. OF THUNDERSTORM DAYS	NO. CORRECTLY FORECAST	% CORRECT	
ADIABATIC ENERGY	443 (412)	356 (347)	80 (85)	124 (117)	103 (96)	83 (82)	319 (295)	253 (251)	79 (85)	169 (135)	103 (96)	61 (70)	0.56 (0.64)
BLACKLIFF 29/29½	445 (414)	355 (338)	75 (80)	141 (137)	100 (96)	71 (70)	304 (277)	255 (255)	77 (85)	169 (135)	100 (96)	59 (70)	0.46 (0.55)

TABLE 17 VERIFICATION STATISTICS FOR "FORECASTS" BASED ON ACTUAL 1200 GMT DATA (CRAWLEY)

AREA B MAY-SEPT 1958-59 1963-64 (INDEPENDENT DATA)

BRACKETS INDICATE STATISTICS EXCLUDING TI CASES

1) VERIFYING TIME 0600-1800 GMT

TECHNIQUE AND CRITICAL INDEX	OVERALL ACCURACY OF FORECASTS			ACCURACY OF 'THUNDERSTORM' FORECASTS			ACCURACY OF 'NO THUNDERSTORM' FORECASTS			INCLUSION IN FORECASTS OF THUNDERSTORMS WHICH OCCURRED			SKILL SCORE
	NUMBER OF FORECASTS	NUMBER CORRECT	% CORRECT	NUMBER OF FORECASTS	NUMBER CORRECT	% CORRECT	NUMBER OF FORECASTS	NUMBER CORRECT	% CORRECT	NO OF THUNDERSTORM DAYS	NO. CORRECTLY FORECAST	% CORRECT	
ADIABATIC ENERGY	607 (572)	500 (498)	82 (86)	149 (139)	97 (97)	65 (63)	458 (433)	403 (403)	88 (93)	152 (117)	97 (87)	64 (74)	0.53 (0.59)
RADCLIFF 23/30	605 (579)	468 (456)	77 (79)	193 (179)	104 (99)	54 (50)	412 (311)	364 (364)	88 (93)	152 (117)	104 (10)	68 (77)	0.45 (0.48)
JEFFERSON 25/26	607 (573)	464 (441)	76 (78)	201 (182)	105 (90)	52 (48)	406 (391)	359 (359)	88 (93)	152 (117)	105 (90)	69 (77)	0.43 (0.46)
RADCLIFF 30/31	605 (579)	472 (446)	78 (81)	135 (124)	77 (66)	57 (53)	470 (444)	395 (380)	84 (86)	152 (117)	77 (66)	51 (56)	0.51 (0.43)
BOYDEN 94/15	612 (577)	442 (426)	72 (73)	230 (212)	107 (89)	47 (42)	382 (365)	335 (335)	88 (92)	154 (119)	107 (89)	69 (75)	0.37 (0.37)
JEFFERSON 24/25	607 (572)	427 (408)	70 (72)	254 (236)	113 (95)	44 (40)	353 (336)	314 (314)	89 (93)	152 (117)	113 (95)	74 (81)	0.35 (0.36)

2) VERIFYING TIME 0600-2400 G.M.T.

TECHNIQUE AND CRITICAL INDEX	OVERALL ACCURACY OF FORECASTS			ACCURACY OF 'THUNDERSTORM' FORECASTS			ACCURACY OF 'NO THUNDERSTORM' FORECASTS			INCLUSION IN FORECASTS OF THUNDERSTORMS WHICH OCCURRED			SKILL SCORE
	NUMBER OF FORECASTS	NUMBER CORRECT	% CORRECT	NUMBER OF FORECASTS	NUMBER CORRECT	% CORRECT	NUMBER OF FORECASTS	NUMBER CORRECT	% CORRECT	NO. OF THUNDERSTORM DAYS	NO. CORRECTLY FORECAST	% CORRECT	
ADIABATIC ENERGY	607 (566)	482 (473)	79 (84)	149 (140)	103 (94)	69 (67)	458 (426)	379 (379)	83 (89)	182 (141)	103 (94)	57 (67)	0.43 (0.56)
JEFFERSON 25/26	607 (574)	464 (446)	76 (78)	201 (183)	120 (102)	60 (56)	406 (391)	344 (344)	85 (90)	192 (141)	120 (102)	66 (72)	0.45 (0.48)
RADCLIFF 23/30	605 (566)	466 (447)	77 (79)	193 (175)	117 (99)	61 (57)	412 (391)	349 (349)	85 (89)	190 (141)	117 (99)	65 (70)	0.46 (0.48)
RADCLIFF 30/31	605 (566)	460 (448)	76 (79)	135 (123)	85 (73)	63 (59)	470 (443)	375 (375)	80 (85)	190 (141)	85 (73)	47 (52)	0.38 (0.42)
JEFFERSON 24/25	607 (564)	433 (413)	71 (73)	254 (234)	131 (111)	52 (47)	353 (334)	302 (302)	86 (91)	192 (141)	131 (111)	72 (79)	0.39 (0.41)
BOYDEN 94/15	612 (571)	450 (426)	74 (75)	230 (206)	126 (102)	55 (49)	382 (365)	324 (324)	85 (89)	184 (143)	126 (102)	68 (71)	0.41 (0.41)

Comparison of these figures with those in Table 10 reveals, not unexpectedly, that the percentage successes and skill scores are generally lower for the independent data. However, the adiabatic energy method is still definitely superior to the other techniques, particularly when the T1 cases are excluded. The Rackliff index, with a threshold of 29/30 appears to be the best of the instability indices. An examination of the contingency tables in Appendix 5 confirms that the vast majority of the days of widespread storms are categorised correctly. The main reason for the fall in skill score, compared with 1960-1962, is an increase in the proportion of UT+ and LP+ days on which storms failed to develop.

Corresponding results for the combined area are given in Appendix 7 (contingency tables for the adiabatic energy method), Appendix 8 (contingency tables for the Rackliff index) and Table 18 (summary of the percentage successes and skill scores). The mean Rackliff index for Crawley and Hemsby was used as the standard, with a threshold value of 29/29½. A comparison with Table 16 shows that the differences between the adiabatic energy and Rackliff skill scores were almost identical for the dependent and independent data. For the dependent data, the adiabatic energy skill scores were slightly higher for the small area than the combined area, whereas with the independent data the reverse was true. This may suggest that the criteria for the combined area were based on slightly more representative data. The association between the actual observation of hail and the LP+ category is again quite noticeable in the tables in Appendix 7.

A further test was performed for area B, by applying the same rules to the midnight data, over the period May to September 1960-1962. These results represent the minimum standard of accuracy that may be achieved in practice, in the circumstances when no attempt is made to forecast the midday values of the predictors i.e. a persistence forecast based on midnight data. Contingency tables for the adiabatic energy method are presented in Appendix 9 and for the other indices in Appendix 10. A statistical summary is given in Table 19. The skill scores and percentage accuracies are considerably lower than when the midday values of the predictors were used. In addition to normal changes in the conditions, this is partly due to the fact that there is a mean difference of about ½°C between the midnight and midday values of the 900 mb. wet-bulb potential temperature the latter, rather surprisingly being the lower. The skill scores would certainly have been higher if the criteria had originally been determined

/from

TABLE 13 VERIFICATION STATISTICS FOR "FORECASTS" BASED ON ACTUAL 1200 GMT. DATA

AREAS A & B MAY-SEPT 1958-59 1963-64 (INDEPENDENT DATA)

BRACKETS INDICATE STATISTICS EXCLUDING TI CASES.

1) VERIFYING TIME 0600-1800 G.M.T.

TECHNIQUE AND CRITICAL INDEX	OVERALL ACCURACY OF FORECASTS			ACCURACY OF 'THUNDERSTORM' FORECASTS			ACCURACY OF 'NO THUNDERSTORM' FORECASTS			INCLUSION IN FORECASTS OF THUNDERSTORMS WHICH OCCURRED			SKILL SCORE
	NUMBER OF FORECASTS	NUMBER CORRECT	% CORRECT	NUMBER OF FORECASTS	NUMBER CORRECT	% CORRECT	NUMBER OF FORECASTS	NUMBER CORRECT	% CORRECT	NO. OF THUNDERSTORM DAYS	NO. CORRECTLY FORECAST	% CORRECT	
ADIABATIC ENERGY	602 (561)	498 (451)	83 (76)	158 (141)	120 (111)	76 (74)	444 (420)	378 (340)	85 (90)	186 (153)	120 (103)	65 (73)	0.58 (0.64)
RADCLIFF 29/43½	605 (572)	461 (445)	76 (78)	216 (203)	129 (116)	60 (57)	389 (369)	332 (329)	85 (90)	186 (153)	129 (116)	69 (76)	0.47 (0.51)

2) VERIFYING TIME 0600-1800 G.M.T.

TECHNIQUE AND CRITICAL INDEX	OVERALL ACCURACY OF FORECASTS			ACCURACY OF 'THUNDERSTORM' FORECASTS			ACCURACY OF 'NO THUNDERSTORM' FORECASTS			INCLUSION IN FORECASTS OF THUNDERSTORMS WHICH OCCURRED			SKILL SCORE
	NUMBER OF FORECASTS	NUMBER CORRECT	% CORRECT	NUMBER OF FORECASTS	NUMBER CORRECT	% CORRECT	NUMBER OF FORECASTS	NUMBER CORRECT	% CORRECT	NO. OF THUNDERSTORM DAYS	NO. CORRECTLY FORECAST	% CORRECT	
ADIABATIC ENERGY	602 (565)	488 (479)	81 (85)	158 (141)	125 (116)	79 (78)	444 (424)	363 (363)	82 (86)	206 (167)	125 (116)	61 (69)	0.55 (0.62)
RADCLIFF 29/43½	605 (568)	461 (445)	76 (78)	216 (200)	139 (123)	64 (62)	389 (368)	322 (322)	83 (87)	206 (167)	139 (123)	67 (73)	0.48 (0.49)

TABLE 19: VERIFICATION STATISTICS FOR 'FORECASTS' BASED ON ACTUAL 0001 GMT DATA (CRAWLEY)

AREA B. MAY-SEPT. 1960-62

BRACKETS INDICATE STATISTICS EXCLUDING TI CASES.

1) VERIFYING TIME 0600-1800 GMT

TECHNIQUE AND CRITICAL INDEX	OVERALL ACCURACY OF FORECASTS: NUMBER OF FORECASTS	NUMBER CORRECT	% CORRECT	ACCURACY OF "THUNDERSTORM" FORECASTS: NUMBER OF FORECASTS	NUMBER CORRECT	% CORRECT	ACCURACY OF "NO THUNDERSTORM" FORECASTS: NUMBER OF FORECASTS	NUMBER CORRECT	% CORRECT	INCLUSION IN FORECASTS OF THUNDERSTORMS WHICH OCCURRED: NO. OF THUNDERSTORM DAYS	NO. CORRECTLY FORECAST	% CORRECT	SKILL SCORE
ADIABATIC ENERGY	453 (425)	352 (342)	78 (80)	116 (115)	69 (59)	59 (51)	337 (319)	283 (283)	84 (89)	123 (95)	69 (59)	56 (62)	0.43 (0.46)
RAWCLIFF 30/31	458 (430)	356 (344)	78 (81)	104 (97)	63 (56)	61 (58)	354 (333)	293 ([illegible])	83 (87)	124 ([illegible])	63 ([illegible])	51 (57)	0.41 (0.45)
RAWCLIFF 29/30	458 (430)	339 (328)	74 (77)	145 (134)	75 (64)	52 (48)	313 (296)	264 (264)	84 (89)	124 ([illegible])	75 (64)	60 (67)	0.38 (0.40)
JEFFERSON 25/26	457 (429)	338 (325)	74 (76)	141 (125)	73 (60)	52 (47)	316 (301)	265 (265)	84 (88)	124 ([illegible])	73 (60)	59 (63)	0.37 (0.39)
JEFFERSON 24/25	457 (429)	322 (305)	70 (71)	187 (170)	88 (71)	47 (42)	270 (251)	234 (234)	87 (90)	124 ([illegible])	88 (71)	71 (74)	0.36 (0.35)
MOD. JEFFERSON 25/26	455 (427)	323 (311)	71 (73)	140 (129)	66 (54)	47 (42)	315 ([illegible])	257 (257)	82 (88)	124 (96)	66 (54)	53 (56)	0.30 (0.30)
MOD. JEFFERSON 24/25	455 (427)	315 (300)	69 (70)	166 (151)	75 (60)	45 (40)	289 (276)	240 (240)	83 (87)	124 (96)	75 (60)	60 (63)	0.30 (0.31)
BOYDEN 94/95	458 (430)	315 (303)	69 (70)	157 (145)	69 (57)	44 (39)	301 (285)	246 (246)	82 (86)	124 (96)	69 (57)	56 (59)	0.27 (0.26)

2) VERIFYING TIME 0600-2400 GMT

TECHNIQUE AND CRITICAL INDEX	OVERALL ACCURACY OF FORECASTS: NUMBER OF FORECASTS	NUMBER CORRECT	% CORRECT	ACCURACY OF 'THUNDERSTORM' FORECASTS: NUMBER OF FORECASTS	NUMBER CORRECT	% CORRECT	ACCURACY OF 'NO THUNDERSTORM' FORECASTS: NUMBER OF FORECASTS	NUMBER CORRECT	% CORRECT	INCLUSION IN FORECASTS OF THUNDERSTORMS WHICH OCCURRED			SKILL SCORE
ADIABATIC ENERGY	453 (418)	339 (329)	75 (79)	116 (106)	73 (63)	63 (59)	337 (312)	266 (266)	79 (85)	144 (109)	73 (63)	51 (58)	0.39 (0.44)
RAWCLIFF 30/31	458 (429)	335 (330)	73 (78)	104 (99)	63 (58)	61 (59)	354 (330)	272 (272)	77 ([illegible])	145 (110)	63 (58)	43 (53)	0.33 (0.41)
RAWCLIFF 29/30	458 (429)	328 (316)	72 (75)	145 (133)	80 (68)	55 (51)	313 (296)	248 (248)	79 ([illegible])	145 (110)	80 (68)	55 (62)	0.34 (0.35)
JEFFERSON 25/26	457 (422)	329 (314)	72 (74)	141 (126)	79 (64)	56 (51)	316 (296)	250 (250)	79 (84)	145 (110)	79 (64)	54 (58)	0.35 (0.37)
JEFFERSON 24/25	457 (422)	317 (297)	69 (70)	187 (167)	96 (76)	51 (46)	270 (255)	221 (221)	82 (87)	145 (110)	96 (76)	66 (69)	0.34 (0.34)
MOD. JEFFERSON 25/26	455 (420)	314 (302)	69 (72)	140 (125)	72 (60)	51 (47)	315 (292)	242 (242)	77 (82)	145 (110)	72 (60)	50 (55)	0.28 (0.31)
MOD. JEFFERSON 24/25	455 (426)	308 (293)	68 (70)	166 (151)	82 (67)	49 (44)	289 (269)	226 (226)	78 (84)	145 (110)	82 (67)	57 (61)	0.28 (0.30)
BOYDEN 94/95	458 (423)	318 (300)	69 (71)	157 (139)	81 (63)	52 (45)	301 (284)	237 (237)	79 (83)	145 (110)	81 (63)	56 (57)	0.31 (0.30)

from midnight data. Table 19 shows that the adiabatic energy method is again superior to the other methods, although the difference is understandably not as marked as when more representative values of the parameters were used. The Rackliff index, with a threshold of 30/31, was the best of the other indices, the higher critical value proving superior, due to the higher 900 mb. wet-bulb potential temperature at midnight. The results confirm that the modified Jefferson index only compares favourably with the other indices when the actual midday conditions are known, so justifying its exclusion from the previous tests.

9. The prediction of widespread storms and large hail.

The association between the severity of storms and the strength of the up-draught has already been emphasised. In addition, a large positive value of the available energy is more likely to be indicative of unstable conditions over a wide area, whereas a small value may only represent local instability which is not typical of the region as a whole. Local features such as topography and aspect will be important in initiating the convection. This implies that E_{max} will attain a large positive value on days of widespread storms.

Table 20 shows, for area B, the relationship between the values of E_{max} and the number of thunderstorm reports, on days in the LP+ category. Data for the whole seven-year period (1958-1964) are recorded, and refer to the time interval 0600-1800 GMT.

TABLE 20:-

Number of days with E_{max} between specified limits for various groups of weather categories. LP+ and UT+ cases. Crawley 1200 GMT ascent.

Area B (0600-1800 GMT) Period May-Sept. 1958-1964.

Classification	E_{max} Joules/kg	Number of days in weather category							
		x	%	T1	%	T2-T3 Ho-H3	%	T4-T6 H4-H6	%
UT+	-	31	34	11	12	29	32	20	22
LP+	30-99	11	37	3	10	11	37	5	17
	100-199	18	32	2	4	17	30	20	35
	200-399	7	17	0	0	12	29	22	54
	≥ 400	7	19	3	8	7	19	20	54

/Results

Results for the UT+ category are also included in the table. The ranges of E_{max} for the LP+ category were selected to discriminate as usefully as possible between the four main classes of weather type. The results for the UT+ and borderline LP+ cases (E_{max} 30-99 j/kg) are similar, being largely associated with fairly local activity or no storms at all. With larger positive values of E_{max}, the proportion of days with widespread activity increases markedly although there appears to be little change in the ratio above about 200 j/kg. When E_{max} exceeds this value in the LP+ category, there is more than a 50% probability of widespread activity.

The corresponding analysis for the combined area is given in Table 21. It will be seen that the results are similar to those for the smaller area.

TABLE 21:-

Number of days with E_{max} between specified limits for various groups of weather categories. LP+ and UT+ cases. Mean of Crawley and Hemsby 1200 GMT ascents. Area A+B (0600-1800 GMT). Period May-Sept. 1958-1964.

Classification	E_{max} Joules/kg	Number of days in weather category							
		x	%	T1	%	T2-T3 H0-H3	%	T4-T6 H4-H6	%
UT+	-	31	36	10	12	27	32	17	20
LP+	0- 99	15	19	6	8	27	35	29	38
	100-199	11	17	2	3	25	38	27	42
	200-399	2	5	1	3	9	24	25	68
	≥ 400	2	12	0	0	5	29	10	59

An alternative way of measuring the severity of the storms is in terms of the maximum size of hail reported at the ground. It was shown in section 3 that the size of the largest hail produced in a thundercloud is likely to be closely associated with the maximum velocity in the updraught. The disadvantage with this measure of severity stems from the rarity of observations of large hail in this country and the fact that the largest hail is unlikely to fall at an observing station. In area B, during the years 1960-1964, there were only 7 reports of hail with a diameter of 1 cm. or greater. No information on hail size was given in the climatological returns for 1958 and 1959. It is interesting to note that hail was actually observed on 33 of the 48 days when very widespread storms

/occurred

occurred over area B. (defined as days with n>4).

The relationship between E_{max} and the largest reported size of hail on days in the LP+ category is given in Tables 22 and 23, for the small and large areas, respectively. The data again refer to the interval 0600-1800 GMT.

Table 22:-

Number of days with the size of the largest hail between specified limits, as a function of E_{max}. LP+ cases only. Crawley 1200 GMT ascent. Area B(0600-1800GMT). Period May-Sept 1960-1964.

Diam of largest hail (cm)	E_{max} (Joules/kg)		
	< 150	150-299	⩾ 300
0.5-0.9	18	10	5
⩾ 1.0	0	3	4

In addition, the value of E_{max} on the day of the Horsham storm (5/9/58), when hail of 3" diameter was reported, was 888 j/kg. On the day of the Wokingham storm (9/7/59) when hail of 2" diameter was reported, the value of E_{max} was 659 j/kg. These results tend to confirm the general conclusions of the theoretical investigation. There is a marked tendency for the larger hail to occur with the higher values of available energy, in the case of area B. Although it is difficult to formulate definite rules on such a small number of cases, a tentative threshold of 300 j/kg. is suggested, above which hail of at least one centimetre in diameter should be forecast. On the basis of Eq. (5c) one would expect a larger value of available energy to be associated with hail of this diameter. Similarly, the equation gives higher energies for hail of the size reported on the days of the Wokingham and Horsham storms. This discrepancy may be due to the various assumptions and approximations that have been made, and could represent some form of systematic bias in the calculated energies. It is important to remember, however, that the value of E_{max} obtained from the 1200 GMT Crawley ascent is unlikely to be wholly representative of conditions at the place and time where the largest hail actually fell. The energy at Crawley will, in general, be less than this local extreme value.

/TABLE

TABLE 23:-

Number of days with the size of the largest hail between specified limits, as a function of E_{max}. LP+ cases only.

Mean of Crawley and Hemsby 1200 GMT ascents.

Area A+B (0600-1800 GMT). Period May-Sept. 1960-1964.

Diam. of largest hail (cm)	E_{max} (Joules/kg)		
	< 150	150-299	⩾ 300
0.5-0.9	30	13	3
⩾ 1.0	6	1	1

Table 23 shows that a connection between E_{max} and the size of the largest hail is not so apparent in the case of the combined area. Large hail is usually a rather local feature and the smoothing introduced by the meaning of two ascents probably obscures the basic relationship.

10. The occurrence of storms in relation to the 900 metre wind.

The contingency tables for the adiabatic energy method indicate that the skill scores would probably show a considerable improvement, if more were known about the factors that inhibit the development of storms on some days in the UT+ and LP+ categories. A subsidiary investigation was initiated for area B and most of the parameters listed in section 7 were considered, without any real success. The most promising results were achieved by relating the development of storms over Area B to the wind velocity at the 900 metre level, as measured by the Crawley 1200 GMT radio-sonde ascent. The LP+, UT+ and ULN cases for the whole seven-year period (1958-1964) were analysed. There were 258 such cases in all, of which 184 were associated with storms between 0600 and 1800 GMT.

Fig.18 shows the weather category for area B (0600-1800 GMT) as a function of the 900 m. wind speed and direction. In conditions of very light winds, the actual direction is obviously unimportant. There were very few failures when the speed was 8 kt. or less; these cases were all included in the category of light and variable winds (Class X). The remaining cases were classified according to the wind direction, and it was found possible to define four main wind regimes.

/Fig.

Fig.19 shows the range of direction appropriate to each of these categories, in a diagrammatic form. The statistics of the failure rate are given in Table 24. No distinction could be made between the LP+, UT+ and ULN Categories.

TABLE 24:-

Failure rate of the LP+, UT+ and ULN cases as a function of the 900m. wind direction. Crawley 1200 GMT ascent. Area B (0600-1800 GMT). Period May-Sept. 1958-1964.

Class	Range of 900 m Wind direction (deg)	Number of cases			Failure Rate %
		Total	Weather category		
			x	T1-T6/H0-H6	
X	All directions speed ≤ 8 kt.	39	6	33	15
A	360-060	17	8	9	47
B	070-150	27	2	25	7
C	160-250	106	43	63	41
D	260-350	69	15	54	22

There is a clear indication from Fig.19 that the highest failure rates are related to those directions where the air is likely to reach area B after a fairly long sea track. This fact is consistent with Saunder's conclusion [26] that it is intrinsically more difficult to forecast thunderstorms for an area near the coast than it is for an area well inland. When considering this diagram, it must be borne in mind that the air trajectories are cyclonically curved, in the majority of instances. The lowest failure rate occurred with Class B, which is associated with a short sea-track from the Continent. Next, in order, were Class X (light variable winds) and Class D. In both these cases, the air has probably been over land for a considerable time prior to the development of convective activity. Subsequent investigation was mainly confined to Classes C and A, for which the failure rate was over 40%.

On days when the Crawley 900 m. wind direction is between 160 and 250°, the low-level air reaching area B has probably been substantially modified by its passage over the water of the English Channel (and eastern Atlantic in some cases). A synoptic study indicated that some of the failures might be correlated with the direction of the 900 m. wind at Camborne. Fig.20 shows the weather category as

/a

a function of the Crawley and Camborne 900 m. wind directions, for those occasions when the Crawley wind direction was between 200 and 300°, with a speed greater than 8 kt. When the Crawley wind veered to 260° or more, there were very few failures. With a slight backing of the wind to 240 or 250°, the proportion of failures increased substantially, particularly when the Camborne wind direction was veered by less than 30°, or backed with respect to the Crawley direction. These cases are enclosed by the box in Fig.20. On occasions when the Camborne wind was veered by 30° or more relative to Crawley, a trough was situated between the stations which had the effect of enhancing the convective activity.

Most of the cases within the box in Fig.20 were associated with a rather similar surface synoptic pattern, in that the airflow over S.E. England formed part of the broad circulation around a depression centred to the north-west or west of the British Isles. As a result, the air mass consisted of polar maritime air that had originally travelled south far to the west of the British Isles and had consequently followed a very long sea track. Cases of hail and thunder inside the box occurred mainly when the low pressure centre was further south and east i.e. over the British Isles. Fig.21 is a vector diagram showing the weather categories for the cases inside the box in Fig.20, as a function of the 1200 GMT 900 m. wind velocity at Long Kesh. This extra parameter produces almost a complete separation of the storm cases. It appears that storms should not be forecast for area B when the Crawley and Camborne 900 m. wind directions are contained within the box in Fig.20, and the Long Kesh wind is also in the south-west sector in Fig.21. With the Long Kesh wind direction in the north-east sector, the depression was usually situated south of latitude 55°N and S.E. England was in its immediate circulation. The gradual ascending motion that generally occurs in the vicinity of a depression centre must tend to favour the development of convective activity in these cases.

Storms occurred over area A on more than half of the occasions when the Crawley, Camborne and Long Kesh winds were unfavourable for their development in area B. In this type of circulation, the low-level air would encounter a long land track prior to reaching area A. Thus, the circumstances are different for the two regions, and the rules that have just been developed are only applicable to area B. These results suggest that the passage over the sea must tend to stabilise the lowest layers, so that any instability which exists aloft is not

/readily

readily released by ordinary daytime heating when the air subsequently moves over the land.

Many failures in Class C (Table 24) occurred with the direction of the 900 m. wind at Crawley between 160 and 230°. It was impossible to establish any useful relationship between these failures and the corresponding wind at Camborne, as was done for the directions 240 and 250°. Also, no link was apparent with the winds at Brest, Trappes, Long Kesh or Hemsby. However, there did appear to be some connection with the wind direction at Aughton. Fig.22 is a vector diagram showing the weather category for area B as a function of the 1200 GMT Aughton 900 m. wind velocity, for those occasions when the Crawley direction was between 160 and 230° inclusive, with a speed exceeding 8 kt. The majority of the failures are grouped within a sector (Y) between 180 and 240°. The results are summarised in Table 25.

TABLE 25:- Summary of the weather categories for zones Y and Z in Fig.22.

Zone	Number of days in weather category		
	x	T1	Ho-H6 T2-T6
Y	18	2	10
Z	6	2	26

There were very few failures when the Aughton wind was backed beyond 180° or when it veered beyond 240°. In the former case, the wind directions are indicative of a depression in the vicinity of the southern half of the British Isles and in the latter case, of a trough line approaching area B. Both these circumstances will be associated with dynamical processes which are likely to favour the development of convective activity. It was found that the occurrence of SFLOCS prior to 0600 GMT in the area from 50 to 53°N and 10°W to 2°E was useful for discriminating between the thunderstorm cases and failures in zone Y. SFLOCS were present on only one of the 18 occasions when no storms occurred, but were present on 7 of the 10 occasions when there was more than just a single thunderstorm report. The occurrence of SFLOCS in the early morning serves as an indication of those situations where dynamical triggering agents are active. To summarise, when the Crawley 900 m. wind direction is between 160 and 230° and the Aughton

/direction

direction is between 180 and 240° inclusive, storms should not be forecast for area B, unless there is evidence of SFLOCS over the area defined above, prior to 0600 GMT.

Although there is a high proportion of failures when the Crawley 900 m. wind direction is between 360 and 060°, the general effect is not too serious, because there are so few cases in this category. It was impossible to draw any definite conclusions from only 17 cases, but an analysis of the Crawley and Hemsby winds suggested that a direct track from the North Sea tended to inhibit storms. In Fig.23, the plotted weather categories show the position from which an air parcel would start, if it were to reach London 8 hours later. It was assumed that the parcel moved with the mean of the Crawley and Hemsby 1200 GMT 900 m. wind velocities. Most of the failures originated over the North Sea, while thunderstorms were largely associated with a track from E. Anglia or Lincolnshire. A comparison of the totals of thunderstorms and SFLOCS for areas A and B is revealing. On these 17 occasions, during the period 0600-1800 GMT, there were only 16 station reports of thunder in area A, compared with 176 in area B. The correspohding SFLOC totals were 77 for area A and 133 for area B. Thus, storms occur even less readily in area A when the flow is from this particular direction.

These extra restrictions on the issue of a positive storm forecast would remove no less than 39 of the 74 failures in Table 24, at the same time missing only an additional 5 days with more than a single thunderstorm report. The rules have not been tested on independent data, but they appear to be well-founded and should produce a significant improvement in the skill scores with independent data.

11. Conclusions.

A method has been presented, based on parcel theory, for forecasting the occurrence of hail and thunder over S.E. England in summer. Tests on independent actual data show that the method is superior to the best of the instability indices in current use, the skill scores being about 0.1 higher on average. Hail appears to occur most frequently in association with the LP+ category and a threshold of 300 j/kg is suggested for hail of 1 cm. diameter. A threshold of 200 j/kg. is proposed for a forecast of widespread storms.

Additional requirements, which must be satisfied for a positive forecast of hail and thunder, are postulated. These extra criteria are related to the synoptic situation and the recent history of the air (in particular the question

/of

of a land or sea track). Two of the years (1960 and 1961) used in the development of the method and the determination of the critical values of the parameters, were years of exceptional thunderstorm activity. Before applying the technique to other data, it might be worthwhile to review the criteria on the basis of the data from the complete seven-year period.

The method should be equally applicable to other areas in the British Isles, although the critical values of the parameters and the local wind restrictions will have to be determined for each region. Improvements and extensions of the method are possible; for example it could be adopted to utilise the forecast thicknesses of 100 mb. layers with a corresponding improvement in the resolution of the scheme.

Finally, this investigation emphasised that the skill score is a very variable quantity which fluctuates considerably from year to year. It would be dangerous to compare the skill scores with those from other investigations, because the values are determined to a certain extent by the procedure adopted for the tests. Reliable comparisons can only be made if the different techniques are compared under identical conditions.

REFERENCES

1. Winston, J.S. — Editor 1956: Forecasting tornadoes and severe thunderstorms. Forecasting guide No.1. Washington D.C. U.S. Weather Bureau 34 pp.

2. Jones, R.F. — Meteorology and supersonic flight. Nature London 212. 1966. p.1181.

3. Jefferson, G.J. — A further development of the instability index. Met. Mag. London 92. 1963. p.313.

4. Bushby, F.H. and Timpson, M.S. — A ten-level atmospheric model and frontal rain. Q.J. London 93. 1967. p.1.

5. Mason, B.J. — Charge generation in thunderstorms. Coroniti S.C. Problems of atmospheric and space electricity. Proceedings of the Third International Conference. Amsterdam 1965. p.239.

6. Mason, B.J. — On the melting of hailstones. Q.J. London 82. 1956. p.209.

7. Coles, V.R. — Current methods of forecasting hail. MRCP. 82. 1961.

8. Douglas, R.H. and Hitschfeld, W. — Patterns of hailstorms in Alberta. Q.J. London 85. 1959. p.105.

9. Petterssen, S. Knighting, E, James, R.W. and Herlofson, N. — Convection in theory and practice. Geofysiske Publikasjoner Oslo 16 (No.10) 1946. p.1-44.

10. Bjerknes, J. — Saturated adiabatic ascent of air through a dry-adiabatically descending environment. Q.J. London 64. 1938. p.325.

11. Scorer, R.S. — Experiments on the convection of isolated masses of buoyant fluid. J. Fluid Mech. London 2. 1957 p.583

12. Byers, H.R. and Braham, R.R. — The thunderstorm. U.S. Dept. of Commerce Washington D.C. 1949.

13. Long, M.J. Hanks, H.H. and Beebe, R.G. — Tropopause penetrations by cumulonimbus clouds. Atmospheric Research and Development Corporation Kansas City Missouri Contract No. AF 19 (628)-2454 Final report 1965 26 pp.

14. Newton, C.W. — Dynamics of severe convective storms. Met. Monographs Lancaster Pa 5 (No. 27) 1963 p.33.

15. Ludlam, F.H. — The hail problem. Nubila Verona Anno I (N1) 1958 p.12.

16. Ludlam, F.H. — The problem of forecasting the occurrence and severity of hailstorms. MRCP 84 1961.

17. Wichmann, H. — Über das Vorkommen und Verhalten des Hagels in Gewitterwolken. Ann. Meteor. Hamburg 4. 1951 p.218.

18. Saunders, W.E. — Tests of thunderstorm forecasting methods. Met.Office Forecasting techniques branch memorandum No.8. London 1965.

19. Siskin, N.S. — The use of a slice method for forecasting convective cloudiness and precipitation. Leningrad GUEMS, Works of All-Union Scientific Meteorological Council Vol.III Synoptic Met. Gidrometeorizdat 1963.

20. Roach, W.T. — An analysis of eight flights by U-2 aircraft over severe storms in Oklahoma. Washington Environ. Sci Serv. Admin. Inst. Environ. Res. Nat. Severe Storms Lab. Tech. Mem. No. 29 1966 p.23.

21. McDonald, J.E. — An aid to computation of terminal fall velocities of spheres. Journal of Met. Lancaster Pa. 17 1960 p.463.

22. Fawbush, E.J. and Miller, R.C. — A method for forecasting hailstone size at the earth's surface. Bull. Amer. Met. Soc. Boston 34 1953 p.235.

23. Foster, D.S. and Bates, F.C. — A hail-size forecasting technique. Bull. Amer. Met. Soc. Boston 37 1956 p.135.

24. Atkinson, B.W. — Some synoptic aspects of thunder outbreaks over South-east England 1951-1960. Weather London 21 1966 p.203.

25. Miller, R.C. and Starrett, L.G. — Thunderstorms in Great Britain. Met. Mag. London 91 1962 p.247.

26. Saunders, W.E. — Further tests of thunderstorm forecasting methods. Met. Office. Forecasting techniques branch memorandum No. 14. London 1967.

27. Rackliff, P.G. — Application of an instability index to regional forecasting. Met. Mag. London 91. 1962 p.113.

28. Boyden, C.J. — A simple instability index for use as a synoptic parameter. Met. Mag. London 92 1963 p.198.

29. Jefferson, G.J. — A modified instability index. Met. Mag. London 92 1963 p.92.

30. Dorsch, R.G. and Hacker, P.T. — A photo-micrographic investigation of the spontaneous freezing temperatures of supercooled water droplets. Tech. Notes nat. adv. Comm. Aero. Washington No. 2142, 1950.

31. Findeisen, W. and Schulz, G. — Experimentelle Untersuchungen über die atmosphärische. Eisteilchenbildung I. Berlin Forsch. Erfahrb. Reichowetterd A No. 27 1944.

32. Hanssen, A.W. — An objective method for thunderstorm forecasts. De Bilt, K. Ned Met. Inst. Wetensch Rapp 62-1, 1962.

33. Faust, H. — "Verdunstungslabilitat" - ein neues Mass der atmosphärischen Labilität. Zeit. Meteorol. Berlin 4 1950 p.97.

34. Johnson, D.H. — Forecast verification; a critical survey of the literature. Unpublished: copy available in the Met. Office Library.

APPENDIX 1

CONTINGENCY TABLES FOR THE

ADIABATIC ENERGY METHOD

CRAWLEY 1200 GMT ASCENT

MAY-SEPTEMBER 1960-62 AREA B DEPENDENT DATA

Verification period 1) 0600-1800 GMT

Actual Weather

Class	x	T1	T2	T3	T4	T5	T6	HO	H1	H2	H3	H4	H5	H6
LN	165	5	2	3	0	0	0	2	0	0	0	0	0	0
CST	22	1	0	1	0	0	0	0	0	0	0	0	0	0
WST	89	8	2	2	0	0	1	0	0	1	0	0	0	0
UT-	26	5	0	0	0	0	0	0	0	0	1	1	1	0
LP-	4	0	0	0	0	0	0	0	0	0	0	0	0	0
DRY	1	0	1	0	0	0	0	0	0	0	0	0	0	0
ULN	0	0	0	1	0	0	0	0	0	0	0	0	0	0
UT+	11	5	6	5	5	2	0	0	1	0	0	3	1	1
LP+	11	4	9	5	3	3	1	3	1	4	5	7	7	5

6 cases with no data

Skill score = 0.66 including T1 cases
0.73 excluding T1 cases

2) 0600-2400 GMT

Actual Weather

Class	x	T1	T2	T3	T4	T5	T6	HO	H1	H2	H3	H4	H5	H6
LN	156	8	4	6	1	0	0	2	0	0	0	0	0	0
CST	22	1	0	0	1	0	0	0	0	0	0	0	0	0
WST	83	11	4	2	0	0	1	0	0	2	0	0	0	0
UT-	23	4	2	1	0	0	0	0	0	0	1	0	3	0
LP-	3	1	0	0	0	0	0	0	0	0	0	0	0	0
DRY	1	0	1	0	0	0	0	0	0	0	0	0	0	0
ULN	0	0	0	1	0	0	0	0	0	0	0	0	0	0
UT+	11	4	5	6	5	3	0	0	1	0	0	3	1	1
LP+	9	6	8	5	3	4	1	2	0	6	4	7	8	5

6 cases with no data

Skill score = 0.59 including T1 cases
0.67 excluding T1 cases

APPENDIX 2a

CONTINGENCY TABLES FOR THE

JEFFERSON INDEX

CRAWLEY 1200 GMT ASCENT

MAY-SEPTEMBER 1960-62 AREA B DEPENDENT DATA

Verification Period 1) 0600-1800 GMT

Actual Weather

INDEX	x	T1	T2	T3	T4	T5	T6	H0	H1	H2	H3	H4	H5	H6
-22	188	8	3	2	0	0	0	3	0	2	0	0	0	0
23	37	3	1	0	1	0	0	1	0	1	0	1	0	0
24	36	3	2	2	0	0	0	0	1	1	0	0	0	1
25	24	4	3	2	2	1	0	0	0	0	3	0	0	0
26	17	6	2	2	0	0	1	0	0	1	0	2	2	0
27	20	3	2	3	1	1	0	1	1	0	1	3	0	1
28	7	1	4	3	2	2	0	0	0	0	2	4	2	1
29+	6	0	3	3	2	1	1	0	0	0	0	1	5	3

Skill score = 0.44 including T1 cases
0.48 excluding T1 cases

2) 0600-2400 GMT

Actual Weather

INDEX	x	T1	T2	T3	T4	T5	T6	H0	H1	H2	H3	H4	H5	H6
-22	181	11	5	3	0	0	0	2	0	4	0	0	0	0
23	33	4	2	3	0	0	0	1	0	1	0	0	1	0
24	31	6	3	1	1	0	0	0	0	2	0	0	1	1
25	22	5	1	4	3	1	0	0	0	0	3	0	0	0
26	16	4	5	2	0	0	1	0	0	1	0	1	3	0
27	19	3	2	3	2	1	0	1	1	0	0	4	0	1
28	7	1	3	3	2	3	0	0	0	0	2	4	2	1
29+	5	1	3	2	2	2	1	0	0	0	0	1	5	3

Skill score = 0.39 including T1 cases
0.45 excluding T1 cases

APPENDIX 2b

CONTINGENCY TABLES FOR THE

JEFFERSON INDEX

CRAWLEY 1200 GMT ASCENT

MAY-SEPTEMBER 1960-62 AREA B DEPENDENT DATA

Verification period 1) 0600-1800 GMT

Actual Weather

INDEX	x	T1	T2	T3	T4	T5	T6	HO	H1	H2	H3	H4	H5	H6
-21	148	5	3	1	0	0	0	2	0	2	0	0	0	0
22	40	3	0	1	0	0	0	1	0	0	0	0	0	0
23	37	3	1	0	1	0	0	1	0	1	0	1	0	0
24	36	3	2	2	0	0	0	0	1	1	0	0	0	1
25	24	4	3	2	2	1	0	0	0	0	3	0	0	0
26	17	6	2	2	0	0	1	0	0	1	0	2	2	0
27	20	3	2	3	1	1	0	1	1	0	1	3	0	1
28+	13	1	7	6	4	3	1	0	0	0	2	5	7	4

Skill score = 0.45 including T1 cases
0.46 excluding T1 cases

2) 0600-2400 GMT

Actual Weather

INDEX	x	T1	T2	T3	T4	T5	T6	HO	H1	H2	H3	H4	H5	H6
-21	141	9	4	2	0	0	0	2	0	3	0	0	0	0
22	40	2	1	1	0	0	0	0	0	1	0	0	0	0
23	33	4	2	3	0	0	0	1	0	1	0	0	1	0
24	31	6	3	1	1	0	0	0	0	2	0	0	1	1
25	22	5	1	4	3	1	0	0	0	0	3	0	0	0
26	16	4	5	2	0	0	1	0	0	1	0	1	3	0
27	19	3	2	3	2	1	0	1	1	0	0	4	0	1
28+	12	2	6	5	4	5	1	0	0	0	2	5	7	4

Skill score = 0.41 including T1 cases
0.45 excluding T1 cases

APPENDIX 2c

CONTINGENCY TABLES FOR THE

MODIFIED JEFFERSON INDEX

CRAWLEY 1200 GMT ASCENT

MAY-SEPTEMBER 1960-62 AREA B DEPENDENT DATA

Verification Period 1) 0600-1800 GMT

Actual Weather

INDEX	x	T1	T2	T3	T4	T5	T6	HO	H1	H2	H3	H4	H5	H6
-22	250	15	3	3	0	1	0	2	1	2	1	1	0	0
23	21	0	0	2	1	0	0	1	0	0	1	1	0	0
24	17	2	3	1	1	0	0	0	0	1	0	0	0	0
25	14	5	0	1	0	1	0	1	0	2	0	0	0	1
26	10	3	4	3	1	0	0	0	1	0	1	0	0	1
27	4	0	2	2	1	0	0	0	0	0	0	1	2	0
28	9	2	3	1	2	0	1	1	0	0	1	5	1	0
29+	10	1	5	4	2	3	1	0	0	0	2	3	6	4

Skill score = 0.50 including T1 cases
0.57 excluding T1 cases

2) 0600-2400 GMT

Actual Weather

INDEX	x	T1	T2	T3	T4	T5	T6	HO	H1	H2	H3	H4	H5	H6
-22	236	21	7	6	0	1	0	2	0	4	1	0	1	0
23	18	2	2	1	0	1	0	0	0	1	1	0	1	0
24	17	1	2	3	1	0	0	0	0	1	0	0	0	0
25	12	4	2	1	0	1	0	1	0	2	0	0	1	1
26	10	2	3	4	2	0	0	0	1	0	1	0	0	1
27	4	0	1	2	1	1	0	0	0	0	0	1	2	0
28	9	2	2	2	2	0	1	1	0	0	1	5	1	0
29+	8	3	5	2	4	3	1	0	0	0	1	4	6	4

Skill score = 0.43 including T1 cases
0.51 excluding T1 cases

APPENDIX 2d

CONTINGENCY TABLES FOR THE

MODIFIED JEFFERSON INDEX

CRAWLEY 1200 GMT ASCENT

MAY-SEPTEMBER 1960-62 AREA B DEPENDENT DATA

Verification period 1) 0600-1800 GMT

Actual Weather

INDEX	x	T1	T2	T3	T4	T5	T6	HO	H1	H2	H3	H4	H5	H6
-21	227	14	2	3	0	1	0	2	1	2	1	1	0	0
22	23	1	1	0	0	0	0	0	0	0	0	0	0	0
23	21	0	1	1	1	0	0	1	0	0	1	1	0	0
24	17	2	2	2	1	0	0	0	0	1	0	0	0	0
25	14	5	0	1	0	1	0	1	0	2	0	0	0	1
26	10	3	4	3	1	0	0	0	1	0	1	0	0	1
27	4	0	2	2	1	0	0	0	0	0	0	1	2	0
28+	19	3	8	5	4	3	2	1	0	0	3	8	7	4

Skill score = 0.51 including T1 cases
0.55 excluding T1 cases

2) 0600-2400 GMT

Actual Weather

INDEX	x	T1	T2	T3	T4	T5	T6	HO	H1	H2	H3	H4	H5	H6
-21	215	19	6	5	0	1	0	2	0	4	1	0	1	0
22	21	2	1	1	0	0	0	0	0	0	0	0	0	0
23	18	2	2	1	0	1	0	0	0	1	1	0	1	0
24	17	1	2	3	1	0	0	0	0	1	0	0	0	0
25	12	4	2	1	0	1	0	1	0	2	0	0	1	1
26	10	2	3	4	2	0	0	0	1	0	1	0	0	1
27	4	0	1	2	1	1	0	0	0	0	0	1	2	0
28+	17	5	7	4	6	3	2	1	0	0	2	9	7	4

Skill score = 0.46 including T1 cases
0.52 excluding T1 cases

APPENDIX 2e

CONTINGENCY TABLES FOR THE

RACKLIFF INDEX

CRAWLEY 1200 GMT ASCENT

MAY-SEPTEMBER 1960-62 AREA B DEPENDENT DATA

Verification period 1) 0600-1800 GMT

Actual Weather

INDEX	x	T1	T2	T3	T4	T5	T6	H0	H1	H2	H3	H4	H5	H6
-27	208	11	4	2	0	0	0	3	0	2	0	0	0	0
28	36	3	2	2	2	1	1	0	0	0	0	0	0	0
29	40	5	6	2	0	0	0	0	0	0	1	0	0	0
30	27	3	1	3	1	1	0	0	0	1	1	3	0	2
31	11	5	1	4	3	3	0	1	2	1	2	1	0	0
32	9	0	2	2	0	0	0	0	0	1	1	3	4	0
33	3	0	2	2	2	0	0	0	0	0	0	0	4	1
34+	1	1	2	0	0	0	1	1	0	0	1	4	1	3

Skill score = 0.47 including T1 cases
0.54 excluding T1 cases

2) 0600-2400 GMT

Actual Weather

INDEX	x	T1	T2	T3	T4	T5	T6	H0	H1	H2	H3	H4	H5	H6
-27	199	15	5	5	0	0	0	3	0	3	0	0	0	0
28	31	6	2	3	2	1	1	0	0	0	0	0	1	0
29	38	4	8	2	1	0	0	0	0	0	1	0	0	0
30	23	6	2	2	1	2	0	0	0	1	0	2	2	2
31	11	3	1	4	4	4	0	0	1	3	2	1	0	0
32	9	0	2	2	0	0	0	0	0	1	1	3	4	0
33	2	0	2	3	2	0	0	0	0	0	0	0	4	1
34+	1	1	2	0	0	0	1	1	0	0	1	4	1	3

Skill score = 0.40 including T1 cases
0.50 excluding T1 cases

APPENDIX 2f

CONTINGENCY TABLES FOR THE

RACKLIFF INDEX

CRAWLEY 1200 GMT ASCENT

MAY-SEPTEMBER 1960-62 AREA B DEPENDENT DATA

Verification period 1) 0600-1800 GMT

Actual Weather

INDEX	x	T1	T2	T3	T4	T5	T6	H0	H1	H2	H3	H4	H5	H6
-26	155	6	2	1	0	0	0	2	0	1	0	0	0	0
27	53	5	2	1	0	0	0	1	0	1	0	0	0	0
28	36	3	2	2	2	1	1	0	0	0	0	0	0	0
29	40	5	6	2	0	0	0	0	0	0	1	0	0	0
30	27	3	1	3	1	1	0	0	0	1	1	3	0	2
31	11	5	1	4	3	3	0	1	2	1	2	1	0	0
32	9	0	2	2	0	0	0	0	0	1	1	3	4	0
33+	4	1	4	2	2	0	1	1	0	0	1	4	5	4

Skill score = 0.46 including T1 cases
0.51 excluding T1 cases

2) 0600-2400 GMT

Actual Weather

INDEX	x	T1	T2	T3	T4	T5	T6	H0	H1	H2	H3	H4	H5	H6
-26	150	8	4	2	0	0	0	2	0	1	0	0	0	0
27	49	7	1	3	0	0	0	1	0	2	0	0	0	0
28	31	6	2	3	2	1	1	0	0	0	0	0	1	0
29	38	4	8	2	1	0	0	0	0	0	1	0	0	0
30	23	6	2	2	1	2	0	0	0	1	0	2	2	2
31	11	3	1	4	4	4	0	0	1	3	2	1	0	0
32	9	0	2	2	0	0	0	0	0	1	1	3	4	0
33+	3	1	4	3	2	0	1	1	0	0	1	4	5	4

Skill score = 0.43 including T1 cases
0.50 excluding T1 cases

APPENDIX 2g

CONTINGENCY TABLES FOR THE

BOYDEN INDEX

CRAWLEY 1200 GMT ASCENT

MAY-SEPTEMBER 1960-62 AREA B DEPENDENT DATA

Verification period 1) 0600-1800 GMT

Actual Weather

INDEX	x	T1	T2	T3	T4	T5	T6	H0	H1	H2	H3	H4	H5	H6
-91	71	1	0	0	0	0	0	0	0	0	0	0	0	0
92	56	3	1	0	0	0	0	2	0	1	1	0	0	0
93	78	10	2	1	0	0	0	0	0	0	0	1	0	0
94	75	4	5	3	2	2	0	0	1	2	2	2	1	1
95	28	5	6	8	3	0	0	1	1	1	1	6	1	1
96	15	3	4	2	1	1	2	2	0	1	1	1	3	3
97	9	2	1	2	2	0	0	0	0	0	1	1	4	1
98+	3	0	1	1	0	2	0	0	0	0	0	0	0	0

Skill score = 0.45 including T1 cases
0.48 excluding T1 cases

2) 0600-2400 GMT

Actual Weather

INDEX	x	T1	T2	T3	T4	T5	T6	H0	H1	H2	H3	H4	H5	H6
-91	69	1	1	1	0	0	0	0	0	0	0	0	0	0
92	51	7	1	0	0	0	0	2	0	2	1	0	0	0
93	79	7	2	1	2	0	0	0	0	0	0	0	1	0
94	67	9	4	6	1	3	0	0	0	3	2	2	2	1
95	25	5	8	8	4	0	0	1	1	1	1	5	2	1
96	15	2	5	3	1	1	2	1	0	2	1	1	3	2
97	6	3	2	1	2	1	0	0	0	0	0	2	4	2
98+	2	1	1	1	0	2	0	0	0	0	0	0	0	0

Skill score = 0.43 including T1 cases
0.49 excluding T1 cases

APPENDIX 3

CONTINGENCY TABLES FOR THE

ADIABATIC ENERGY METHOD

MEAN OF CRAWLEY AND HEMSBY 1200 GMT ASCENTS

MAY-SEPTEMBER 1960-62 COMBINED AREA A+B DEPENDENT DATA

Verification period 1) 0600-1800 GMT

Actual Weather

CLASS	x	T1	T2	T3	T4	T5	T6	H0	H1	H2	H3	H4	H5	H6
LN	132	1	2	0	1	0	0	1	0	0	0	0	0	0
CST	12	0	0	0	0	0	0	0	0	0	1	0	0	0
WST	106	18	4	2	1	0	0	2	0	1	1	0	0	0
UT-	15	7	4	1	1	0	0	0	1	0	1	0	0	0
LP-	3	0	0	0	0	0	0	0	0	0	0	0	0	0
DRY	0	1	1	0	0	0	0	0	0	0	0	0	0	0
ULN	0	0	0	0	0	0	0	0	0	0	0	0	0	0
UT+	14	7	3	9	4	2	1	0	0	0	0	1	0	2
LP+	9	2	7	8	5	7	3	1	3	2	7	5	12	9

16 cases with no data

Skill score = 0.61 including T1 cases
0.71 excluding T1 cases

2) 0600-2400 GMT

Actual Weather

CLASS	x	T1	T2	T3	T4	T5	T6	H0	H1	H2	H3	H4	H5	H6
LN	124	5	3	3	0	0	1	1	0	0	0	0	0	0
CST	12	0	0	0	0	0	0	0	0	0	1	0	0	0
WST	99	16	9	4	0	1	0	3	0	1	2	0	0	0
UT-	15	4	4	2	1	1	0	0	1	0	1	0	1	0
LP-	3	0	0	0	0	0	0	0	0	0	0	0	0	0
DRY	0	0	2	0	0	0	0	0	0	0	0	0	0	0
ULN	0	0	0	0	0	0	0	0	0	0	0	0	0	0
UT+	13	4	6	10	4	1	1	0	0	0	0	1	1	2
LP+	8	2	6	8	6	9	3	1	2	3	6	2	12	12

16 cases with no data

Skill score = 0.56 including T1 cases
0.64 excluding T1 cases

APPENDIX 4

CONTINGENCY TABLES FOR THE

RACKLIFF INDEX

MEAN OF CRAWLEY AND HEMSBY 1200 GMT ASCENTS

MAY-SEPTEMBER 1960-62 COMBINED AREAS A+B DEPENDENT DATA

Verification period 1) 0600-1800 GMT

Actual Weather

INDEX	x	T1	T2	T3	T4	T5	T6	H0	H1	H2	H3	H4	H5	H6
-27½	193	13	6	2	1	0	0	3	0	1	0	0	1	0
28	22	3	2	0	0	0	0	0	0	0	1	0	0	0
28½	19	4	0	1	1	0	1	0	1	0	1	0	0	0
29	17	5	2	1	2	1	0	0	0	0	0	0	0	0
29½	14	3	4	3	1	2	0	0	0	0	1	1	0	0
30	9	2	2	4	1	3	1	0	0	0	1	1	0	0
30½	3	1	1	2	3	0	0	0	0	0	0	0	1	2
31+	16	5	4	7	3	3	2	1	3	2	6	4	10	9

14 cases with no data

Skill score = 0.52 including T1 cases
0.59 excluding T1 cases

2) 0600-2400 GMT

Actual Weather

INDEX	x	T1	T2	T3	T4	T5	T6	H0	H1	H2	H3	H4	H5	H6
-27½	182	16	9	6	0	1	0	3	0	1	1	0	0	1
28	21	3	1	1	0	0	0	0	0	0	1	0	1	0
28½	15	4	3	1	1	0	1	1	1	0	1	0	0	0
29	17	4	2	1	2	1	0	0	0	0	0	0	1	0
29½	14	0	6	4	0	2	1	0	0	0	1	0	1	0
30	9	0	3	5	1	3	1	0	0	0	1	1	0	0
30½	3	1	1	2	2	1	0	0	0	0	0	0	0	3
31+	15	3	5	7	5	4	2	1	2	3	5	2	11	10

14 cases with no data

Skill score = 0.46 including T1 cases
0.55 excluding T1 cases

APPENDIX 5

CONTINGENCY TABLES FOR THE

ADIABATIC ENERGY METHOD

CRAWLEY 1200 GMT ASCENT

MAY-SEPTEMBER 1958-59 1963-64 AREA B INDEPENDENT DATA

Verification period 1) 0600-1800 GMT

Actual Weather

CLASS	x	T1	T2	T3	T4	T5	T6	H0	H1	H2	H3	H4	H5	H6
LN	236	8	2	0	0	0	0	0	0	2	1	0	0	0
CST	21	1	2	0	0	0	0	0	0	0	1	0	0	0
WST	99	11	5	3	0	1	0	0	0	1	1	0	0	0
UT-	37	5	1	3	2	0	0	0	0	0	0	1	0	0
LP-	6	0	0	1	2	0	0	0	0	0	0	0	1	0
DRY	4	0	0	0	0	0	0	0	0	0	0	0	0	0
ULN	0	0	0	0	0	1	0	0	0	0	0	0	0	0
UT+	20	6	5	8	2	1	1	0	0	2	2	1	3	0
LP+	32	4	5	10	13	3	1	3	1	0	1	10	12	2

5 cases with no data

Skill score = 0.53 including T1 cases
0.59 excluding T1 cases

2) 0600-2400 GMT

Actual Weather

CLASS	x	T1	T2	T3	T4	T5	T6	H0	H1	H2	H3	H4	H5	H6
LN	228	14	3	0	0	0	0	0	0	1	2	0	1	0
CST	19	2	2	0	1	0	0	0	0	0	1	0	0	0
WST	94	9	9	5	1	1	0	0	0	1	1	0	0	0
UT-	30	6	4	5	2	1	0	0	0	0	0	1	0	0
LP-	4	1	0	2	2	0	0	0	0	0	0	0	1	0
DRY	4	0	0	0	0	0	0	0	0	0	0	0	0	0
ULN	0	0	0	0	0	1	0	0	0	0	0	0	0	0
UT+	17	4	9	7	3	2	1	0	0	0	3	2	3	0
LP+	29	5	5	10	13	5	1	2	1	0	2	8	11	5

5 cases with no data

Skill score = 0.48 including T1 cases
0.56 excluding T1 cases

APPENDIX 6a

CONTINGENCY TABLES FOR THE

JEFFERSON INDEX

CRAWLEY 1200 GMT ASCENT

MAY-SEPTEMBER 1958-59 1963-64 AREA B INDEPENDENT DATA

Verification period 1) 0600-1800 GMT

Actual Weather

INDEX	x	T1	T2	T3	T4	T5	T6	HO	H1	H2	H3	H4	H5	H6
-22	214	9	4	0	0	0	0	2	0	1	1	0	0	0
23	50	3	0	2	0	0	0	0	1	1	0	0	1	0
24	50	5	4	1	0	1	1	0	0	1	1	0	0	0
25	45	3	0	2	1	0	0	0	0	0	1	0	1	0
26	41	6	2	5	2	1	0	0	0	2	0	1	0	0
27	22	4	4	3	5	1	0	1	0	0	0	6	0	0
28	16	3	5	6	4	1	0	0	0	0	2	1	4	0
29+	17	2	1	6	7	2	1	0	0	0	1	4	10	2

5 cases with no data

Skill score = 0.43 including T1 cases
0.46 excluding T1 cases

2) 0600-2400 GMT

Actual Weather

INDEX	x	T1	T2	T3	T4	T5	T6	HO	H1	H2	H3	H4	H5	H6
-22	210	10	6	1	0	0	0	2	0	1	1	0	0	0
23	47	6	0	2	0	0	0	0	1	0	0	0	2	0
24	45	5	6	2	1	1	1	0	0	0	3	0	0	0
25	42	2	3	2	2	0	0	0	0	0	1	0	1	0
26	36	3	8	7	1	2	0	0	0	1	1	1	0	0
27	19	6	4	3	5	2	0	0	0	0	1	4	2	0
28	13	3	5	7	4	3	0	0	0	0	1	2	3	1
29+	13	6	0	5	9	2	1	0	0	0	1	4	8	4

5 cases with no data

Skill score = 0.45 including T1 cases
0.49 excluding T1 cases

APPENDIX 6b

CONTINGENCY TABLES FOR THE

JEFFERSON INDEX

CRAWLEY 1200 GMT ASCENT

MAY-SEPTEMBER 1958-59 1963-64 AREA B INDEPENDENT DATA

Verification period 1) 0600-1800 GMT

Actual Weather

INDEX	x	T1	T2	T3	T4	T5	T6	H0	H1	H2	H3	H4	H5	H6
-21	165	3	4	0	0	0	0	2	0	1	1	0	0	0
22	49	6	0	0	0	0	0	0	0	0	0	0	0	0
23	50	3	0	2	0	0	0	0	1	1	0	0	1	0
24	50	5	4	1	0	1	1	0	0	1	1	0	0	0
25	45	3	0	2	1	0	0	0	0	0	1	0	1	0
26	41	6	2	5	2	1	0	0	0	2	0	1	0	0
27	22	4	4	3	5	1	0	1	0	0	0	6	0	0
28+	33	5	6	12	11	3	1	0	0	0	3	5	14	2

5 cases with no data

Skill score = 0.35 including T1 cases
0.36 excluding T1 cases

2) 0600-2400 GMT

Actual Weather

INDEX	x	T1	T2	T3	T4	T5	T6	H0	H1	H2	H3	H4	H5	H6
-21	163	4	5	0	0	0	0	2	0	1	1	0	0	0
22	47	6	1	1	0	0	0	0	0	0	0	0	0	0
23	47	6	0	2	0	0	0	0	1	0	0	0	2	0
24	45	5	6	2	1	1	1	0	0	0	3	0	0	0
25	42	2	3	2	2	0	0	0	0	0	1	0	1	0
26	36	3	8	7	1	2	0	0	0	1	1	1	0	0
27	19	6	4	3	5	2	0	0	0	0	1	4	2	0
28+	26	9	5	12	13	5	1	0	0	0	2	6	11	5

5 cases with no data

Skill score = 0.39 including T1 cases
0.41 excluding T1 cases

APPENDIX 6c

CONTINGENCY TABLES FOR THE

RACKLIFF INDEX

CRAWLEY 1200 GMT ASCENT

MAY-SEPTEMBER 1958-59 1963-64 AREA B INDEPENDENT DATA

Verification period 1) 0600-1800 GMT

Actual Weather

INDEX	x	T1	T2	T3	T4	T5	T6	H0	H1	H2	H3	H4	H5	H6
-27	245	14	3	0	0	0	1	2	0	2	1	1	0	0
28	70	6	3	2	0	0	0	0	0	0	1	0	0	0
29	49	1	3	4	2	2	0	0	0	0	0	0	0	0
30	31	3	2	6	6	1	0	0	1	1	1	1	4	1
31	32	8	2	5	5	0	0	0	0	1	1	3	4	0
32	15	2	2	5	5	2	1	0	0	1	1	3	2	0
33	8	1	4	2	1	1	0	1	0	0	1	1	4	1
34+	3	0	1	1	0	0	0	0	0	0	0	3	2	0

7 cases with no data

Skill score = 0.39 including T1 cases
0.43 excluding T1 cases

2) 0600-2400 GMT

Actual Weather

INDEX	x	T1	T2	T3	T4	T5	T6	H0	H1	H2	H3	H4	H5	H6
-27	241	12	6	2	0	0	1	2	0	1	2	1	1	0
28	65	6	6	3	1	0	0	0	0	0	1	0	0	0
29	43	3	7	3	3	2	0	0	0	0	0	0	0	0
30	26	6	2	7	5	3	0	0	1	1	1	0	5	1
31	28	7	4	7	6	0	0	0	0	0	2	3	1	3
32	13	2	4	3	5	4	1	0	0	0	1	3	3	0
33	6	3	3	2	2	1	0	0	0	0	2	1	4	1
34+	3	0	0	2	0	0	0	0	0	0	0	3	2	0

7 cases with no data

Skill score = 0.38 including T1 cases
0.42 excluding T1 cases

APPENDIX 6d

CONTINGENCY TABLES FOR THE

RACKLIFF INDEX

CRAWLEY 1200 GMT ASCENT

MAY-SEPTEMBER 1958-59 1963-64 AREA B INDEPENDENT DATA

Verification period 1) 0600-1800 GMT

Actual Weather

INDEX	x	T1	T2	T3	T4	T5	T6	H0	H1	H2	H3	H4	H5	H6
-26	181	8	2	0	0	0	0	1	0	2	1	1	0	0
27	64	6	1	0	0	0	1	1	0	0	0	0	0	0
28	70	6	3	2	0	0	0	0	0	0	1	0	0	0
29	49	1	3	4	2	2	0	0	0	0	0	0	0	0
30	31	3	2	6	6	1	0	0	1	1	1	1	4	1
31	32	8	2	5	5	0	0	0	0	1	1	3	4	0
32	15	2	2	5	5	2	1	0	0	1	1	3	2	0
33+	11	1	5	3	1	1	0	1	0	0	1	4	6	1

7 cases with no data

Skill score = 0.45 including T1 cases
0.48 excluding T1 cases

2) 0600-2400 GMT

Actual Weather

INDEX	x	T1	T2	T3	T4	T5	T6	H0	H1	H2	H3	H4	H5	H6
-26	178	8	4	1	0	0	0	1	0	1	1	1	1	0
27	63	4	2	1	0	0	1	1	0	0	1	0	0	0
28	65	6	6	3	1	0	0	0	0	0	1	0	0	0
29	43	3	7	3	3	2	0	0	0	0	0	0	0	0
30	26	6	2	7	5	3	0	0	1	1	1	0	5	1
31	28	7	4	7	6	0	0	0	0	0	2	3	1	3
32	13	2	4	3	5	4	1	0	0	0	1	3	3	0
33+	9	3	3	4	2	1	0	0	0	0	2	4	6	1

7 cases with no data

Skill score = 0.46 including T1 cases
0.48 excluding T1 cases

APPENDIX 6e

CONTINGENCY TABLES FOR THE

BOYDEN INDEX

CRAWLEY 1200 GMT ASCENT

MAY-SEPTEMBER 1958-59 1963-64 AREA B INDEPENDENT DATA

Verification period 1) 0600-1800 GMT

Actual Weather

INDEX	x	T1	T2	T3	T4	T5	T6	H0	H1	H2	H3	H4	H5	H6
-91	63	2	2	0	0	0	0	0	0	0	1	0	0	0
92	78	1	0	0	0	0	0	0	0	0	0	0	0	0
93	90	6	2	0	0	0	0	0	0	4	0	0	1	0
94	104	8	6	2	1	1	1	3	1	0	2	0	3	0
95	61	10	4	7	3	1	0	1	0	1	1	7	3	0
96	37	6	4	9	7	1	0	0	0	0	1	2	3	1
97	21	1	1	3	7	2	0	0	0	0	0	2	2	0
98+	4	1	1	4	2	1	1	0	0	0	1	1	4	1

Skill score = 0.37 including T1 cases
0.37 excluding T1 cases

2) 0600-2400 GMT

Actual Weather

INDEX	x	T1	T2	T3	T4	T5	T6	H0	H1	H2	H3	H4	H5	H6
-91	62	3	2	0	0	0	0	0	0	0	1	0	0	0
92	76	1	1	1	0	0	0	0	0	0	0	0	0	0
93	86	7	3	1	1	0	0	0	0	2	1	0	1	1
94	100	6	11	3	1	1	1	2	1	0	3	0	3	0
95	53	13	8	8	2	2	0	1	0	0	2	6	4	0
96	31	6	6	8	9	3	0	0	0	0	1	3	3	1
97	17	3	1	3	8	3	0	0	0	0	0	2	1	1
98+	3	2	0	5	2	1	1	0	0	0	1	0	4	2

Skill score = 0.41 including T1 cases
0.41 excluding T1 cases

APPENDIX 7

CONTINGENCY TABLES FOR THE

ADIABATIC ENERGY METHOD

MEAN OF CRAWLEY AND HEMSBY 1200 GMT ASCENTS

MAY-SEPTEMBER 1958-59 1963-64 COMBINED AREA A+B INDEPENDENT DATA

Verification period 1) 0600-1800 GMT

Actual Weather

CLASS	x	T1	T2	T3	T4	T5	T6	HO	H1	H2	H3	H4	H5	H6
LN	191	8	4	1	0	0	1	0	0	0	1	0	0	0
CST	16	2	1	0	0	0	0	0	0	0	2	0	0	0
WST	129	11	10	4	0	2	0	1	0	1	0	0	0	0
UT-	35	3	5	3	1	2	0	0	0	0	0	1	0	0
LP-	4	0	0	0	1	0	0	0	0	0	0	0	0	0
DRY	3	0	1	0	0	0	0	0	0	0	0	0	0	0
ULN	0	0	0	0	0	0	0	0	0	0	0	0	0	0
UT+	17	3	4	7	2	1	0	0	0	1	3	0	3	0
LP+	21	6	8	21	9	6	2	2	0	2	6	6	17	11

10 cases with no data

Skill score = 0.58 including T1 cases
0.64 excluding T1 cases

2) 0600-2400 GMT

Actual Weather

CLASS	x	T1	T2	T3	T4	T5	T6	HO	H1	H2	H3	H4	H5	H6
LN	187	8	6	2	0	0	1	0	0	0	1	0	0	1
CST	16	2	1	0	0	0	0	0	0	0	2	0	0	0
WST	125	11	8	9	1	2	0	0	0	1	1	0	0	0
UT-	29	6	4	5	2	2	0	0	0	0	1	1	0	0
LP-	3	1	0	0	1	0	0	0	0	0	0	0	0	0
DRY	3	0	1	0	0	0	0	0	0	0	0	0	0	0
ULN	0	0	0	0	0	0	0	0	0	0	0	0	0	0
UT+	17	2	3	7	4	1	0	0	0	1	3	0	2	1
LP+	16	7	8	16	14	8	2	2	0	2	4	7	18	13

10 cases with no data

Skill score = 0.55 including T1 cases
0.62 excluding T1 cases

APPENDIX 8

CONTINGENCY TABLES FOR THE

RACKLIFF INDEX

MEAN OF CRAWLEY AND HEMSBY 1200 GMT ASCENTS

MAY-SEPTEMBER 1958-59 1963-64 COMBINED AREA A+B INDEPENDENT DATA

Verification period 1) 0600-1800 GMT

Actual Weather

INDEX	x	T1	T2	T3	T4	T5	T6	H0	H1	H2	H3	H4	H5	H6
-27½	246	11	8	4	0	1	1	1	0	0	1	0	0	0
28	33	2	4	1	0	0	0	0	0	1	0	0	0	0
28½	31	5	2	1	0	0	0	0	0	0	2	0	0	0
29	22	2	2	5	0	2	1	0	0	0	0	0	0	0
29½	19	2	2	3	0	3	0	0	0	0	2	0	2	0
30	15	3	2	5	3	1	0	0	0	1	0	1	2	1
30½	17	2	3	3	2	0	0	0	0	0	0	1	0	1
31+	36	6	10	14	8	4	1	2	0	2	7	5	16	9

7 cases with no data

Skill score = 0.47 including T1 cases
0.51 excluding T1 cases

2) 0600-2400 GMT

Actual Weather

INDEX	x	T1	T2	T3	T4	T5	T6	H0	H1	H2	H3	H4	H5	H6
-27½	240	12	7	7	1	1	1	1	0	0	2	0	0	1
28	33	2	2	3	0	0	0	0	0	1	0	0	0	0
28½	30	4	3	2	0	0	0	0	0	0	2	0	0	0
29	19	3	3	5	1	2	1	0	0	0	0	0	0	0
29½	17	2	3	1	3	3	0	0	0	0	2	0	2	0
30	13	5	2	2	5	1	0	0	0	1	1	1	2	1
30½	15	1	3	5	3	0	0	0	0	0	0	0	0	2
31+	32	8	8	14	9	6	1	1	0	2	5	7	16	11

7 cases with no data

Skill score = 0.48 including T1 cases
0.49 excluding T1 cases

APPENDIX 9

CONTINGENCY TABLES FOR THE

ADIABATIC ENERGY METHOD

CRAWLEY 0001 GMT ASCENT

MAY-SEPTEMBER 1960-62 AREA B INDEPENDENT DATA

Verification period 1) 0600-1800 GMT

Actual Weather

CLASS	x	T1	T2	T3	T4	T5	T6	HO	H1	H2	H3	H4	H5	H6
LN	147	6	5	2	2	1	2	1	1	0	0	1	1	0
CST	8	1	0	0	0	0	0	1	0	0	0	0	0	0
WST	77	6	2	4	1	0	0	0	0	2	0	0	0	0
UT-	41	5	4	0	1	0	0	0	0	1	0	2	0	0
LP-	9	0	0	0	0	0	0	1	0	0	0	0	0	0
DRY	1	0	1	0	0	0	0	0	0	0	0	0	0	0
ULN	0	0	0	0	0	0	0	0	0	0	0	0	0	0
UT+	21	3	3	3	0	0	0	0	0	0	4	1	2	3
LP+	26	7	6	7	4	4	0	1	1	2	2	7	6	3

6 cases with no data

Skill score = 0.43 including T1 cases
0.46 excluding T1 cases

2) 0600-2400 GMT

Actual Weather

CLASS	x	T1	T2	T3	T4	T5	T6	HO	H1	H2	H3	H4	H5	H6
LN	137	11	3	6	3	2	2	1	0	1	0	1	2	0
CST	8	1	0	0	0	0	0	1	0	0	0	0	0	0
WST	72	8	4	5	1	0	0	0	0	2	0	0	0	0
UT-	39	5	6	0	1	0	0	0	0	1	0	1	1	0
LP-	9	0	0	0	0	0	0	1	0	0	0	0	0	0
DRY	1	0	1	0	0	0	0	0	0	0	0	0	0	0
ULN	0	0	0	0	0	0	0	0	0	0	0	0	0	0
UT+	19	4	3	2	2	0	0	0	0	0	3	2	2	3
LP+	24	6	7	8	3	5	0	1	1	3	2	6	7	3

6 cases with no data

Skill score = 0.39 including T1 cases
0.44 excluding T1 cases

APPENDIX 10a

CONTINGENCY TABLES FOR THE

JEFFERSON INDEX

CRAWLEY 0001 GMT ASCENT

MAY-SEPTEMBER 1960-62 AREA B INDEPENDENT DATA

Verification period 1) 0600-1800 GMT

Actual Weather

INDEX	x	T1	T2	T3	T4	T5	T6	HO	H1	H2	H3	H4	H5	H6
-22	158	3	7	1	1	0	0	4	1	2	1	0	0	0
23	41	4	1	1	0	0	1	0	0	0	0	0	0	0
24	35	4	2	0	1	0	0	0	0	1	0	0	0	1
25	31	4	2	3	1	1	1	1	0	0	0	1	1	0
26	23	5	2	2	1	0	0	0	0	0	0	1	2	0
27	19	3	1	3	2	0	0	0	1	2	1	2	0	1
28	11	1	1	3	1	0	0	0	0	0	2	1	2	1
29+	15	4	5	3	1	4	0	0	0	0	2	6	4	3

2 cases with no data

Skill score = 0.37 including T1 cases
0.38 excluding T1 cases

2) 0600-2400 GMT

Actual Weather

INDEX	x	T1	T2	T3	T4	T5	T6	HO	H1	H2	H3	H4	H5	H6
-22	151	5	6	5	1	1	0	3	0	4	1	0	1	0
23	39	4	2	2	0	0	1	0	0	0	0	0	0	0
24	31	6	2	1	1	0	0	0	0	2	0	0	0	1
25	29	5	3	3	1	1	1	1	0	0	0	1	1	0
26	21	6	3	1	2	0	0	0	0	0	0	1	2	0
27	16	5	1	2	4	0	0	0	1	2	1	2	0	1
28	10	1	2	3	0	1	0	0	0	0	1	1	3	1
29+	15	3	5	4	1	4	0	0	0	0	2	5	5	3

2 cases with no data

Skill score = 0.35 including T1 cases
0.37 excluding T1 cases

APPENDIX 10b

CONTINGENCY TABLES FOR THE

JEFFERSON INDEX

CRAWLEY 0001 GMT ASCENT

MAY-SEPTEMBER 1960-62 AREA B INDEPENDENT DATA

Verification period 1) 0600-1800 GMT

Actual Weather

INDEX	x	T1	T2	T3	T4	T5	T6	HO	H1	H2	H3	H4	H5	H6
-21	131	2	4	1	0	0	0	3	0	2	1	0	0	0
22	27	1	3	0	1	0	0	1	1	0	0	0	0	0
23	41	4	1	1	0	0	1	0	0	0	0	0	0	0
24	35	4	2	0	1	0	0	0	0	1	0	0	0	1
25	31	4	2	3	1	1	1	1	0	0	0	1	1	0
26	23	5	2	2	1	0	0	0	0	0	0	1	2	0
27	19	3	1	3	2	0	0	0	1	2	1	2	0	1
28+	26	5	6	6	2	4	0	0	0	0	4	7	6	4

2 cases with no data

Skill score = 0.36 including T1 cases
0.35 excluding T1 cases

2) 0600-2400 GMT

Actual Weather

INDEX	x	T1	T2	T3	T4	T5	T6	HO	H1	H2	H3	H4	H5	H6
-21	125	5	4	3	1	0	0	2	0	3	1	0	0	0
22	26	0	2	2	0	1	0	1	0	1	0	0	1	0
23	39	4	2	2	0	0	1	0	0	0	0	0	0	0
24	31	6	2	1	1	0	0	0	0	2	0	0	0	1
25	29	5	3	3	1	1	1	1	0	0	0	1	1	0
26	21	6	3	1	2	0	0	0	0	0	0	1	2	0
27	16	5	1	2	4	0	0	0	1	2	1	2	0	1
28+	25	4	7	7	1	5	0	0	0	0	3	6	8	4

2 cases with no data

Skill score = 0.34 including T1 cases
0.34 excluding T1 cases

APPENDIX 10c

CONTINGENCY TABLES FOR THE

MODIFIED JEFFERSON INDEX

CRAWLEY 0001 GMT ASCENT

MAY-SEPTEMBER 1960-62 AREA B INDEPENDENT DATA

Verification period 1) 0600-1800 GMT

Actual Weather

INDEX	x	T1	T2	T3	T4	T5	T6	H0	H1	H2	H3	H4	H5	H6
-22	213	11	8	4	1	0	0	3	1	3	2	1	0	1
23	16	2	1	1	1	0	1	1	0	0	1	1	0	0
24	11	0	2	0	1	1	1	0	0	0	0	0	0	0
25	17	3	2	0	1	0	0	1	0	0	0	0	1	1
26	23	2	3	0	1	0	0	0	0	0	0	0	0	0
27	14	3	2	2	0	0	0	0	0	2	1	0	2	0
28	11	3	0	2	1	0	0	0	0	0	0	1	0	1
29+	26	4	3	7	2	4	0	0	1	0	2	8	6	3

4 cases with no data

Skill score = 0.30 including T1 cases
0.30 excluding T1 cases

2) 0600-2400 GMT

Actual Weather

INDEX	x	T1	T2	T3	T4	T5	T6	H0	H1	H2	H3	H4	H5	H6
-22	201	17	8	7	3	0	0	2	0	5	2	1	1	1
23	15	2	1	2	1	0	1	1	0	0	1	1	0	0
24	10	1	2	0	1	1	1	0	0	0	0	0	0	0
25	16	3	1	1	1	0	0	1	0	1	0	0	1	1
26	22	2	4	0	1	0	0	0	0	0	0	0	0	0
27	13	4	2	2	0	0	0	0	0	2	0	1	2	0
28	8	3	2	2	1	1	0	0	0	0	0	1	0	1
29+	25	3	4	7	2	5	0	0	1	0	2	6	8	3

4 cases with no data

Skill score = 0.28 including T1 cases
0.31 excluding T1 cases

APPENDIX 10d

CONTINGENCY TABLES FOR THE

MODIFIED JEFFERSON INDEX

CRAWLEY 0001 GMT ASCENT

MAY-SEPTEMBER 1960-62 AREA B INDEPENDENT DATA

Verification period 1) 0600-1800 GMT

Actual Weather

INDEX	x	T1	T2	T3	T4	T5	T6	H0	H1	H2	H3	H4	H5	H6
-21	190	9	7	3	1	0	0	2	1	3	2	0	0	0
22	23	2	1	1	0	0	0	1	0	0	0	1	0	1
23	16	2	1	1	1	0	1	1	0	0	1	1	0	0
24	11	0	2	0	1	1	1	0	0	0	0	0	0	0
25	17	3	2	0	1	0	0	1	0	0	0	0	1	1
26	23	2	3	0	1	0	0	0	0	0	0	0	0	0
27	14	3	2	2	0	0	0	0	0	2	1	0	2	0
28+	37	7	3	9	3	4	0	0	1	0	2	9	6	4

4 cases with no data

Skill score = 0.30 including T1 cases
0.29 excluding T1 cases

2) 0600-2400 GMT

Actual Weather

INDEX	x	T1	T2	T3	T4	T5	T6	H0	H1	H2	H3	H4	H5	H6
-21	179	15	7	6	2	0	0	1	0	5	2	0	1	0
22	22	2	1	1	1	0	0	1	0	0	0	1	0	1
23	15	2	1	2	1	0	1	1	0	0	1	1	0	0
24	10	1	2	0	1	1	1	0	0	0	0	0	0	0
25	16	3	1	1	1	0	0	1	0	1	0	0	1	1
26	22	2	4	0	1	0	0	0	0	0	0	0	0	0
27	13	4	2	2	0	0	0	0	0	2	0	1	2	0
28+	33	6	6	9	3	6	0	0	1	0	2	7	8	4

4 cases with no data

Skill score = 0.28 including T1 cases
0.30 excluding T1 cases

APPENDIX 10e

CONTINGENCY TABLES FOR THE

RACKLIFF INDEX

CRAWLEY 0001 GMT ASCENT

MAY-SEPTEMBER 1960-62 AREA B INDEPENDENT DATA

Verification period 1) 0600-1800 GMT

Actual Weather

INDEX	x	T1	T2	T3	T4	T5	T6	H0	H1	H2	H3	H4	H5	H6
-27	184	7	6	2	1	1	0	2	0	2	1	0	0	0
28	31	3	4	3	2	0	2	2	1	0	0	0	0	1
29	49	7	1	0	0	0	0	0	0	0	0	0	1	0
30	29	4	2	4	2	0	0	0	0	0	0	0	0	0
31	22	1	1	2	2	1	0	1	0	1	3	1	1	0
32	6	2	4	1	0	1	0	0	1	1	1	2	3	3
33	5	3	2	3	0	2	0	0	0	0	0	4	2	0
34+	8	1	1	1	1	0	0	0	0	1	1	4	2	2

1 case with no data

Skill score = 0.41 including T1 cases
0.46 excluding T1 cases

2) 0600-2400 GMT

Actual Weather

INDEX	x	T1	T2	T3	T4	T5	T6	H0	H1	H2	H3	H4	H5	H6
-27	173	10	7	7	1	2	0	2	0	2	1	0	1	0
28	28	5	3	4	2	0	2	1	0	3	0	0	0	1
29	47	8	2	0	0	0	0	0	0	0	0	0	1	0
30	24	7	4	2	4	0	0	0	0	0	0	0	0	0
31	22	1	1	1	2	2	0	1	0	1	2	2	1	0
32	6	1	4	2	0	1	0	0	1	1	1	1	4	3
33	5	3	2	3	0	2	0	0	0	0	0	4	2	0
34+	8	0	1	2	1	0	0	0	0	1	1	3	3	2

1 case with no data

Skill score = 0.33 including T1 cases
0.41 excluding T1 cases

APPENDIX 10f

CONTINGENCY TABLES FOR THE

RACKLIFF INDEX

CRAWLEY 0001 GMT ASCENT

MAY-SEPTEMBER 1960-62 AREA B INDEPENDENT DATA

Verification period 1) 0600-1800 GMT

Actual Weather

INDEX	x	T1	T2	T3	T4	T5	T6	H0	H1	H2	H3	H4	H5	H6
-26	146	4	5	0	1	0	0	1	0	2	0	0	0	0
27	38	3	1	2	0	1	0	1	0	0	1	0	0	0
28	31	3	4	3	2	0	2	2	1	0	0	0	0	1
29	49	7	1	0	0	0	0	0	0	0	0	0	1	0
30	29	4	2	4	2	0	0	0	0	0	0	0	0	0
31	22	1	1	2	2	1	0	1	0	1	3	1	1	0
32	6	2	4	1	0	1	0	0	1	1	1	2	3	3
33+	13	4	3	4	1	2	0	0	0	1	1	8	4	2

1 case with no data

Skill score = 0.38 including T1 cases
0.40 excluding T1 cases

2) 0600-2400 GMT

Actual Weather

INDEX	x	T1	T2	T3	T4	T5	T6	H0	H1	H2	H3	H4	H5	H6
-26	138	6	5	4	1	1	0	1	0	2	0	0	1	0
27	35	4	2	3	0	1	0	1	0	0	1	0	0	0
28	28	5	3	4	2	0	2	1	0	3	0	0	0	1
29	47	8	2	0	0	0	0	0	0	0	0	0	1	0
30	24	7	4	2	4	0	0	0	0	0	0	0	0	0
31	22	1	1	1	2	2	0	1	0	1	2	2	1	0
32	6	1	4	2	0	1	0	0	1	1	1	1	4	3
33+	13	3	3	5	1	2	0	0	0	1	1	7	5	2

1 case with no data

Skill score = 0.34 including T1 cases
0.38 excluding T1 cases

APPENDIX 10g

CONTINGENCY TABLES FOR THE

BOYDEN INDEX

CRAWLEY 0001 GMT ASCENT

MAY-SEPTEMBER 1960-62 AREA B INDEPENDENT DATA

Verification period 1) 0600-1800 GMT

Actual Weather

INDEX	x	T1	T2	T3	T4	T5	T6	H0	H1	H2	H3	H4	H5	H6
-91	73	1	1	0	0	0	0	0	0	1	0	0	0	0
92	52	2	3	0	1	0	0	1	0	0	1	0	0	0
93	66	5	2	2	3	0	0	2	2	1	0	0	0	0
94	55	8	4	3	1	1	1	0	0	1	2	3	1	2
95	59	6	4	5	2	1	0	1	0	2	3	6	3	2
96	19	4	4	4	0	0	0	1	0	0	0	2	2	1
97	6	2	3	1	0	2	1	0	0	0	0	0	3	1
98+	4	0	0	1	1	1	0	0	0	0	0	0	0	0

1 case with no data

Skill score = 0.27 including T1 cases
0.28 excluding T1 cases

2) 0600-2400 GMT

Actual Weather

INDEX	x	T1	T2	T3	T4	T5	T6	H0	H1	H2	H3	H4	H5	H6
-91	69	3	0	3	0	0	0	0	0	1	0	0	0	0
92	50	1	3	2	0	1	0	0	0	1	1	0	1	0
93	65	4	3	1	4	1	0	2	1	2	0	0	0	0
94	53	9	5	1	3	1	1	0	0	1	2	2	2	2
95	51	10	6	6	2	1	0	1	0	3	2	6	4	2
96	16	5	4	6	0	0	0	1	0	0	0	2	2	1
97	5	3	3	1	0	2	1	0	0	0	0	0	3	1
98+	4	0	0	1	1	1	0	0	0	0	0	0	0	0

1 case with no data

Skill score = 0.31 including T1 cases
0.30 excluding T1 cases

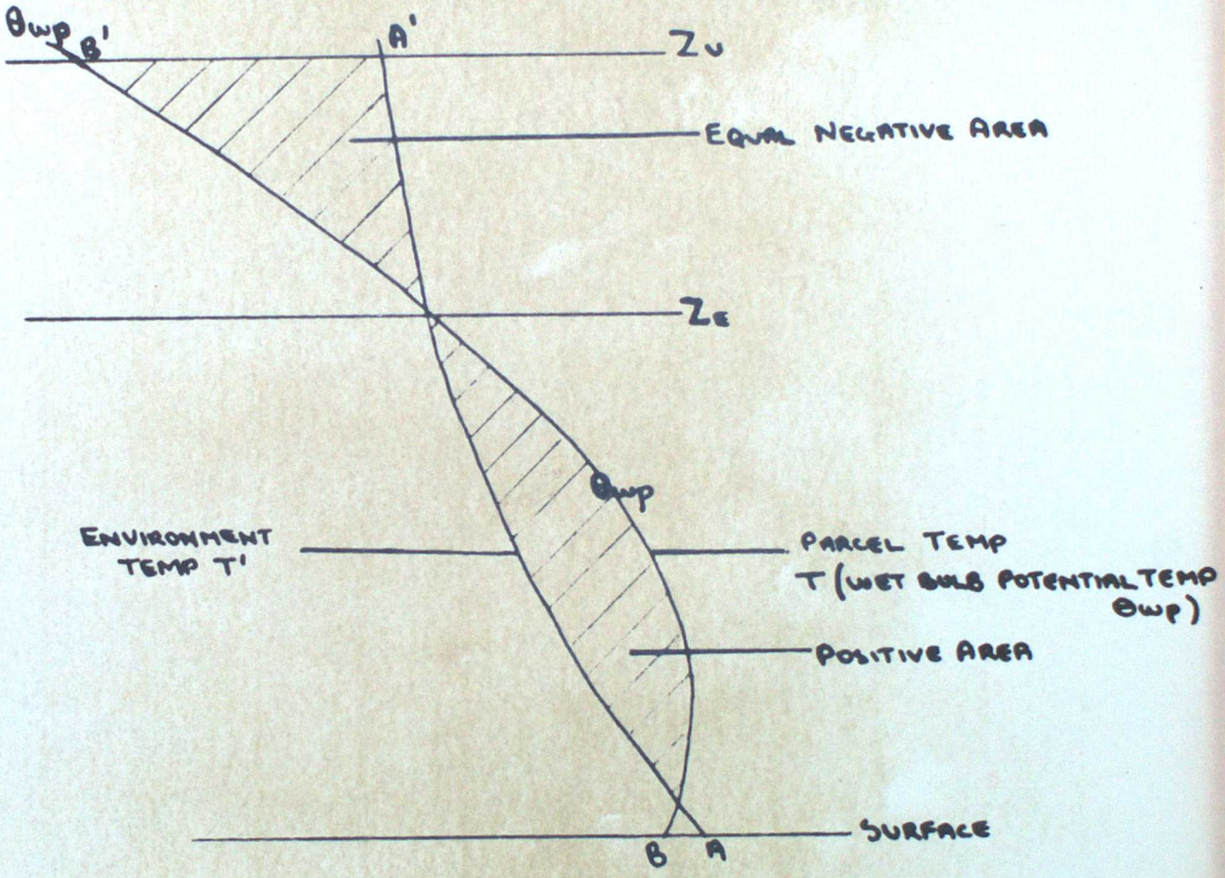

FIG. 1 SCHEMATIC DIAGRAM OF TEPHIGRAM

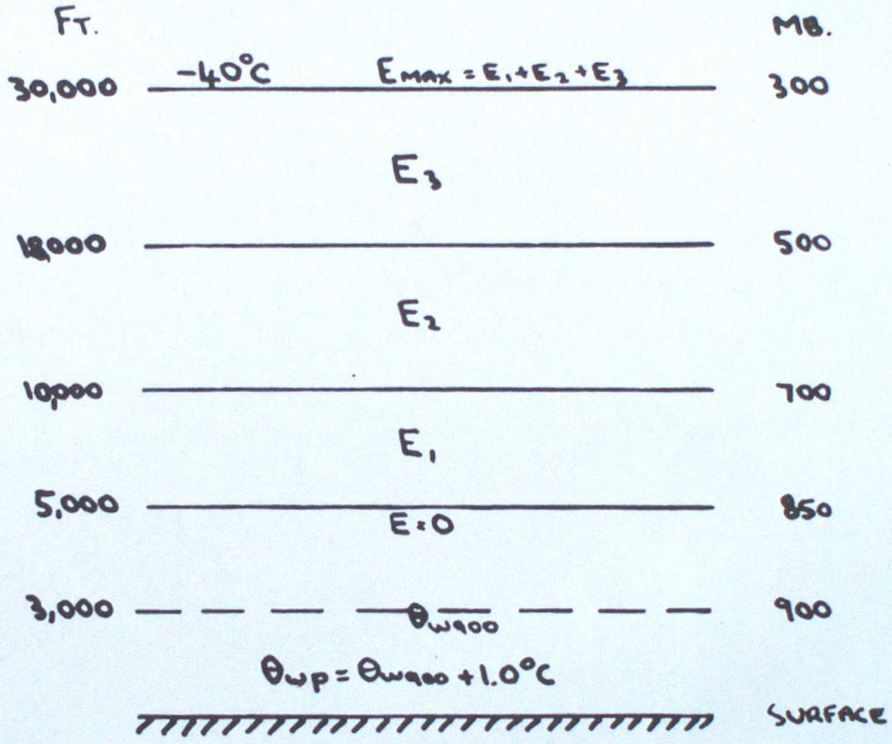

FIG. 2 BASIC SCHEME FOR CALCULATING EMAX

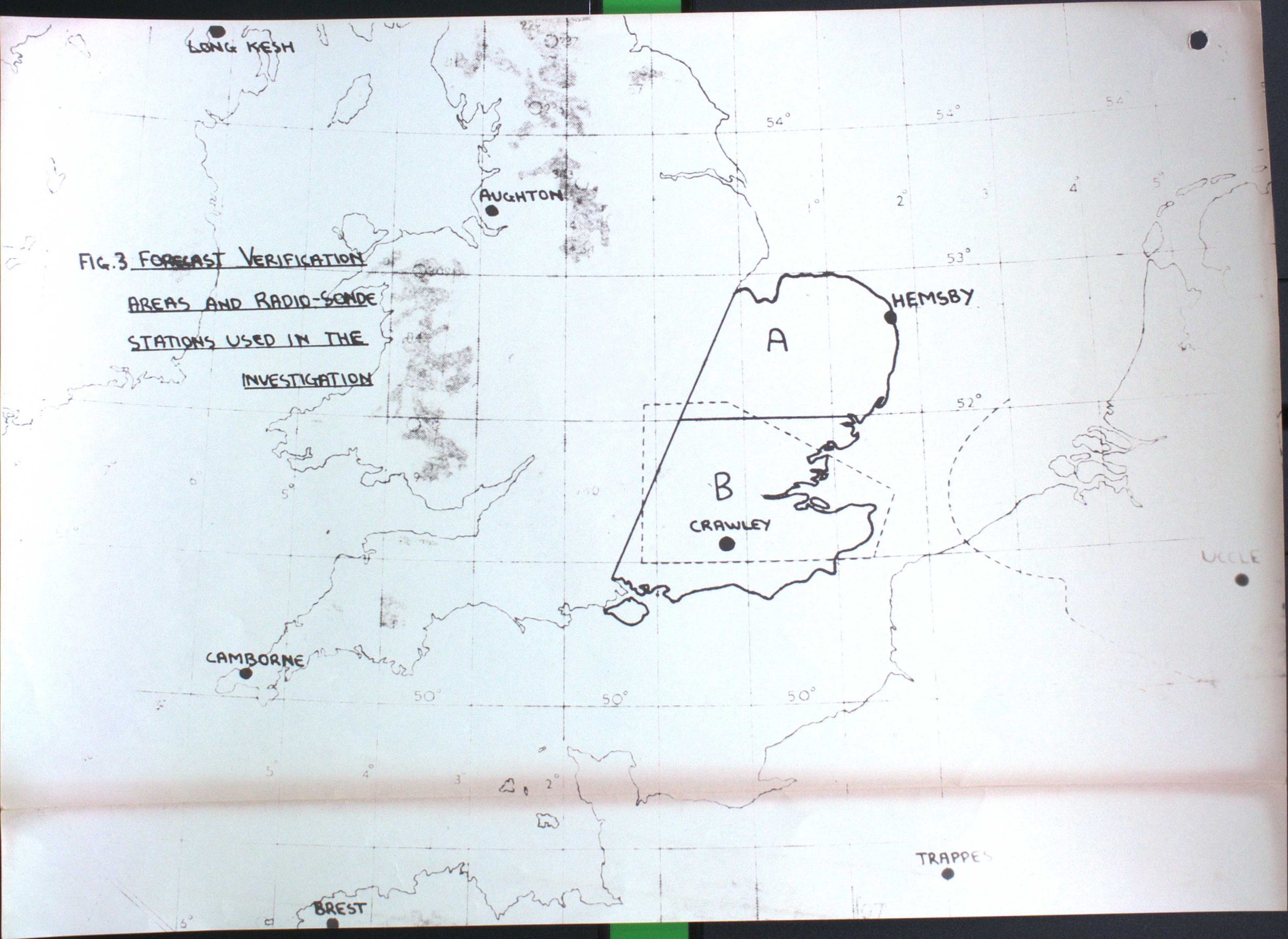

FIG. 3 FORECAST VERIFICATION AREAS AND RADIO-SONDE STATIONS USED IN THE INVESTIGATION

FIG. 4:- WEATHER CATEGORY FOR AREA B (0600-1800 G.M.T.) AS A FUNCTION OF E_2 AND θ_{wp} (CRAWLEY 1200 G.M.T. ASCENT). PERIOD MAY-SEPT. 1960-62

ALL LN CASES ARE EXCLUDED

SQUARE BRACKETS INDICATE THAT E_3 IS POSITIVE

E_2 (JOULES/KG.)

1000
800
600
400
200
0
-200
-400
-600
-800
-1000
-1200
-1400
-1600
-1800

COLD

WARM

2 4 6 8 10 12 14 16 18 20

PARCEL WET BULB POTENTIAL TEMPERATURE θ_{wp} (°C)

FIG. 5:- WEATHER CATEGORY FOR AREA B (0600-1800 G.M.T) AS A FUNCTION OF E_2 AND θ_{WP} (CRAWLEY 1200 G.M.T ASCENT). PERIOD MAY-SEPT 1960-62

DAYS WITH $E_{MAX} \geq 30$ JOULES/KG

SQUARE BRACKETS INDICATE THAT E_3 IS POSITIVE

E_2 (JOULES/KG)

1000
800
600
400
200
0
-200
-400
-600
-800
-1000
-1200
-1400
-1600
-1800

COLD

WARM

2 4 6 8 10 12 14 16 18 20

PARCEL WET BULB POTENTIAL TEMPERATURE θ_{WP} (°C)

FIG 6:- WEATHER CATEGORY FOR WARM ZONE CASES AS A FUNCTION OF $(E_2 - E_1)$ AND θ_{wp}

CRAWLEY 1200 G.M.T AVERN. AREA B (0600-1800 G.M.T) PERIOD MAY-SEPT. 1960-62

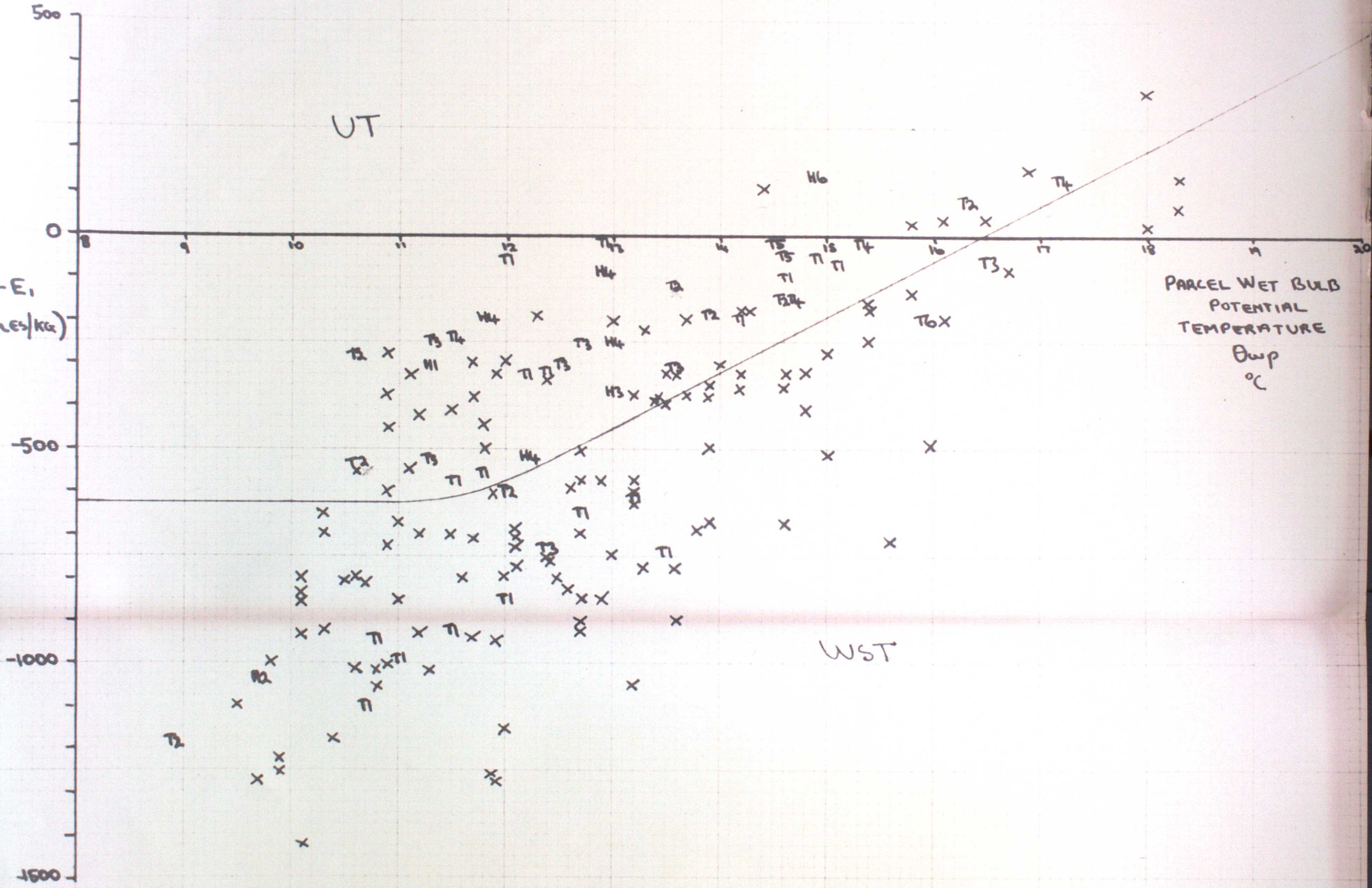

FIG 7.- WEATHER CATEGORY FOR COLD ZONE CASES WITH $E_{max} < 30$ JOULES/KG AS A FUNCTION OF (E_2-E_1) AND θ_{wp} CRAWLEY 1200 G.M.T. ASCENT. AREA B (0600-1800 GMT.). PERIOD MAY-SEPT 1960-62

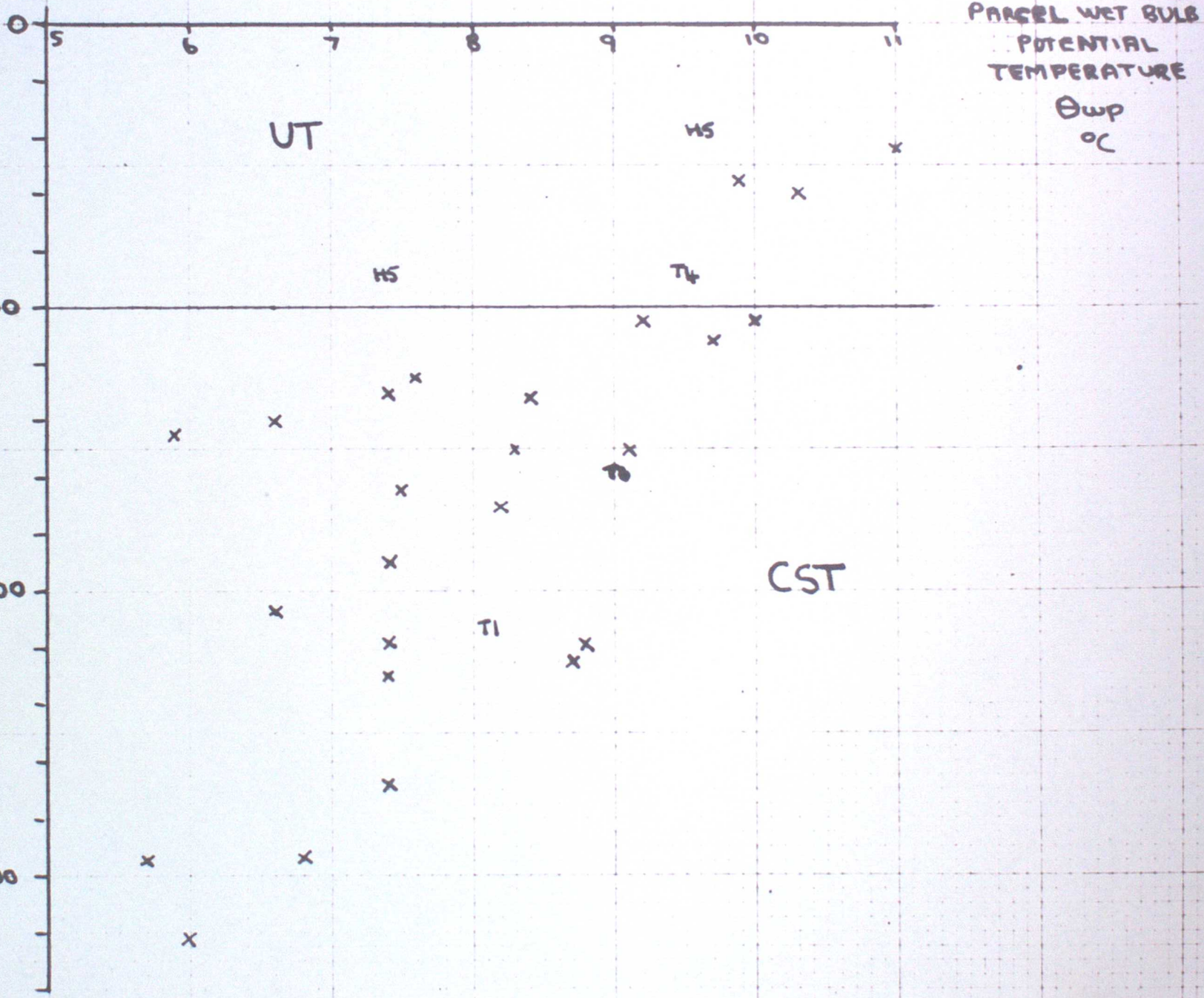

FIG. 8:- FINITE DIFFERENCE GRID FOR EVALUATING THE LAPLACIAN OF THE CONTOUR HEIGHT AND SURFACE PRESSURE FIELDS

FIG 9:- WEATHER CATEGORY FOR THE UNSTABLE TYPE (UT) CASES AS A FUNCTION OF THE 1200 G.M.T. VORTICITY INDICES AT THE SURFACE AND 700 MB. CRAWLEY 1200 G.M.T. ASCENT AREA B (0600-1800 G.M.T.) PERIOD MAY-SEPT 1960-62

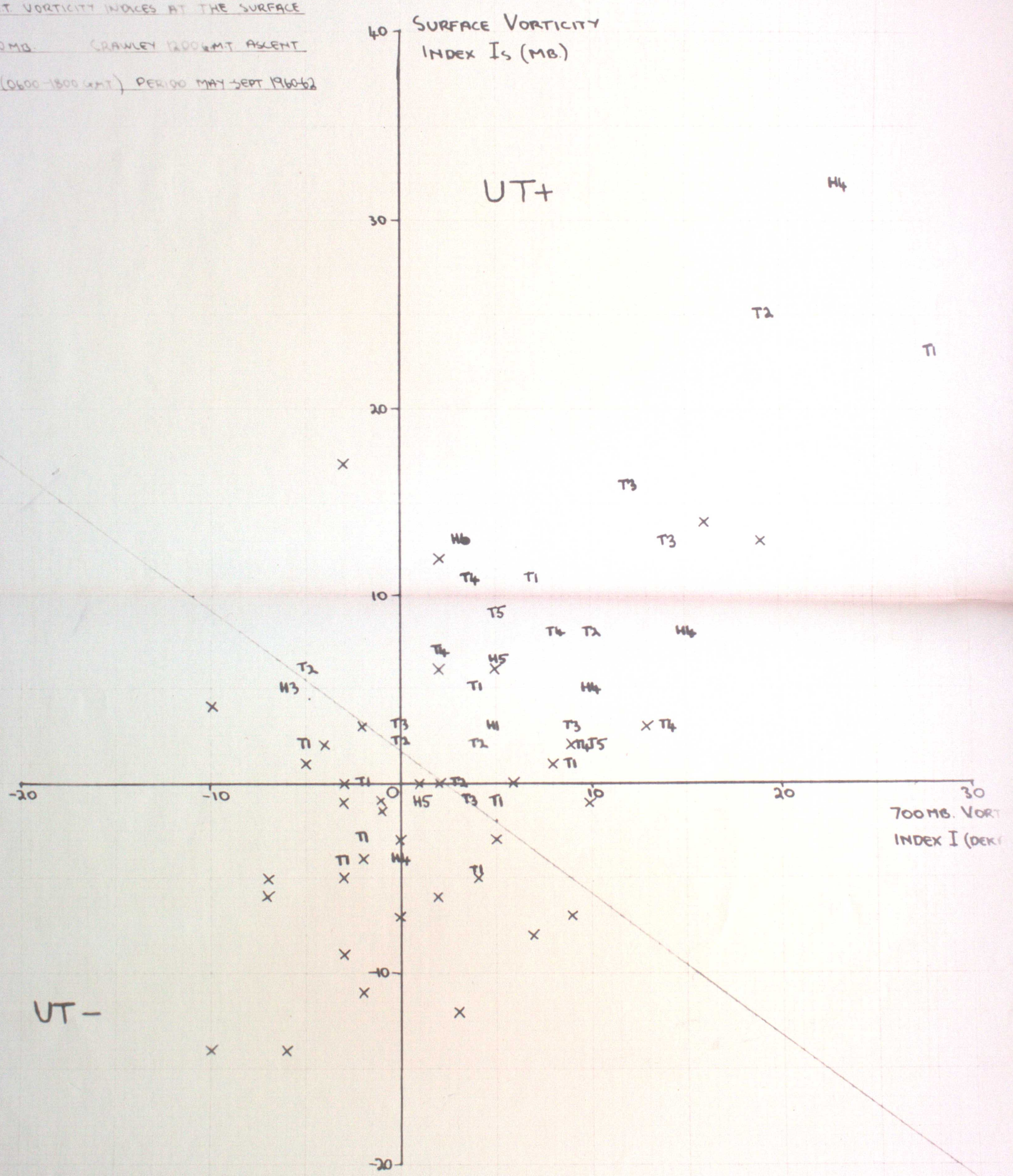

FIG. 10 :- WEATHER CATEGORY FOR THE LARGE POSITIVE ENERGY (LP) CASES AS A FUNCTION OF THE 1200 G.M.T. VORTICITY INDICES AT THE SURFACE AND 700 MB. CRAWLEY 1200 G.M.T. ASCENT AREA B (0600-1800 G.M.T). PERIOD MAY-SEPT 1961&62

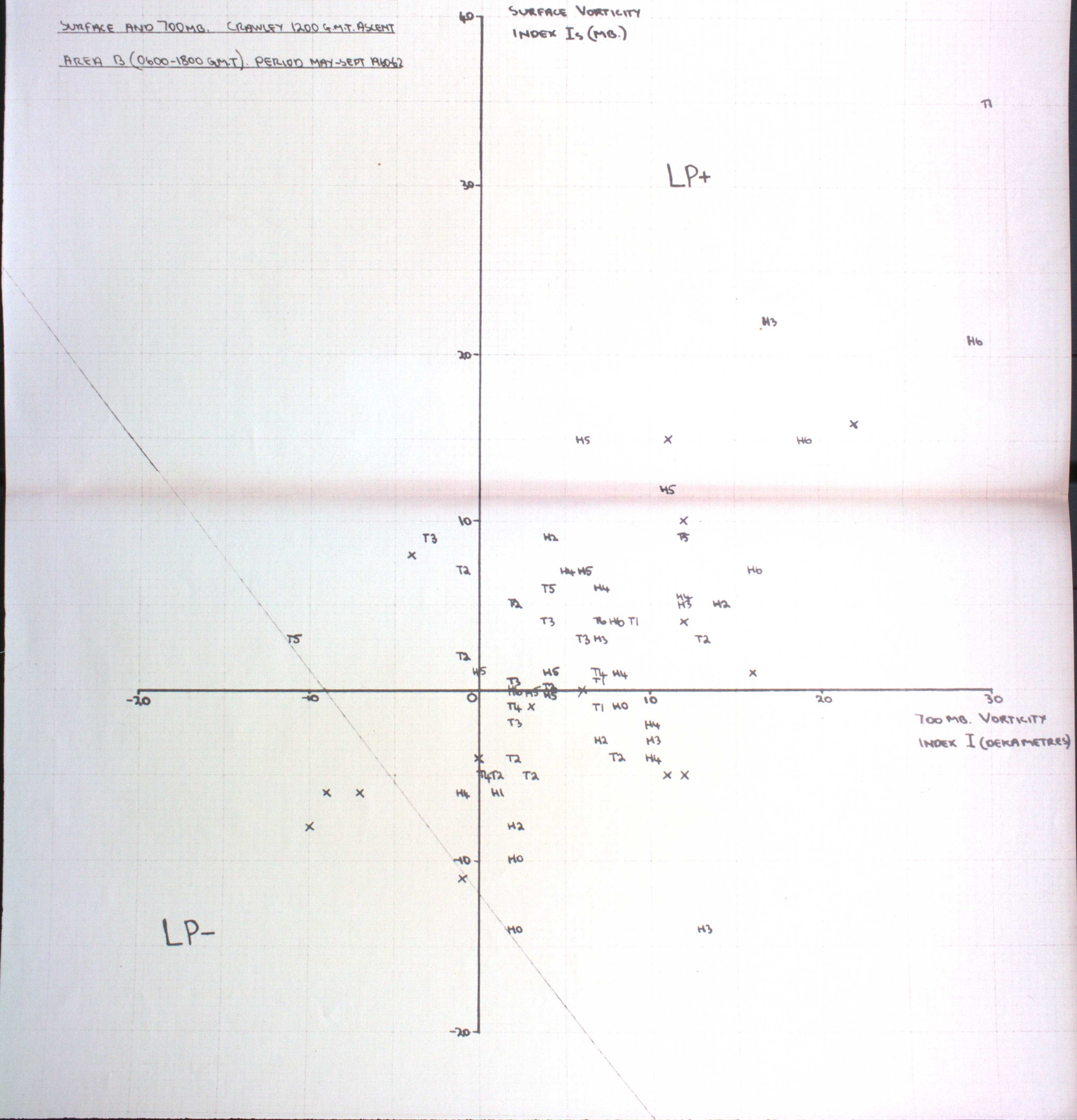

FIG. 11 :- FLOW DIAGRAM OF HAIL-THUNDERSTORM FORECASTING SCHEME FOR AREA B

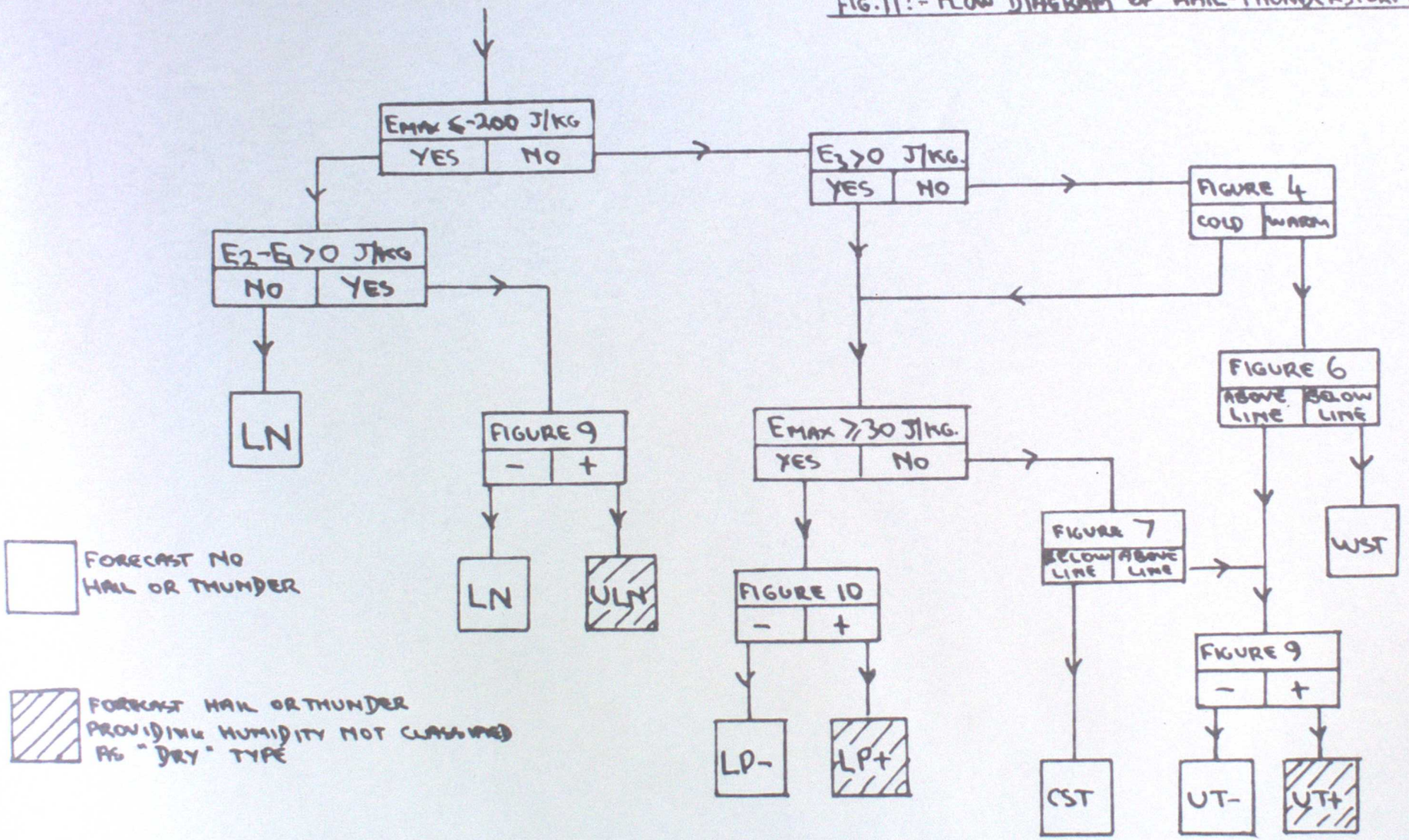

FIG. 12:- WEATHER CATEGORY FOR AREA A+B (0600-1800 G.M.T) AS A FUNCTION OF E_2 AND θ_{wp} (MEAN OF CRAWLEY AND HEMSBY 1200 G.M.T. ASCENTS. PERIOD MAY-SEPT. 1960+62

ALL LN CASES ARE EXCLUDED

SQUARE BRACKETS INDICATE THAT E_3 IS POSITIVE

COLD

WARM

E_2 (JOULES/KG.)

PARCEL WET BULB POTENTIAL TEMPERATURE θ_{wp} (°C)

1000
800
600
400
200
0
-200
-400
-600
-800
-1000
-1200
-1400
-1600
-1800

2 4 6 8 10 12 14 16 18 20

FIG.13 :- WEATHER CATEGORY FOR AREA A+B (0600-1800 G.M.T) AS A FUNCTION OF E_2 AND θ_{wp} (MEAN OF CRAWLEY AND HEMSBY 1200 GMT ASCENTS). PERIOD MAY-SEPT 1960-62. DAYS WITH $E_{MAX} \geqslant 0$ JOULES/KG.

SQUARE BRACKETS INDICATE THAT E_3 IS POSITIVE

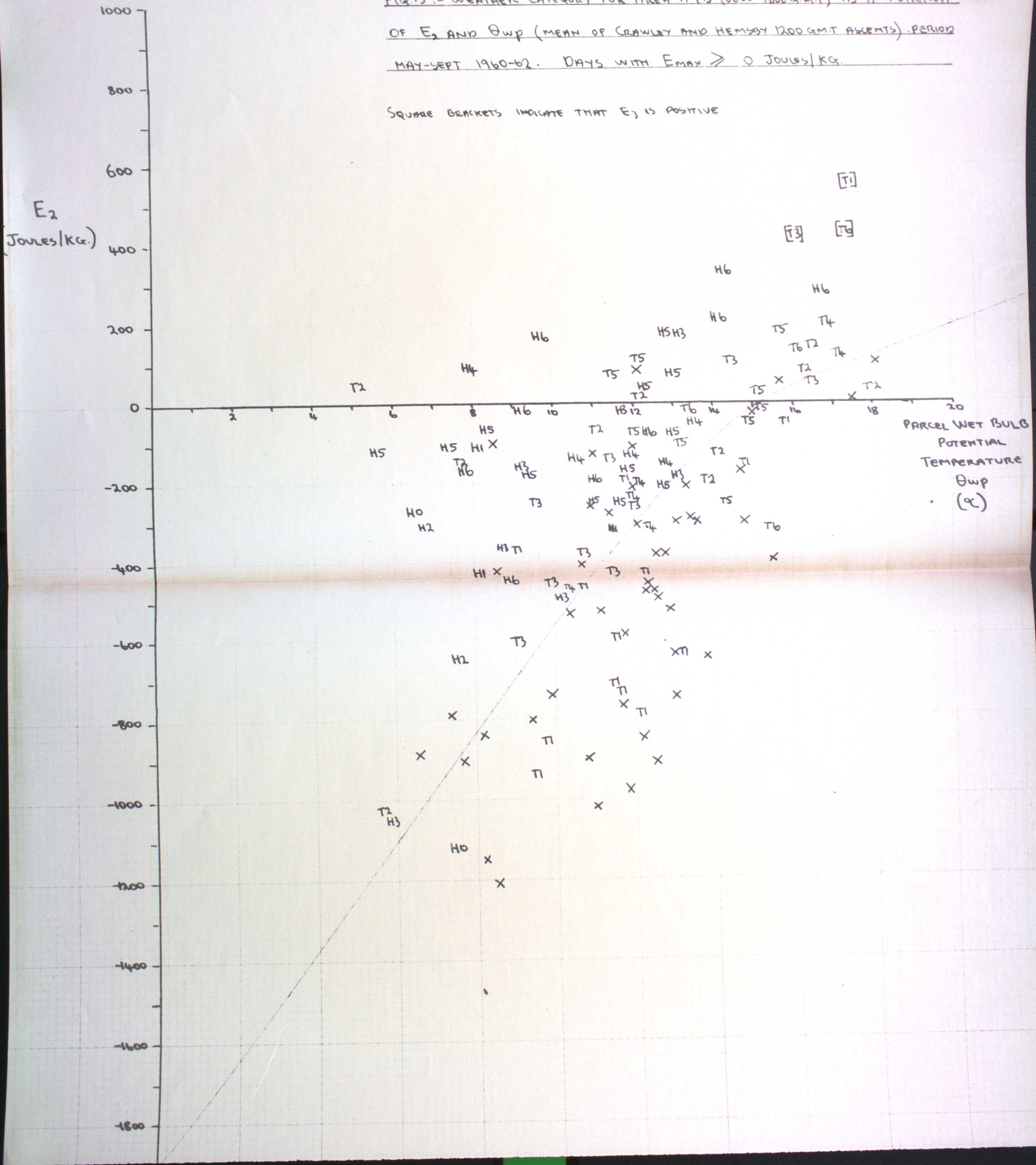

FIG 14:- WEATHER CATEGORY FOR WARM ZONE CASES AS A FUNCTION OF (E_2-E_1) AND θ_{wp}

MEAN OF CRAWLEY AND HEMSBY 1200 G.M.T. ASCENTS AREA A+B (0600-1800 G.M.T.) PERIOD MAY-SEPT 1960-62

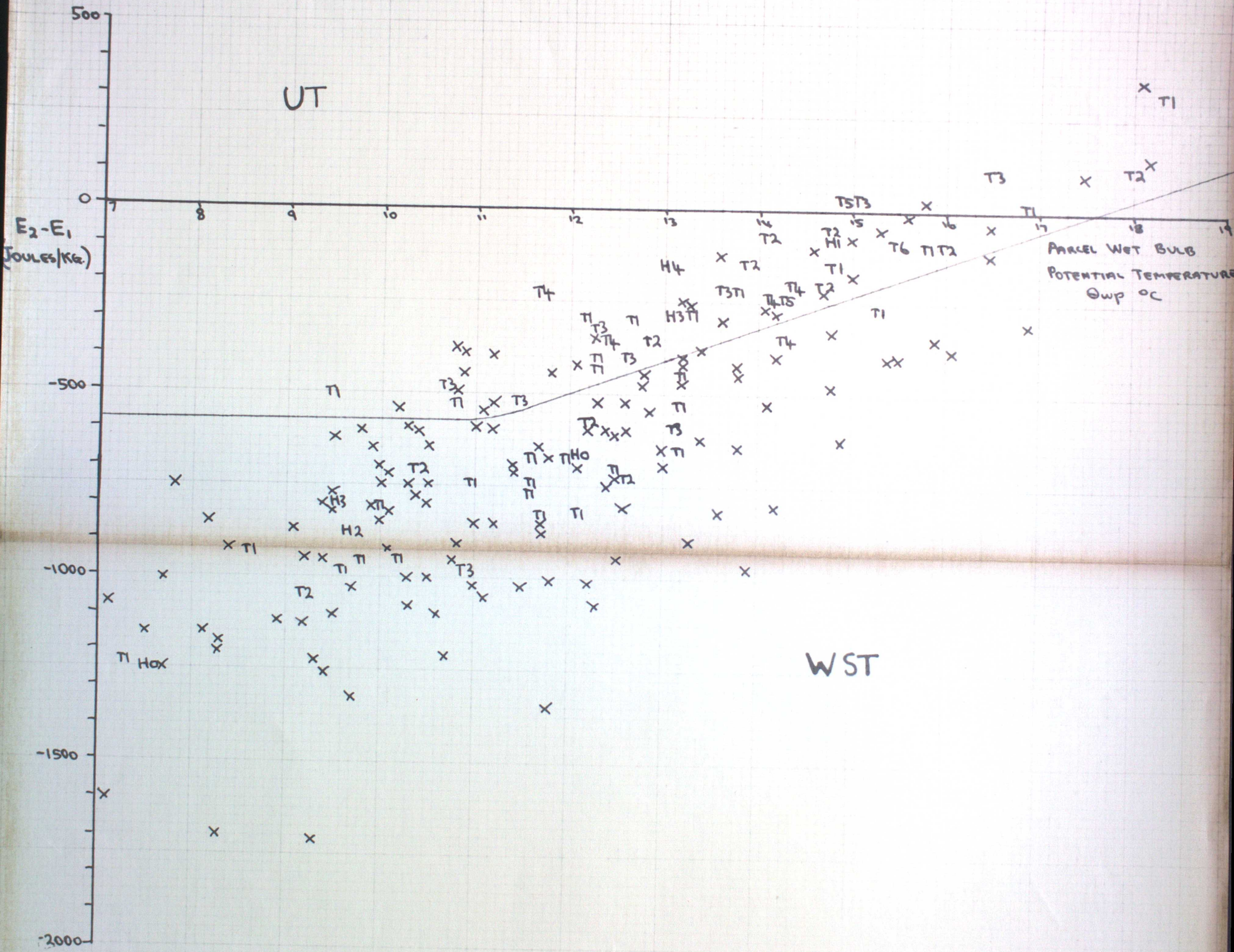

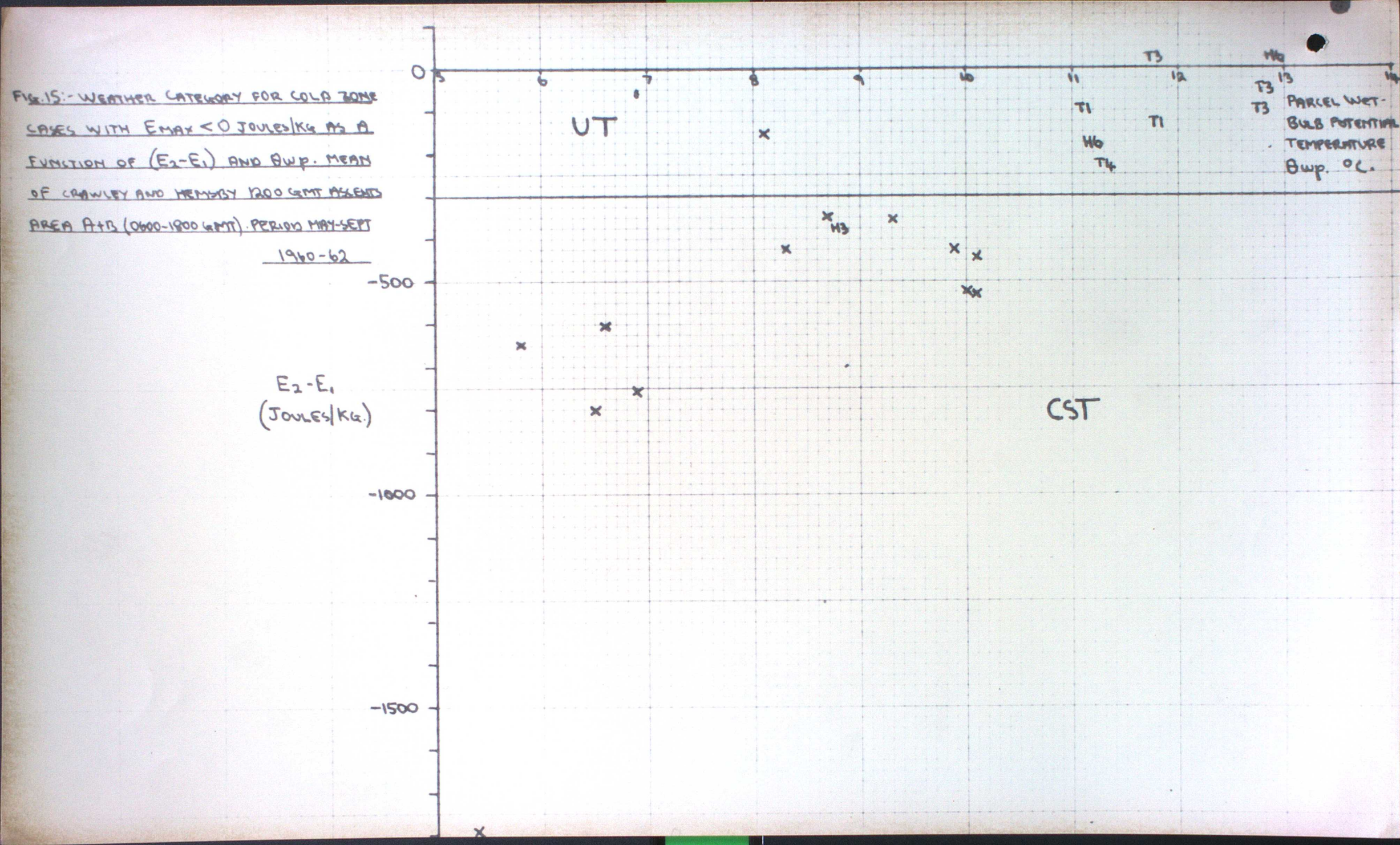

FIG. 15:- WEATHER CATEGORY FOR COLA ZONE CASES WITH $E_{MAX} < 0$ JOULES/KG AS A FUNCTION OF $(E_2 - E_1)$ AND θ_{wp}. MEAN OF CRAWLEY AND HEMSBY 1200 GMT ASCENTS AREA A+B (0600-1800 GMT). PERIOD MAY-SEPT 1960-62

FIG 16:- WEATHER CATEGORY FOR THE UNSTABLE TYPE (UT) CASES AS A FUNCTION OF THE 1200 G.M.T. VORTICITY INDICES AT THE SURFACE AND 700 MB. MEAN OF CRAWLEY AND HEMSBY 1200 G.M.T. ASCENTS. AREA A+B (0600-1800 GMT) PERIOD MAY-SEPT. 1960-62.

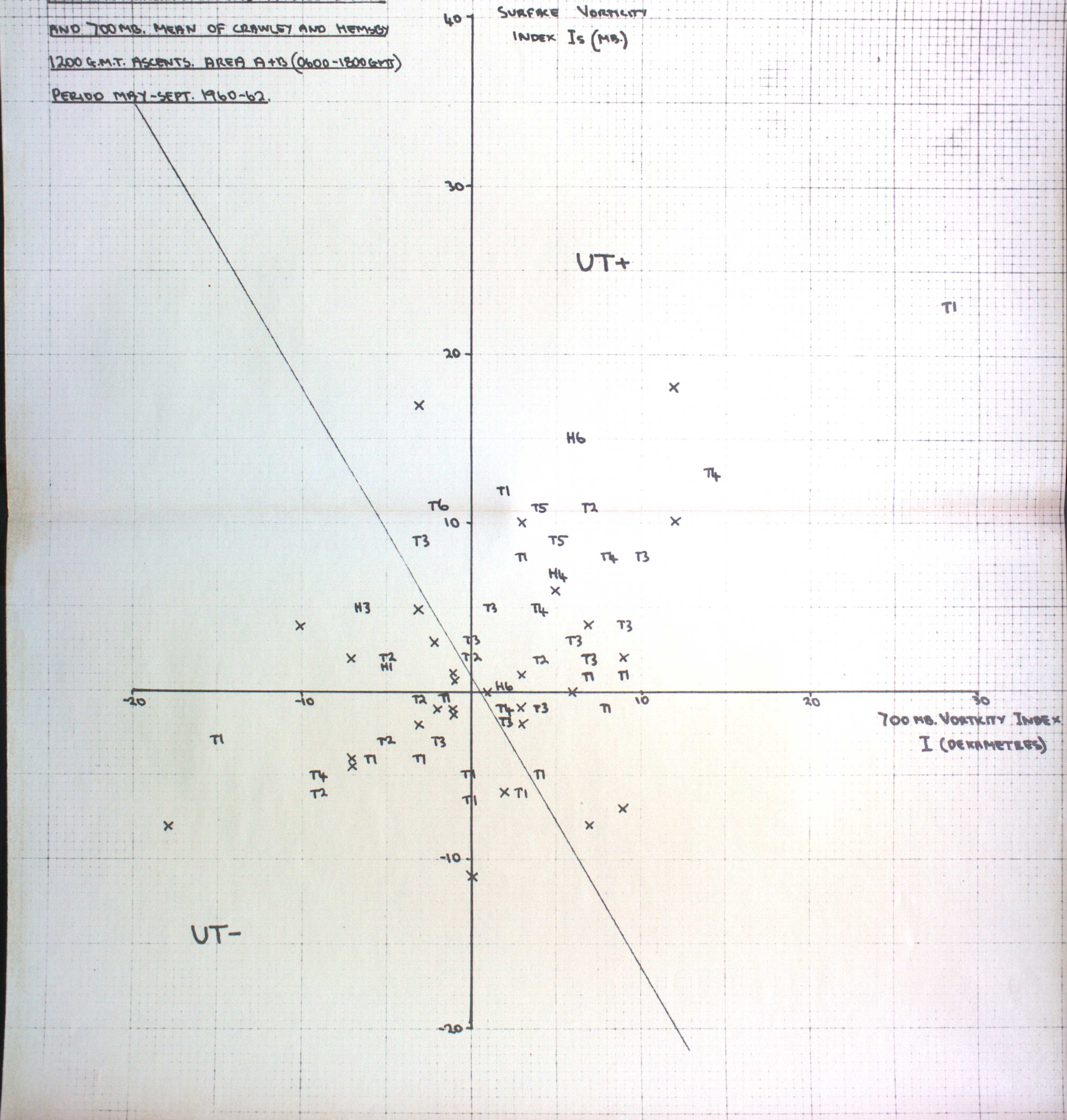

FIG. II:- WEATHER CATEGORY FOR THE LARGE POSITIVE ENERGY (LP) CASES AS A FUNCTION OF THE 1200 G.M.T. VORTICITY INDICES AT THE SURFACE AND 700MB. MEAN OF CRAWLEY AND HEMSBY 1200 G.M.T. ASCENTS. AREA A+B (0600-1800 G.M.T.) PERIOD MAY-SEPT. 1960-62

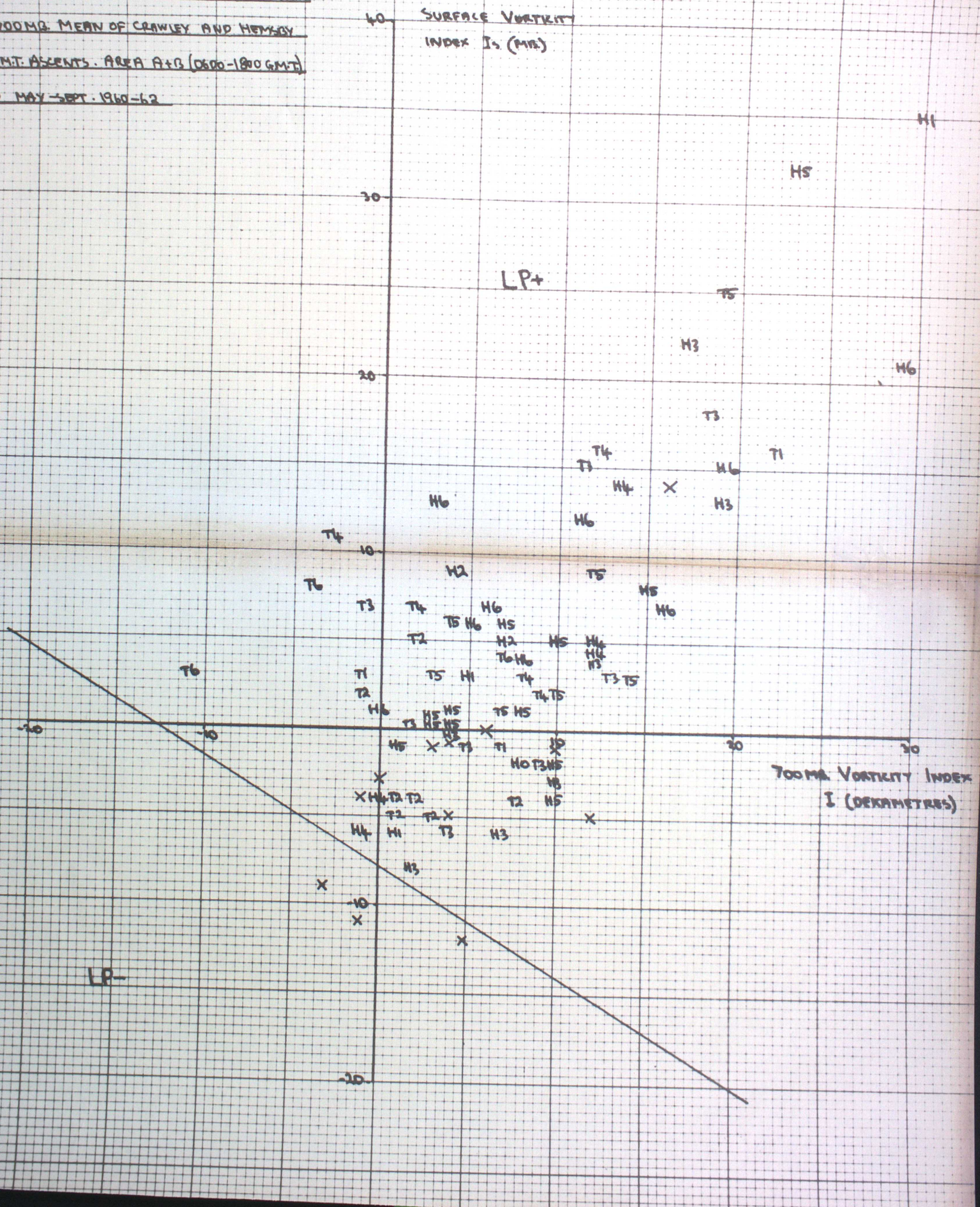

FIG. 18 WEATHER CATEGORY FOR AREA B (0600 - 1800 GMT)
AS A FUNCTION OF THE WIND SPEED AND
DIRECTION AT 900M (CRAWLEY 1200 GMT ASCENT)
LP+ UT+ ULN CASES ONLY. PERIOD MAY-SEPT 1958-66

G.M.T. CRAWLEY
SPEED
00M
(T.)

CLASS A

CLASS B

CLASS C

1200 GMT CRAWLEY
WIND DIRECTION AT 900M (°)

FIG. 18 WEATHER CATEGORY FOR AREA B (0900 - 1800 GMT) AS A FUNCTION OF THE WIND SPEED AND DIRECTION AT 900M (CRAWLEY 1200 GMT ASCENT) LP+ UT+ ULN CASES ONLY. PERIOD MAY-SEPT 1958-64

1200 G.M.T. CRAWLEY WIND SPEED AT 900M (KT.)

CLASS A

CLASS B

CLASS C

1200 GMT CRAWLEY WIND DIRECTION AT 900M (°)

CLASS C

CLASS D

CLASS X

120 140 160 180 200 220 240 260 280 300 320 340 (360)

1200 GMT CRAWLEY

WIND DIRECTION AT 900M (°)

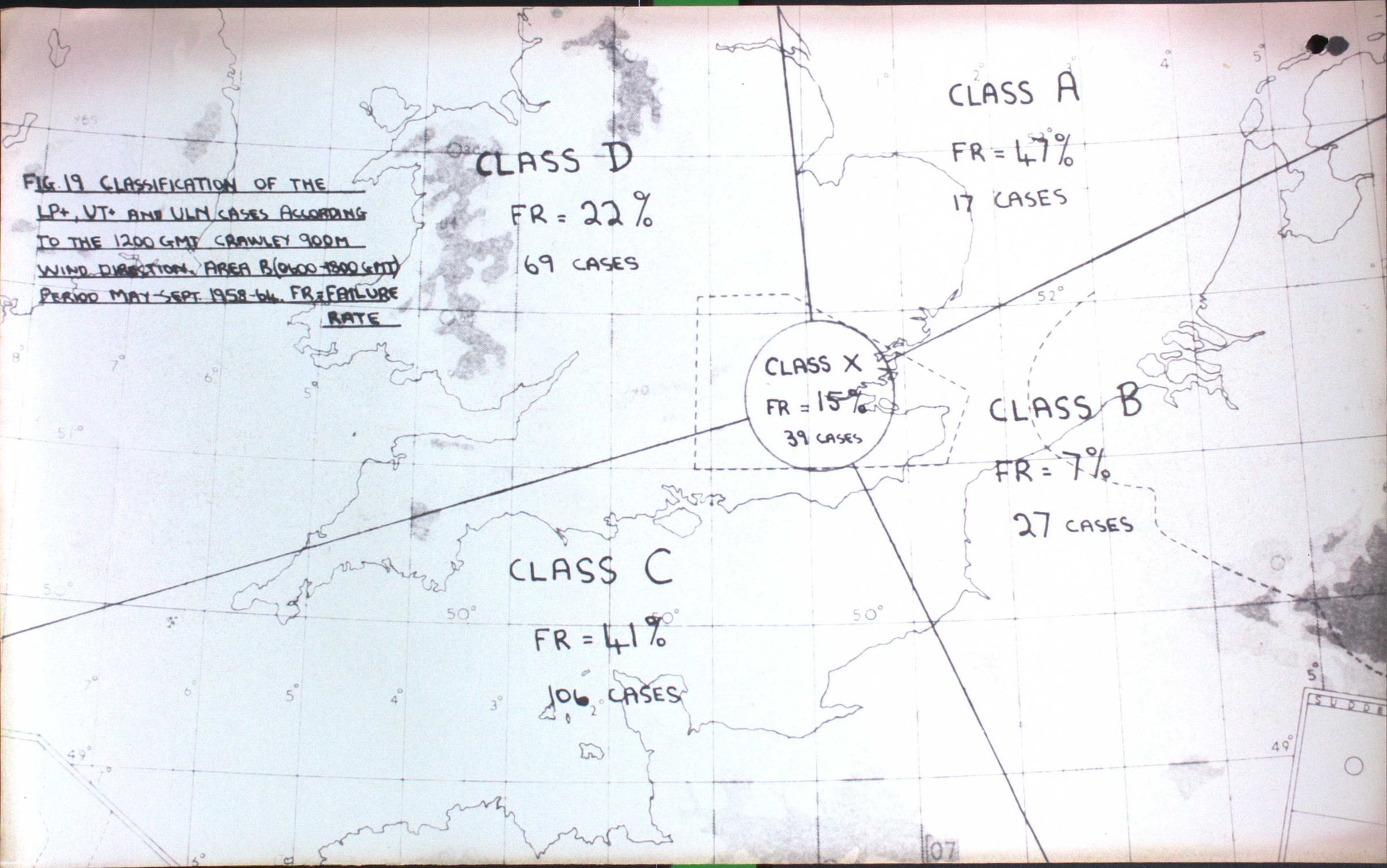

FIG. 19 CLASSIFICATION OF THE LP+, VT+ AND ULN CASES ACCORDING TO THE 1200 GMT CRAWLEY 900M WIND DIRECTION. AREA B (0600-1800 GMT) PERIOD MAY-SEPT. 1958-64. FR = FAILURE RATE

FIG. 20 WEATHER CATEGORY FOR AREA B (0600–1800 GMT) AS A FUNCTION OF THE 1200 GMT 900M WIND DIRECTIONS AT CRAWLEY AND CAMBORNE LA, UT + ULN CASES ONLY WITH CRAWLEY WIND DIRECTION 200–300° AND SPEED ≥ 8KT. PERIOD MAY–SEPT 1958–64

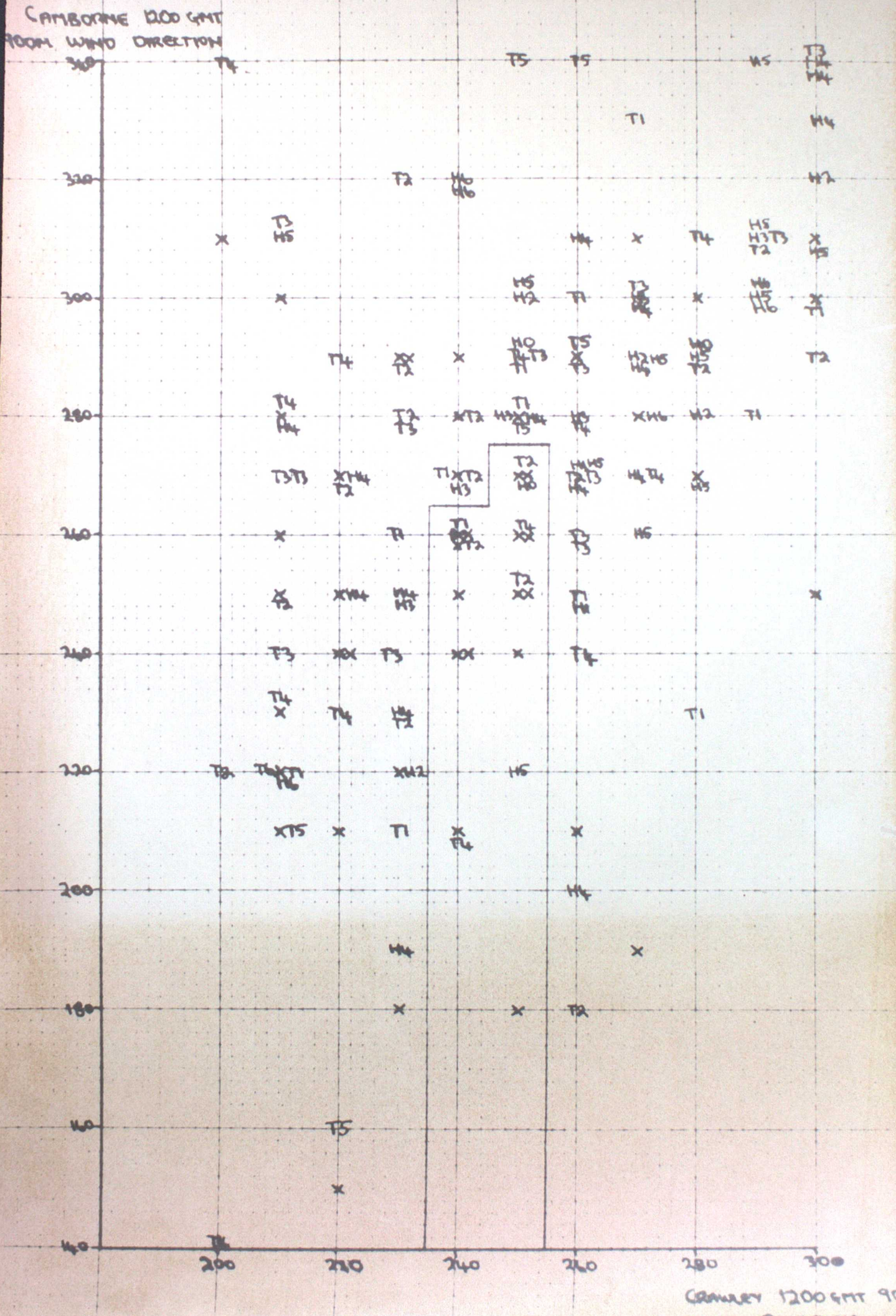

FIG. 21 WEATHER CATEGORY FOR CASES INSIDE THE BOX IN FIG. 20 AS A FUNCTION OF THE 1200 GMT WIND VELOCITY AT LONG KESH.

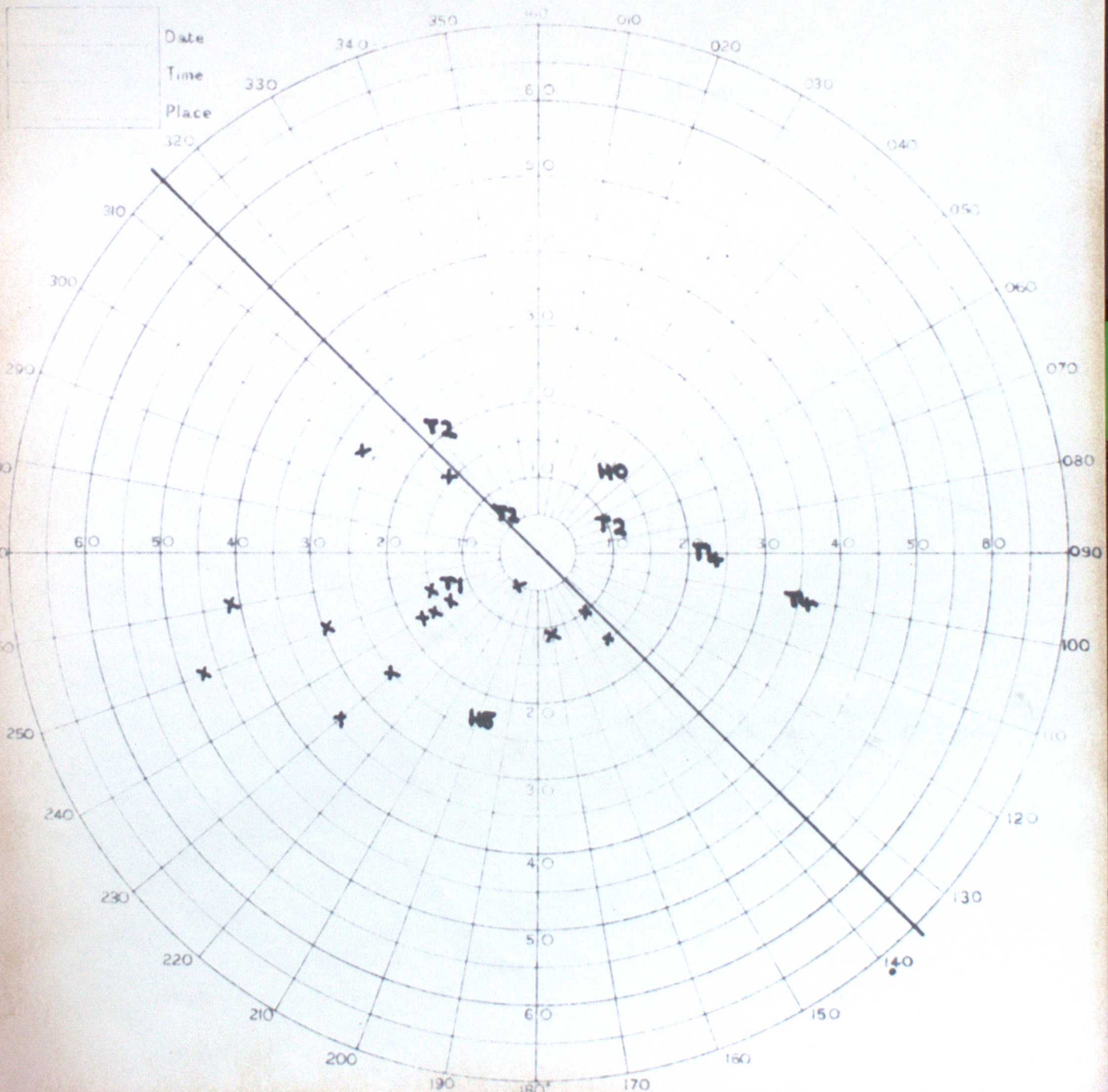

FIG. 22 WEATHER CATEGORY FOR AREA B (0900-1800 GMT) AS A FUNCTION OF THE 1200 GMT 900M WIND VELOCITY AT AVIATION LPT UT+ ULN CASES WITH CRAWLEY WIND DIRECTION 160-230° AND SPEED >8KT. PERIOD MAY-SEPT 1958-64

PLOTTED DOUBLE SCALE

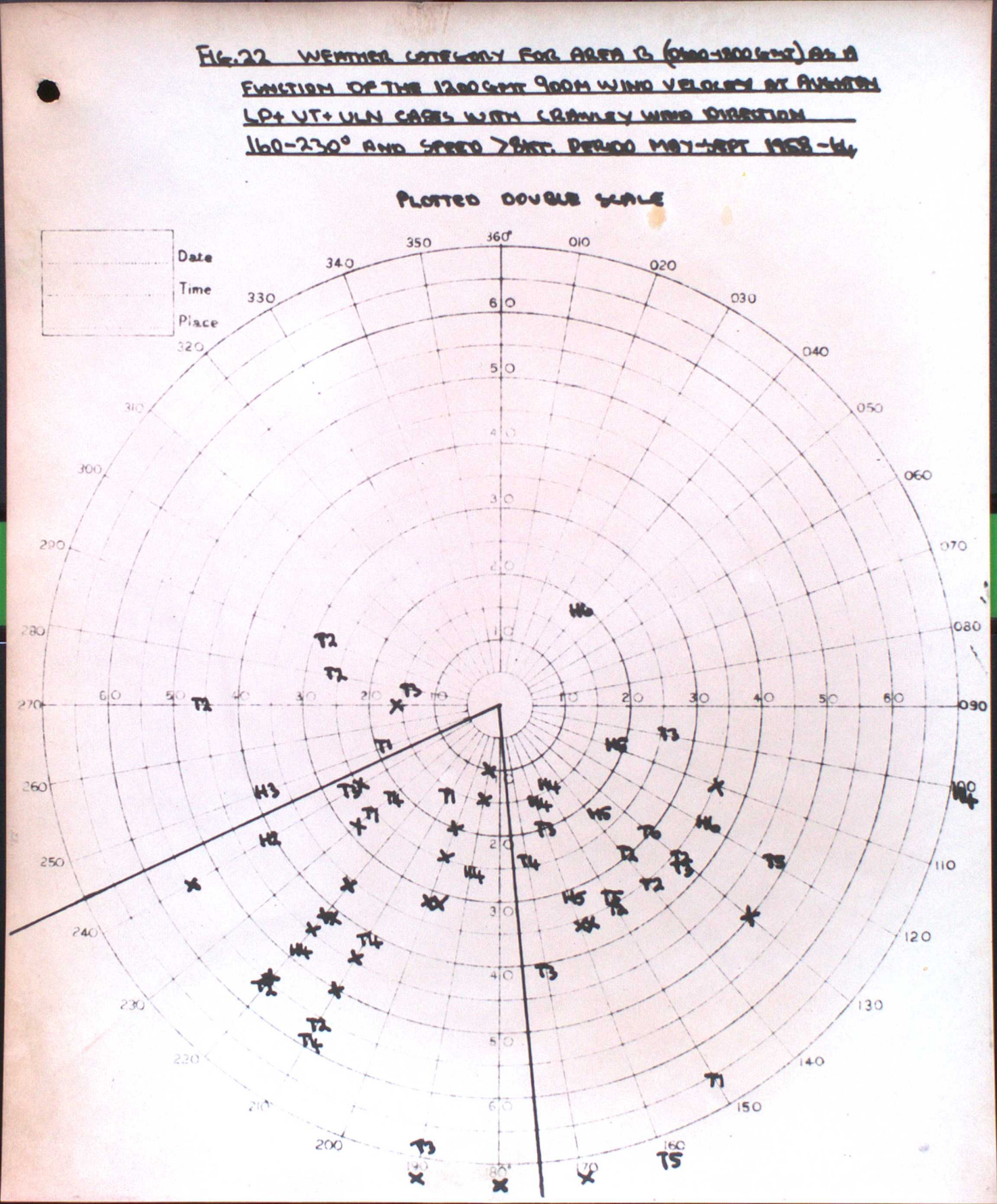

FIG. 23 WEATHER CATEGORY FOR AREA B (0600-1800 GMT) AS A FUNCTION OF THE 8-HOUR DISPLACEMENT OF AN AIR PARCEL MOVING WITH THE MEAN OF THE CRAWLEY AND HERSTMON 1200 GMT 900 m WIND VELOCITIES. LP+ UT+ T5 VLM CASES WITH CRAWLEY WIND DIRECTION 360-060° AND SPEED > 8 KT. PERIOD MAY - SEPTEMBER 1958-64